



# **Macquarie Harbour Oxygen Process model (FRDC 2016-067)**

**CSIRO Final Report**

Karen Wild-Allen, John Andrewartha, Mark Baird, Lev Bodrossy, Elizabeth Brewer, Ruth Eriksen, Jenny Skerratt, Andrew Reville, Kendall Sherrin, Dan Wild

June 2020

FRDC Project No **2016/067**

## Macquarie Harbour Oxygen Process model (FRDC 2016-067) CSIRO Final Report

FRDC 2016-067

June 2020

### Ownership of Intellectual property rights

Copyright (and any other intellectual property rights) in this publication are owned by the Fisheries Research and Development Corporation, CSIRO and UTAS-IMAS.

This publication (and any information sourced from it) should be attributed to:

Wild-Allen, K., Andrewartha, J., Baird, M., Bodrossy, L., Brewer, E., Eriksen, R., Skerratt, J., Reville, A., Sherrin, K., Wild, D. (2020) Macquarie Harbour Oxygen Process model (FRDC 2016-067): CSIRO Final Report. CSIRO Oceans & Atmosphere, Hobart, Australia

### Creative Commons licence

All material in this publication is licensed under a Creative Commons Attribution 3.0 Australia Licence, save for content supplied by third parties, logos and the Commonwealth Coat of Arms.



Creative Commons Attribution 3.0 Australia Licence is a standard form licence agreement that allows you to copy, distribute, transmit and adapt this publication provided you attribute the work. A summary of the licence terms is available from <https://creativecommons.org/licenses/by/3.0/au/>. The full licence terms are available from <https://creativecommons.org/licenses/by-sa/3.0/au/legalcode>.

Inquiries regarding the licence and any use of this document should be sent to: [frdc@frdc.com.au](mailto:frdc@frdc.com.au)

### Disclaimer

The authors do not warrant that the information in this document is free from errors or omissions. The authors do not accept any form of liability, be it contractual, tortious, or otherwise, for the contents of this document or for any consequences arising from its use or any reliance placed upon it. The information, opinions and advice contained in this document may not relate, or be relevant, to a readers particular circumstances. Opinions expressed by the authors are the individual opinions expressed by those persons and are not necessarily those of the publisher, research provider or the FRDC.

The Fisheries Research and Development Corporation plans, invests in and manages fisheries research and development throughout Australia. It is a statutory authority within the portfolio of the federal Minister for Agriculture, Fisheries and Forestry, jointly funded by the Australian Government and the fishing industry.

CSIRO advises that the information contained in this publication comprises general statements based on scientific research. The reader is advised and needs to be aware that such information may be incomplete or unable to be used in any specific situation. No reliance or actions must therefore be made on that information without seeking prior expert professional, scientific and technical advice. To the extent permitted by law, CSIRO (including its employees and consultants) excludes all liability to any person for any consequences, including but not limited to all losses, damages, costs, expenses and any other compensation, arising directly or indirectly from using this publication (in part or in whole) and any information or material contained in it.

#### Researcher Contact Details

Name: Dr Karen Wild-Allen  
Address: CSIRO Oceans & Atmosphere,  
GPO Box 1538  
Hobart, TAS 7001  
Phone: +61 3 5232 5010  
Email: [karen.wild-allen@csiro.au](mailto:karen.wild-allen@csiro.au)

#### FRDC Contact Details

Address: 25 Geils Court  
Deakin ACT 2600  
Phone: 02 6285 0400  
Fax: 02 6285 0499  
Email: [frdc@frdc.com.au](mailto:frdc@frdc.com.au)  
Web: [www.frdc.com.au](http://www.frdc.com.au)

In submitting this report, the researcher has agreed to FRDC publishing this material in its edited form.

# Table of Contents

Acknowledgments.....	4
Glossary .....	4
Executive Summary.....	5
1 Profiling Mooring.....	8
2 Near Real-Time and Short-Term Forecast Model.....	11
2.1 Model Implementation .....	11
2.2 Model Validation .....	13
2.3 Harbour Recharge.....	18
3 Visualisation Dashboard .....	23
4 Biogeochemical Process Model .....	24
4.1 Summary of model implementation .....	24
4.2 Summary of model skill compared to observations.....	25
4.3 Simulated seasonal cycle .....	31
4.4 Oxygen and nitrogen budget analysis .....	43
4.5 Model scenario simulations .....	51
4.6 Analysis of scenario simulations.....	53
5 New Observations.....	66
5.1 Optical properties.....	66
5.2 Water column profiles.....	68
5.3 Phytoplankton composition .....	72
5.4 Phosphate addition process study .....	76
5.5 Dissolved oxygen drawdown process study.....	83
6 Conclusions.....	89
7 Recommendations.....	92
8 References .....	93
9 Appendix: Summary figures of model comparison with observations .....	96

# Acknowledgments

This work has been funded by the FRDC project 2016 - 067 'Understanding oxygen dynamics and the importance for benthic recovery in Macquarie Harbour' and delivers the 4<sup>th</sup> milestone report to IMAS (FRDC project lead).

We thank the Australian Bureau of Meteorology for weather forecast, hind-cast data and observations and the EPA, DPIIWE Marine Farming Branch, Tassal, HAC and Petuna for making data available to the project. We thank HAC, Petuna and Tassal for operational support in maintaining the CSIRO profiling mooring and IMAS staff for assistance with fieldwork. We thank Lesley Clementson, Monika Wozniak, Bozena Wojtasiewicz and Dion Frampton for assistance with optical and picoplankton sample analysis and Tim Malthus for constructive review.

## Glossary

BEMP	Broadscale Environmental Monitoring Program
Bias	Bias refers to the tendency of a measurement process to over- or under-estimate the value of a population parameter
BGA	Blue-green algae sensor (senses phycoerythrin pigment, PE)
CDOM	colour dissolved organic matter
Chl a	chlorophyll a
CSIRO1 or 2	CSIRO Profiling mooring location 1 (central harbour) or 2 (north harbour closer to entrance)
CTD	Conductivity Temperature Depth profiler
d2	Statistical metric, aka see Willmott index (below and in methods section)
DIN	Dissolved inorganic nitrogen (NH <sub>4</sub> plus NO <sub>x</sub> )
DIP	dissolved inorganic phosphorous
DOC	dissolved organic carbon
DON	dissolved organic nitrogen
DPIIWE	Tasmanian government Department of Primary Industry, Parks, Water and the Environment
EMS	Environmental modelling suite is the CSIRO hydrodynamic biogeochemical sediment wave spectral model as a whole and in this study refers to the set up for Macquarie Harbour model
EPA	Tasmanian Environment Protection Authority
HAC	Huon Aquaculture
Kd(PAR)	light attenuation coefficient
mae	mean absolute error
mape	mean absolute percentage error
MODIS	Moderate Resolution Imaging Spectroradiometer
NH <sub>3</sub> <sup>-</sup> + NH <sub>4</sub> <sup>+</sup>	ammonium
NO <sub>x</sub>	nitrate plus nitrite
NTU	Nephelometric Turbidity Unit
PE	Phycoerythrin pigment found in blue green algae (BGA)
rms	root mean square
secchi	measurement of water transparency (depth in m)
TSS	total suspended solids
WHA	World Heritage Area
Willmott index	statistical metric that is a standardized measure of the degree of model prediction error and varies between 0 and 1. A value of 1 indicates a perfect match, and 0 indicates no agreement at all. Hydrodynamic models suitable values fit for purpose are above 0.85 and BGC models 0.40 (see methods section).

# Executive Summary

Good water quality is fundamental for the maintenance of healthy aquatic ecosystems and their provision of beneficial ecosystem services. Good water quality is essential for sustainable aquaculture which can be compromised by elevated sediment loads, nutrient enrichment, algal blooms and depletion of dissolved oxygen. Sources of sediment and nutrients to the coastal marine environment include river loads, oceanic influx, resuspended benthic material and anthropogenic discharge from urban centres and fish farms. The localised impact of these cumulative loads on water quality is determined by physical dispersal and biogeochemical assimilation. Understanding the seasonal and regional variation in water quality can inform the sustainable management of anthropogenic discharge and aquaculture activities to minimise the effects of nutrient enrichment, algal blooms and depletion of dissolved oxygen.

This report delivers CSIRO's Final Report for the project: Understanding oxygen dynamics and the importance for benthic recovery in Macquarie Harbour (FRDC 2016-067). Specifically, we report on:

1. the maintenance of the CSIRO profiler and ongoing delivery of near real time and short term forecast model results
2. updates to the visualisation dashboard
3. a description of the simulated harbour water quality, evaluation of oxygen and nitrogen budgets, scenario results and analysis
4. analysis of observational process studies for phosphate addition and oxygen drawdown

The CSIRO profiling mooring continues to operate and has delivered an impressive dataset of hourly profiles of temperature, salinity, dissolved oxygen, chlorophyll, BGA and CDOM fluorescence in near real time since June 2019 with very little down time. These data (together with available IMAS mooring string data and fish farm data) are routinely used to assess the performance of the operational hydrodynamic and oxygen tracer model that runs in near real time with a short-term forecast. Recently the forecast has been extended out to +10 days, using BOM ACCESS-G, although the accuracy of the harbour forecast is limited by the accuracy of the meteorological forecast and estimated river flows, both of which can deteriorate significantly over this extended forecast period.

The visualisation dashboard has been upgraded to deliver a robust and secure platform consistent with latest developments on similar platforms (e.g. the Storm Bay Information System). Output from the mooring and operational model are available on the Macquarie Harbour dashboard at: <https://macqmodelling.csiro.au/> [user login: CSIRO; password: HitchikersGuide], to inform stakeholders of evolving and predicted harbour conditions. A recent example demonstrating stakeholder use of the dashboard occurred in February 2020, when farmers were informed (with 3 days notice), of a predicted intrusion event and risk of reduced near surface dissolved oxygen in areas of the harbour shown on the dashboard.

A biogeochemical and optical water quality model has been implemented for Macquarie Harbour and generally reproduces the hydrodynamics, biogeochemical cycling and dissolved oxygen conditions observed in 2017-18 very well. The model performed best in the main harbour basin with slightly poorer skill near the Gordon and King Rivers, due to unconstrained uncertainty in river flows and biogeochemical loads. For simulated properties and scales that were not observed the model provides a hypothesis of system dynamics consistent with the properties that were observed at the sites within the Harbour.

Surface water in the harbour is seasonally warmer in summer and cooler in winter resulting in a persistent temperature inversion in winter and spring, maintained by the strong salinity driven density gradient. Should low river flow occur in winter or spring this could potentially allow overturning of the water column to re-establish a stable thermal structure.

Surface waters have very low phosphorous content with model and observations suggesting a deficit in phosphorous supply for phytoplankton growth (c.f. Redfield 16 mol N : 1 mol P). Simulated nutrient concentrations at depth were generally higher in 2017 and lower in 2018, particularly for nitrogen, due to a corresponding reduction in fish farm nutrient load in 2018. The largest input of nitrogen to the harbour in 2017-18 was from rivers (45%), fish farms and sewerage (25%), and marine intrusions (23%) [note that for the Gordon river only 30% of the nitrogen load was labile (reactive) material c.f. 100% of fish farm and sewerage treatment plant waste]; nitrogen loss from the harbour was by export to the ocean (80%), and by sediment and water column denitrification (20%). The simulated harbour nitrogen budget shows a small net deficit of -100 tN/y, suggesting that the harbour was not in steady state but was eroding nitrogen to the surrounding environment. Given the relatively large fluxes of nitrogen into and out of the system, and the uncertainty in river nutrient loads, the absolute accuracy of this budget should be treated with caution.

Phytoplankton growth throughout the harbour is limited by light (CDOM and detrital matter dominate total absorption) and low nutrient concentrations in surface waters. Peak concentrations of chlorophyll were simulated at around 15m depth towards the northern end of the harbour which was subject to greater marine phosphorous supply and more transparent water in summer. It should be noted, that phytoplankton increase their pigment concentration under low light conditions and chlorophyll concentration does not directly correspond to phytoplankton biomass.

Dissolved oxygen concentrations in harbour surface waters are generally high, whilst concentrations at depth are depleted, primarily due to stratification and slow flushing of deep water in the harbour. No anoxic (<1% oxygen saturation) water or sediment areas were simulated by the biogeochemical model. Mean conditions simulated in 2017-18 showed that 14% of the whole harbour water volume and 33% of the sediment surface area was hypoxic (1-30% oxygen saturation) with the World Heritage Area (WHA) more impacted than the other basins. Oxygen budget analysis found the largest influx of oxygen to the harbour was from rivers (66%), marine input (10%) and air-sea flux (6%); the greatest loss terms were from export to the ocean (87%), biogeochemical remineralisation processes in the sediment (8%) and estimated farmed fish respiration (3%). Seasonal analysis for 2017-18 showed a net increase in harbour oxygen in winter and less consistently in autumn, and a net loss of oxygen in spring. The simulated harbour oxygen budget is very close to balanced being in deficit by only around -2900 tO/y. Given the large fluxes of oxygen into and out of the harbour, the accuracy of this small net sum should be considered in the context of potential uncertainty in the estimates of river flow and harbour entrance bathymetry.

Scenario simulations were achieved for drier (lower river flow) and wetter (higher river flow) conditions. Under reduced river flow, there was ~20% greater influx of marine water into the deeper parts of the harbour and reduced hypoxia; with increased river flow, marine influx was suppressed (by ~20%), deep water residence time increased and hypoxia increased. These patterns were persistent when scenarios were extended for a further 2 years and strong linear relationships were found between river flow, marine influx of oxygen and hypoxia. Further scenario simulations were achieved to explore reduced anthropogenic load on harbour water quality (by omission of fish farm respiration and nutrient loads). This reduction in anthropogenic load resulted in a 50% reduction in hypoxic water and a 40% reduction in hypoxic sediment compared to the 2017-18 model run and was persistent in

the extended model run. The reduced anthropogenic load scenarios showed a larger reduction in hypoxia under comparable ocean oxygen influx c.f. all other scenarios.

The phosphate addition process study achieved the targeted range of phosphate spikes and demonstrated rapid phosphate draw-down within 24 hours in both dark and light incubations, plus ongoing utilisation of phosphate over 48 hours in the light incubation. Picoplankton analyses showed an increase in total eukaryotes over time and pigment data indicated the presence of cryptophytes and diatoms. Molecular analysis of 16S and 18S ribosomal DNA samples were however inconclusive and no significant reactions to the addition of phosphate were detected [although the experimental timeframe may not have been long enough to observe significant cell division]. On balance, this experiment suggests that phosphate limitation may not be a major factor shaping the Macquarie Harbour microbial community and that light limitation due to high levels of CDOM in surface waters may have a greater influence.

The oxygen drawdown process study found that, following aeration of Macquarie harbour water collected from 10 m and 20 m, there was a substantial increase in the activity of specialised bacteria known as copiotrophs; these increased 25x within 8 and 100x within 18 hours. These bacteria are known to utilise labile organic carbon and we also observed a simultaneous uptake of available ammonium. Our results show that, even at 80% dissolved oxygen saturation, the activity of these bacteria would have been suppressed, which indicates that if more dissolved oxygen were to become available at depth, it would likely be rapidly utilised by these bacteria (assuming sufficient availability of labile carbon and nitrogen).

In conclusion this body of work integrates multiple lines of evidence to characterise the water quality and oxygen dynamics of Macquarie Harbour. Through modelling studies we now understand that river flows control the flushing time and influx of marine water and together with anthropogenic load, this ultimately defines the hypoxic condition of the harbour. Our observations confirm the skill of the model and identify the key microbial communities driving the biogeochemical cycling of nutrients, the remineralisation of organic matter and the ecological drawdown of oxygen. The findings documented in this report are available to inform ongoing sustainable management of the harbour to minimise the deleterious impacts of anthropogenic activities on water quality and local environmental values.

Recommendations for future work are:

1. To improve the accuracy of the hydrodynamic model, by installing river flow gauges on the lower reaches of the Franklin-Gordon and King-Queen River catchments, and prioritising repair of any failure in the Strahan tide gauge.
2. To improve the accuracy of the hydrodynamic and oxygen tracer 10 day forecast, by investing in ensemble model forecasting (using the available range of BoM model forecasts), data assimilation of near real time data sets, a catchment model (including predicted dam releases) and an automated alert system to improve appropriate forecast delivery.
3. To deliver a superior monitoring data set, by strategically analysis, review and better integration of industry, EPA and research sampling programs.
4. To better characterise the impact of contrasting anthropogenic loads and seasonal dam releases on water quality, by running additional model scenarios (especially in the context of evolving hydro demand).
5. To better understand the fate of anthropogenic harbour loads on the west coast shelf and local environmental values, by extending the analysis of model results and using remote sensing.

# 1 Profiling Mooring

In October 2018, the CSIRO profiling mooring was relocated from a position in the centre of the harbour, to a position closer to the entrance, and near to where the entrance channel meets the main harbour basin (Figure 1.1). The intention of this move was to attempt to capture the recharge events whereby incoming oceanic water spills out of the shallow channel and down the slope into the deeper water of the harbour. The mooring has generally operated well in the new location from 3rd October 2018 to May 2020 with only 2 significant outages of 1.5 months each in autumn and winter of 2019. The outage in mid-February 2019 was due to a faulty port plug and a broken wind generator. The outage in May-June was due to further mechanical issues along with a servicing and upgrade of the mooring to include the addition of an ADCP.

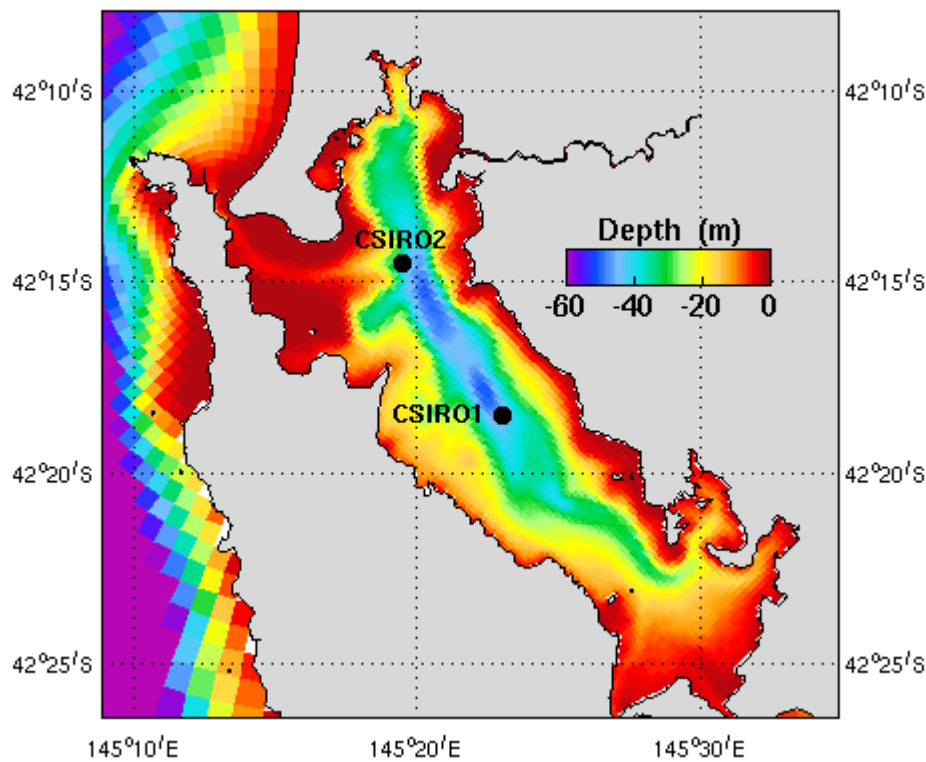
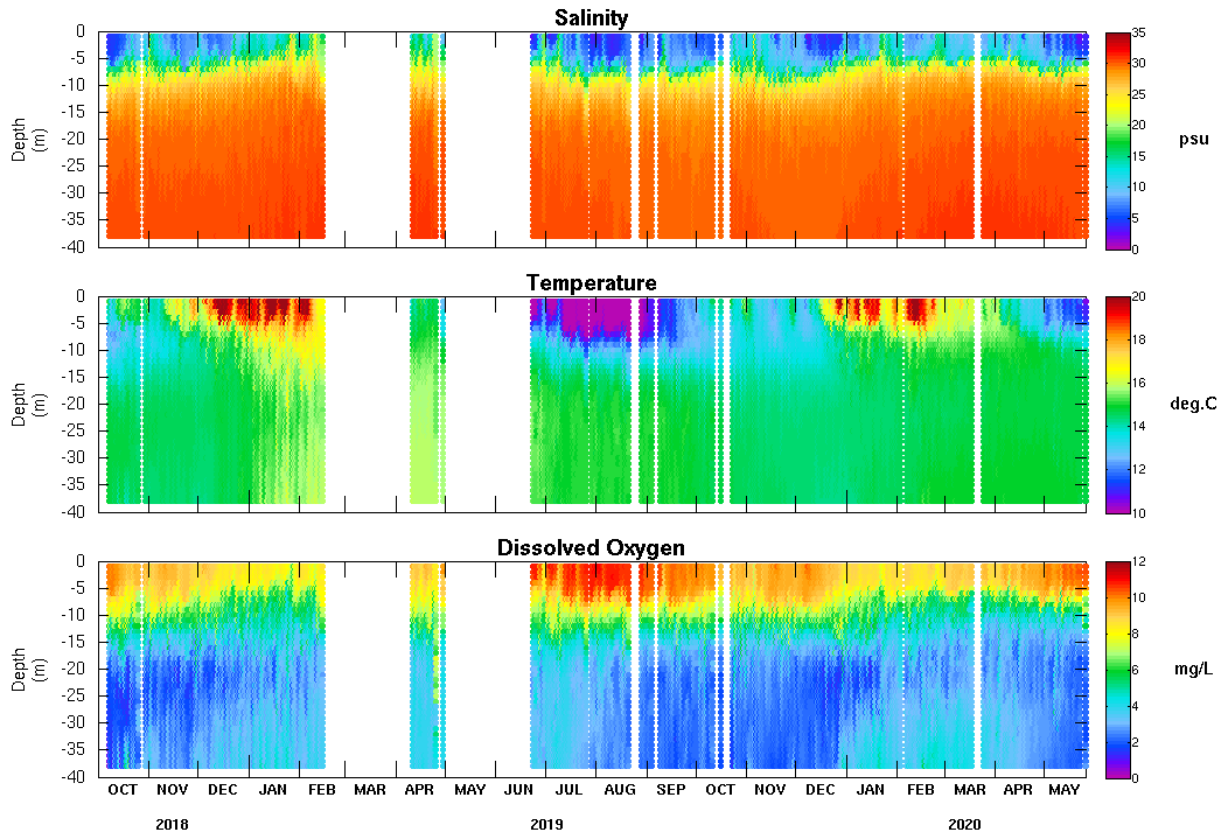


Figure 1.1: Locations of the past (CSIRO1) and present (CSIRO2) profiler deployments in Macquarie Harbour.

During the operational period, the sensors have excelled in capturing all facets of the oceanography within the harbour. These include the intense stratification which exists in the harbour, as well as the seasonal warming and cooling of the surface layer as high surface temperatures, throughout December and January, are followed by much cooler temperatures in July and August (Figure 1.2).

## MACQUARIE HARBOUR - CSIRO2 Mooring



## MACQUARIE HARBOUR - CSIRO2 Mooring

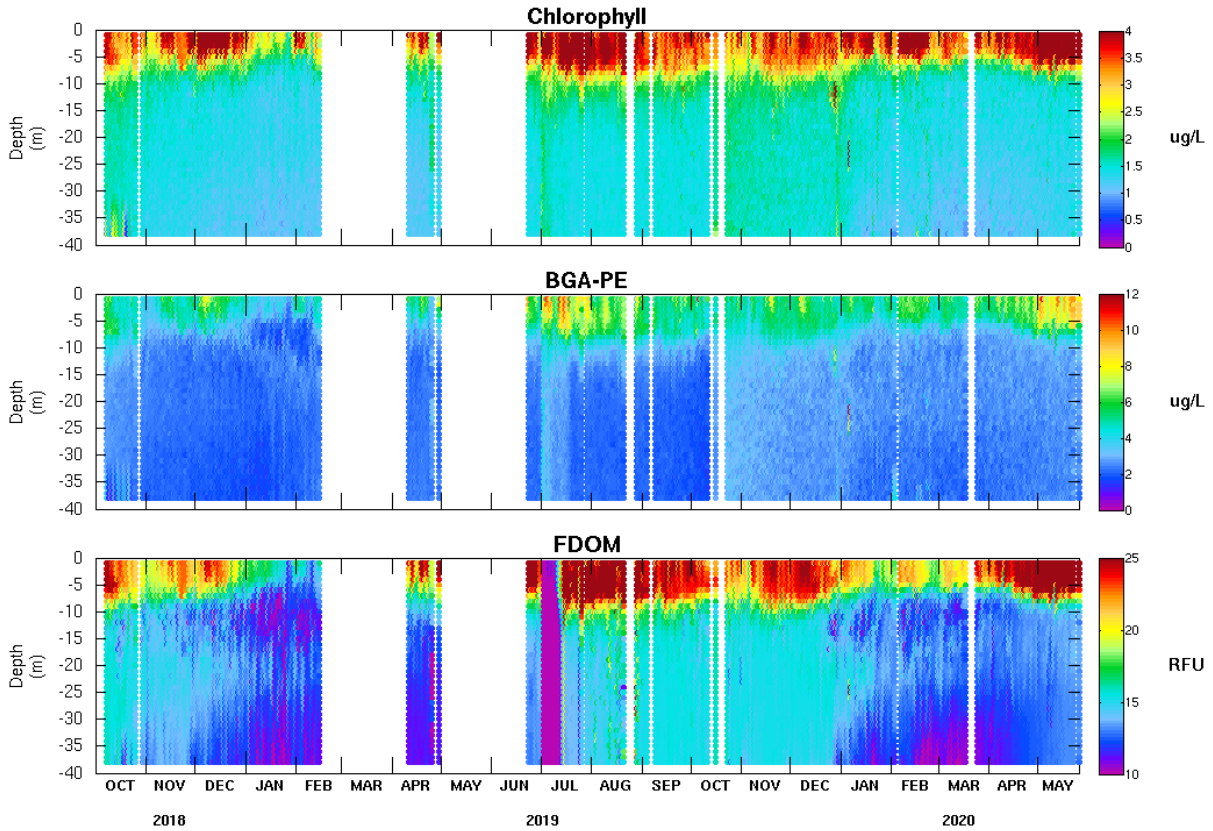


Figure 1.2: Time series of data from the profiling mooring following its relocation to the CSIRO2 site in October 2018.

The profiling mooring salinity data (Figure 1.2 top panel) shows a very distinct halocline, separating fresh water between 0 and 10 PSU, from the deeper saline water at or near 30 PSU all year round. Temperatures (Figure 1.2 second panel) range from 8 to 22 °C. in the surface layers, but in the deeper water they remain at approximately 15 °C all year round. Dissolved oxygen (Figure 1.2 third panel) is generally above 6 mg/l in the surface layers, being at a maximum of about 11 mg/l in winter. Below the halocline, and unlike salinity and temperature, DO does experience seasonal variability, with the lowest levels of around 2 mg/l occurring at the mooring location in winter-spring, and higher levels of up to 5 mg/l occurring in summer-autumn. These higher levels are brought about by oceanic recharge occurring on the incoming tide, and predominantly in summer-autumn. In summer-autumn surface salinities are higher as a result of lower river flows, mixing is diminished, and this allows denser oxygen-rich ocean water to enter the harbour, sink over the sill and enter the deeper parts of the harbour. In 2018, bottom recharge begins in early December, and persists until late July 2019. In 2019, bottom recharge began in late December, and started to wane in mid-April 2020, although there could be a resurgence in early winter if further rains are delayed and river flow remains low.

As well as being related to the strength of the halocline, the DO recharge also appears to be closely related to the actual thickness of the halocline. The salinity and oxygen data of Figure 1.2, for both Nov 2018 and Dec 2019, suggest that there is a threshold thickness of about 6m below which recharge takes place. This is further demonstrated in Figure 1.3 where estimated total river inflow decreases from its high winter levels to about 200 m<sup>3</sup>s<sup>-1</sup> in late December 2019. The halocline then reduces from 8-10 m to approximately 6 m and oxygen levels start to significantly increase, more so at the lower depths. In mid-April 2020, the halocline depth increases again to approximately 7m, as a result of strong autumn rains, and DO at 35m starts to decline again. At the time of writing, in late May, there is an easing of the rain, and the halocline is thinning (but note surface salinity is not increasing, see Figure 1.2) and bottom DO is starting to increase again.

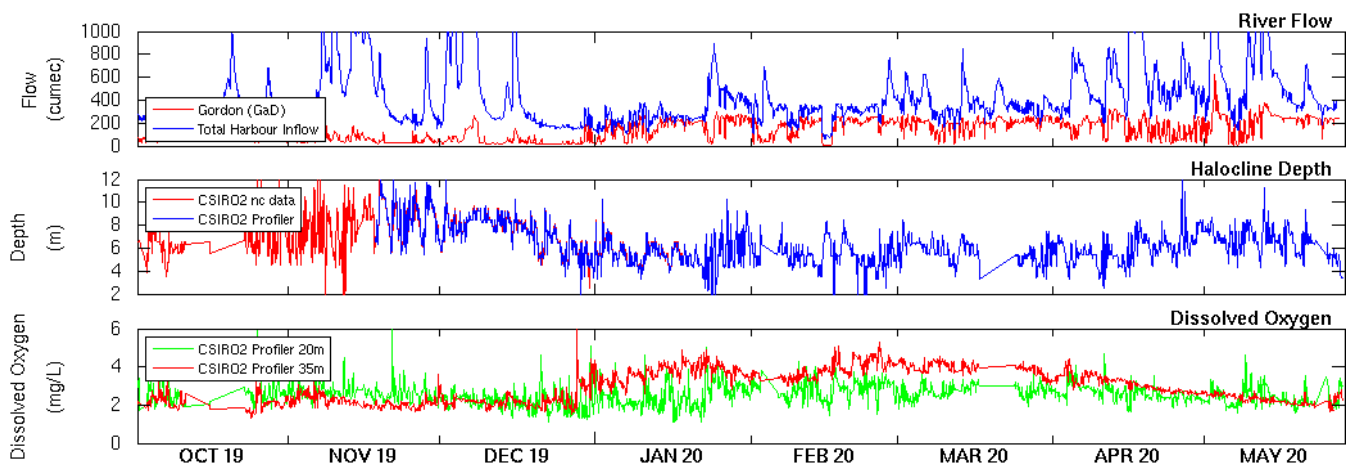


Figure 1.3: Time series of river flow, halocline depth and dissolved oxygen at the CSIRO2 mooring location.

Whilst general recharge is evident at the mooring location individual episodic recharge events are not as well resolved as initially hoped. This may be due to the mooring not being located exactly at the mouth of the entrance channel, possibly due to a shift in the bottom topography of the entrance channel, relative to the charted bathymetry that was used to position the mooring. This possibility is further discussed in the modelling section below.

## 2 Near Real-Time and Short-Term Forecast Model

### 2.1 Model Implementation

The near real-time hydrodynamic and oxygen tracer model of Macquarie Harbour has been previously described in detail (Andrewartha & Wild-Allen 2017; Wild-Allen et al., 2019 & 2020). Recent example outputs from the model, of temperature, salinity and oxygen tracer fields are plotted in Figures 2.1 and 2.2.

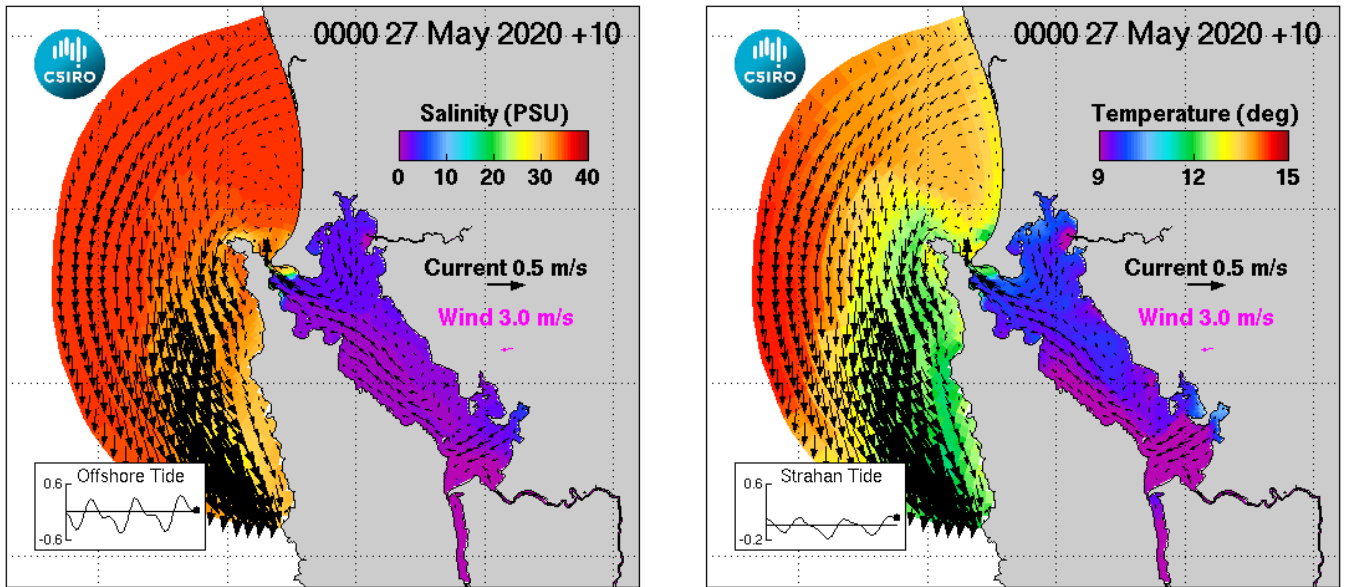


Figure 2.1: Simulated surface fields of salinity (left) & temperature (right) from the near real-time hydrodynamic & oxygen tracer model.

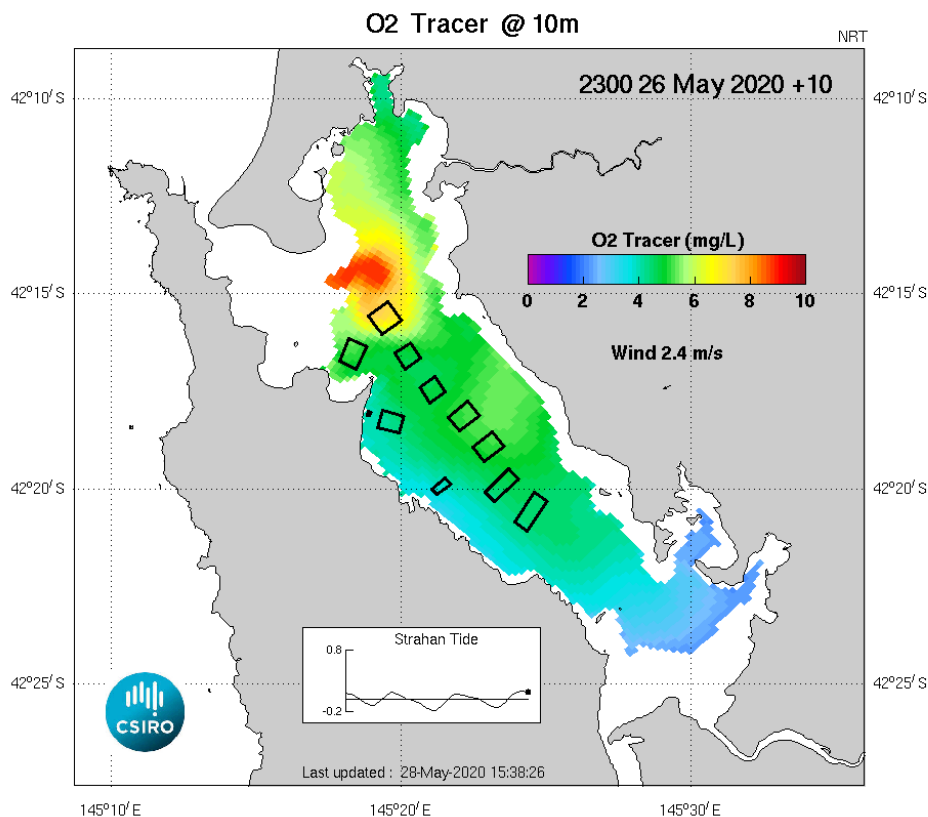


Figure 2.2: Simulated field of oxygen tracer at 10m depth from the near real-time hydrodynamic & oxygen tracer model.

The hydrodynamic and oxygen tracer model was initiated prior to 2016, and continues to operate in near real-time with comprehensive results displayed on the web dashboard at:

<https://macqmodelling.csiro.au> [user login: CSIRO; password: HitchikersGuide].

Following the initial implementation of the model, the simulated concentrations of oxygen have from time to time slowly drifted away from observed values. Corrections to this drift have been invoked periodically – a task made relatively difficult by the long residence time of the water mass in the harbour, and hence long model runs required to assess any changes. At these times of re-adjustment the model has been re-initialised with updated distributions of water quality from IMAS mooring data and CSIRO profiler observations, with modified horizontal and vertical mixing terms, and with modified distributions of water-column ‘artificial’ BOD. There was a long absence in river flow data from May 2019 to January 2020 due to broken flow gauges on the Franklin and Collingwood Rivers and during this period, river flow had to be estimated which further compromised the accuracy of the model. The missing data was internally logged by the broken gauges and when this data became available the model was reinitialised on 1<sup>st</sup> July 2019; the near real time model has run essentially uninterrupted from then to the present.

Originally, both the near real time (NRT) and forecast models were forced meteorologically with BoM’s ACCESS-R data, and forced on the offshore open boundary with BoM’s OceanMAPS data. Sea-level on the offshore boundary was derived from OceanMAPS data assimilated with low-frequency data from the Tassal sea-level gauge near Strahan, and with global tides superimposed. River flow data was obtained from Hydro for the Gordon-below-Franklin station (Upper Gordon River), the John Butters power station (King River) and Fincham Crossing station (Franklin River). Flows for other catchments, including the Lower Franklin, were derived by scaling the observations from Fincham Crossing, according to catchment area.

The length and availability of all the above data sets meant that the model only had a forecast range of approximately 2 days. (and this in the absence of any forecast river flows which had to be extrapolated from the most up-to-date observations.)

More recently the forecast ability of the model has been considerably extended by replacing ACCESS-R with ACCESS-G. The latter is spatially coarser (although the recent ACCESS-G3 is finer resolution than the original ACCESS-G2) but it has a forecast range of 10 days. To capitalize on this benefit, a catchment model has been developed for the Upper Franklin River, that converts forecast rainfall from ACCESS-G to forecast river flow for the Franklin. Example output from the model, including a comparison with observations, is given in the bottom panel of Figure 2.3. Predictions by the catchment model appear to be quite good, with most errors likely being due to inaccuracies in the ACCESS-G rainfall predictions. Note that the catchment model only forecasts river flow for one location (Fincham Crossing) and so river flows for the other catchments are derived, as before, by scaling these predictions according to catchment area.

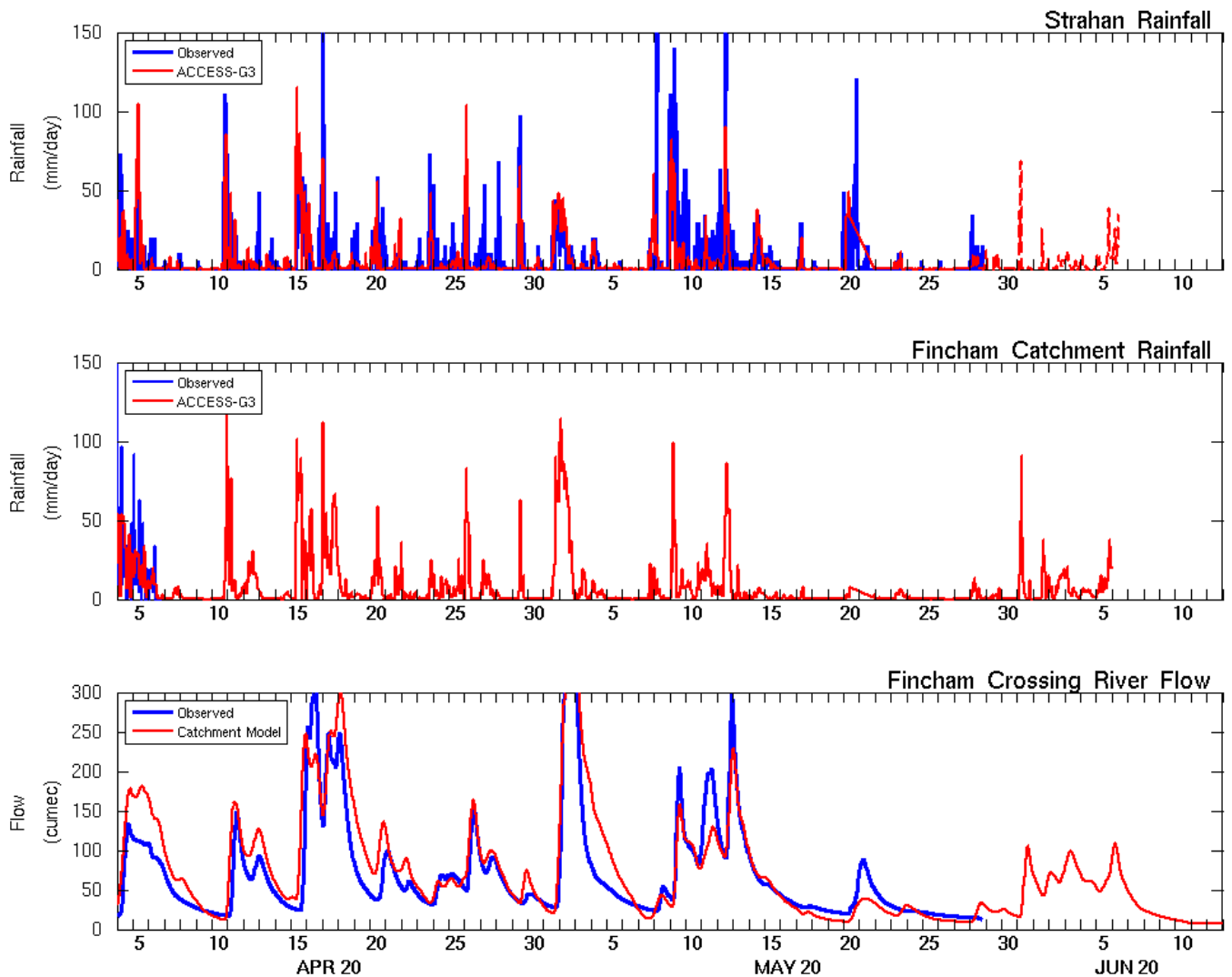


Figure 2.3: Time-series of rainfall at Strahan (top), rainfall in the Upper Franklin catchment (middle), and observed & predicted Franklin River flow (bottom).

The use of ACCESS-G for the forecast mode of the model (the high resolution ACCESS-VT is still used for the NRT mode), and implementation of the catchment model, has meant that the hydrodynamic model can now forecast out to +10 days, notwithstanding a number of assumptions. These are: firstly, sea-level assimilation cannot be implemented in forecast mode, secondly the low-frequency ocean boundary forcing needs to be extrapolated forward in time, and thirdly, flows for Gordon-above-Dennison and John Butters stations need to be assigned as constant values, based on average releases from the dams. The accuracy of the model forecast is primarily related to the accuracy of the meteorological forecast and predicted river forcing, both of which can deteriorate significantly over the extended +10 day forecast period.

## 2.2 Model Validation

The latest version of the near real-time model, applied from July 2019 to the present, is now reproducing very well the observed sea-level, temperature, salinity and oxygen signals at the CSIRO2 location (Figures 2.4, 2.5, 2.6, 2.7, 2.8, 2.9).

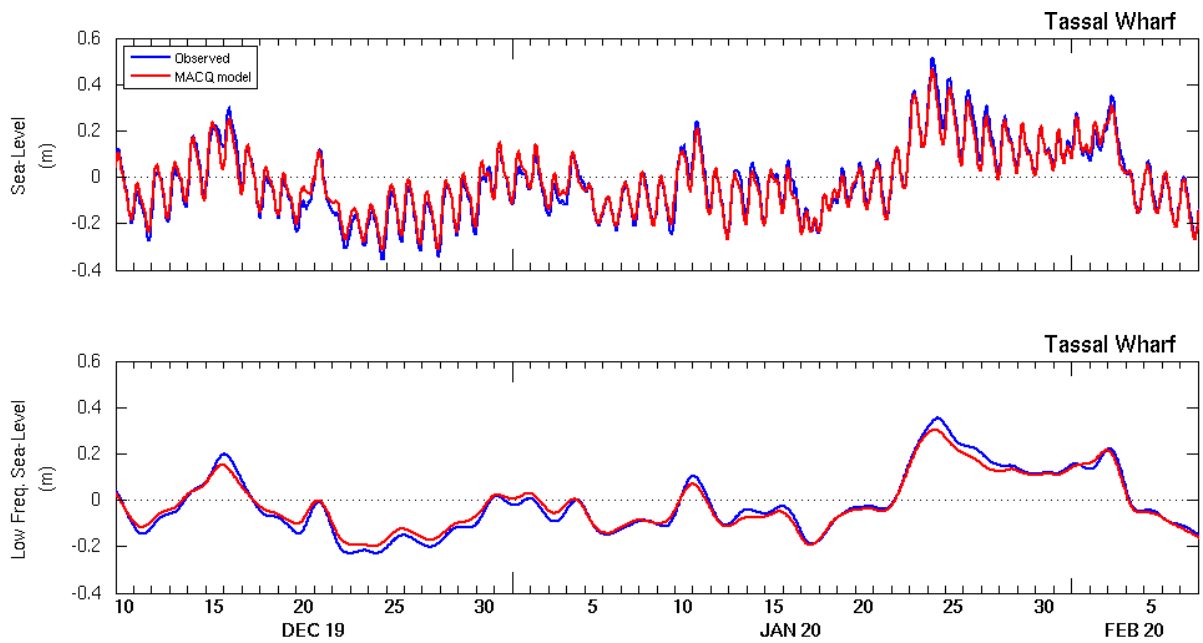


Figure 2.4: Comparison of simulated sea-level with observed sea-level, for both raw and low-pass filtered signals, collected from the Tassal Wharf.

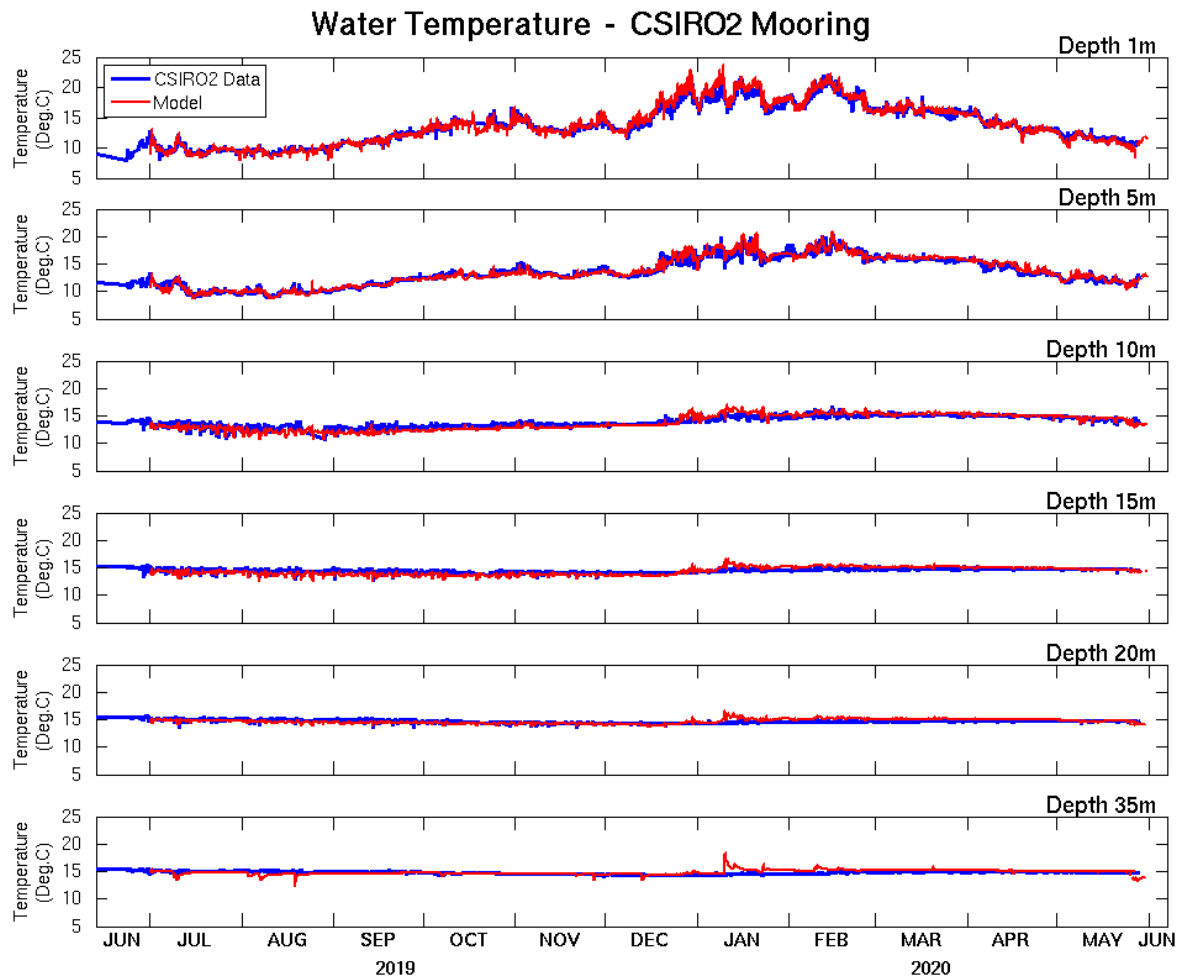


Figure 2.5: Time-series comparison of simulated and observed water temperature for 6 depths at the CSIRO2 mooring location.

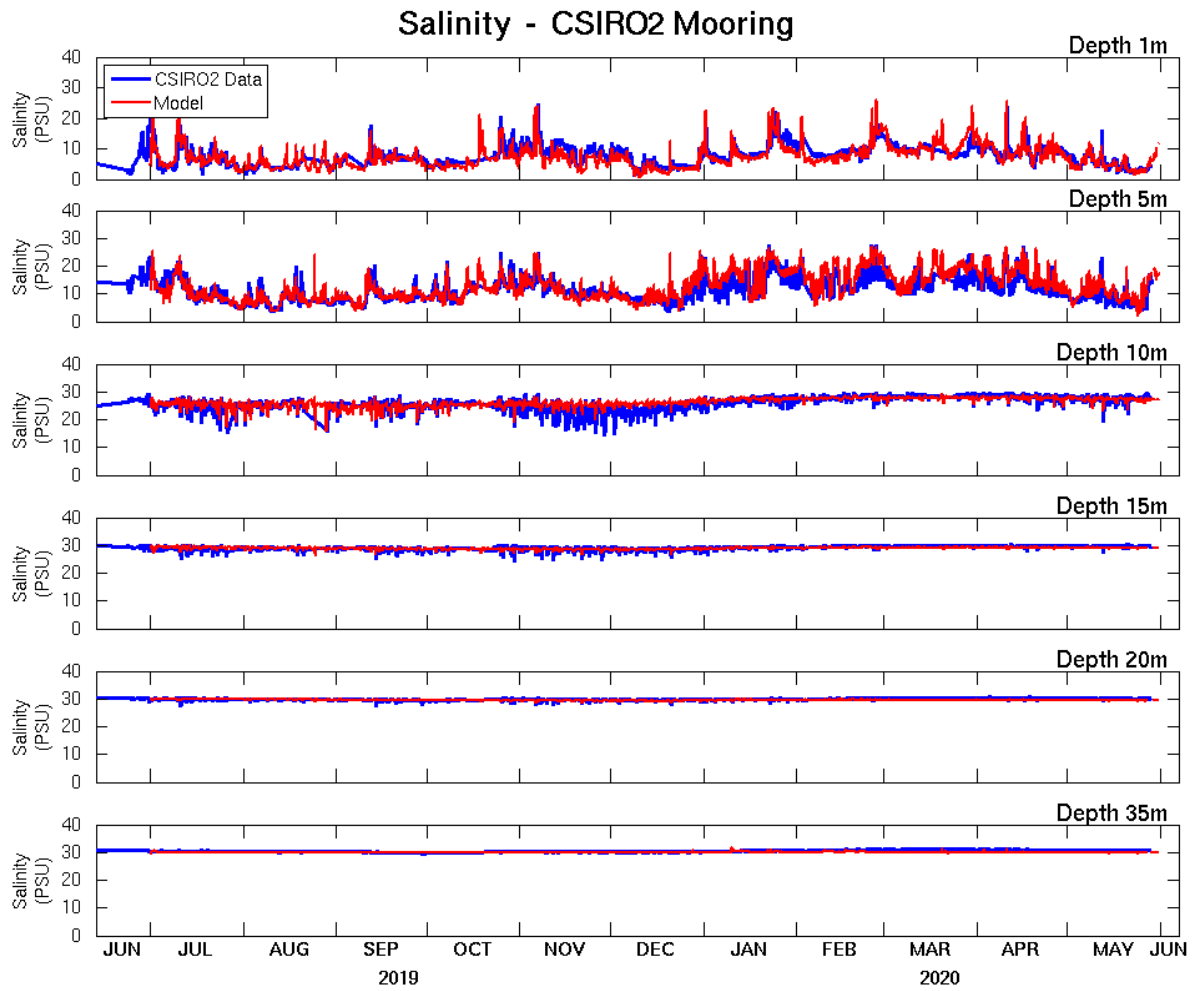


Figure 2.6: Time-series comparison of simulated and observed salinity for 6 depths at the CSIRO2 mooring location.

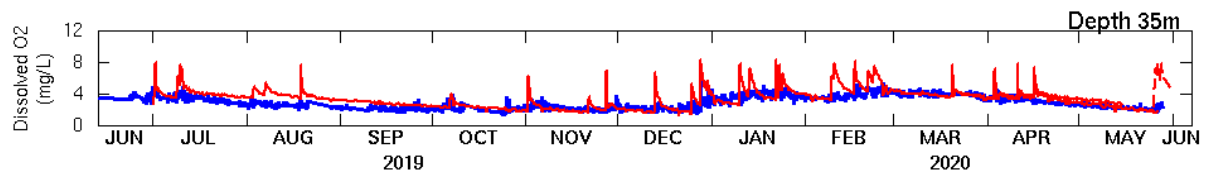


Figure 2.7: Time-series comparison of simulated oxygen tracer with observed dissolved oxygen, at a depth of 35m at the CSIRO2 mooring location.

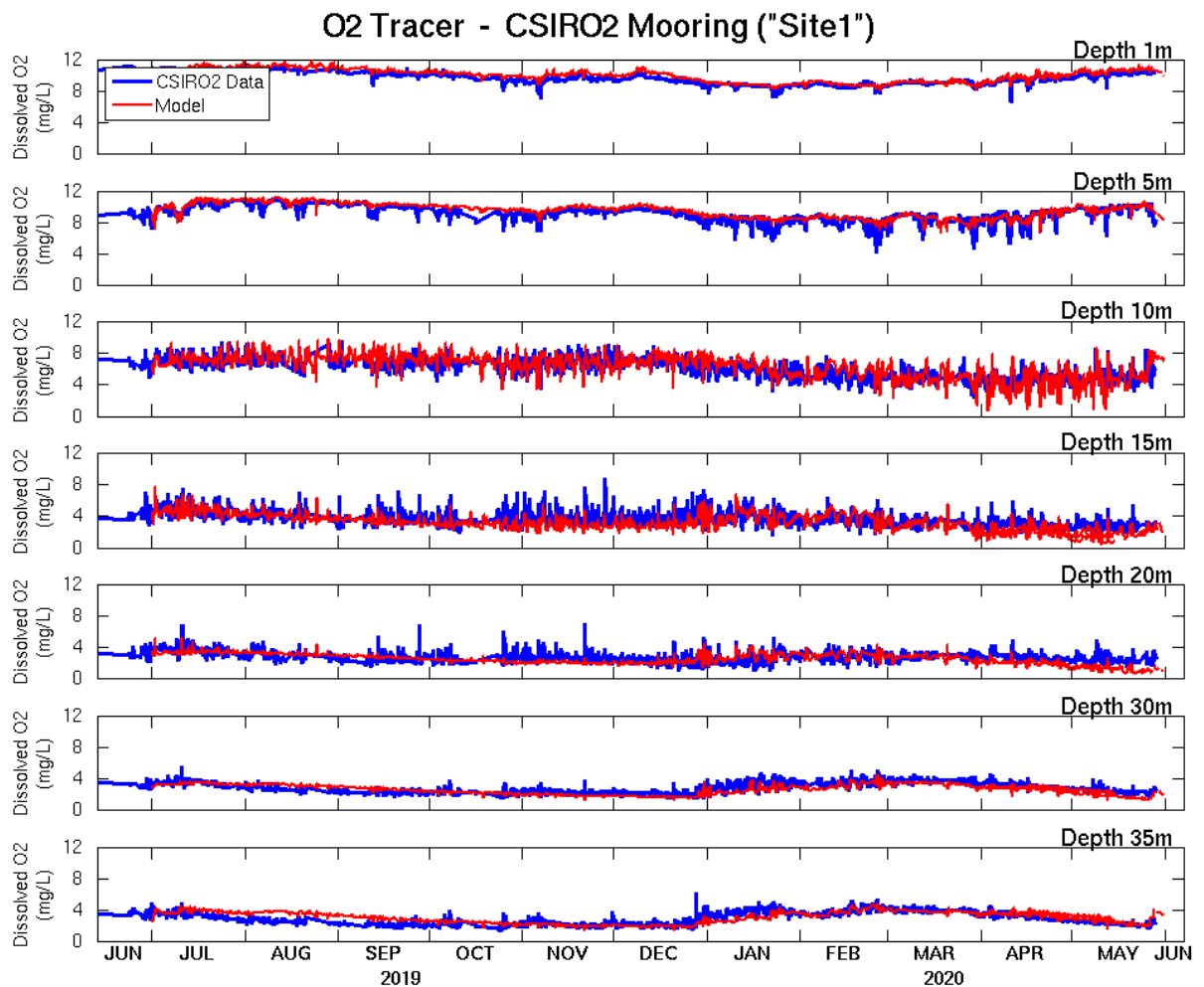
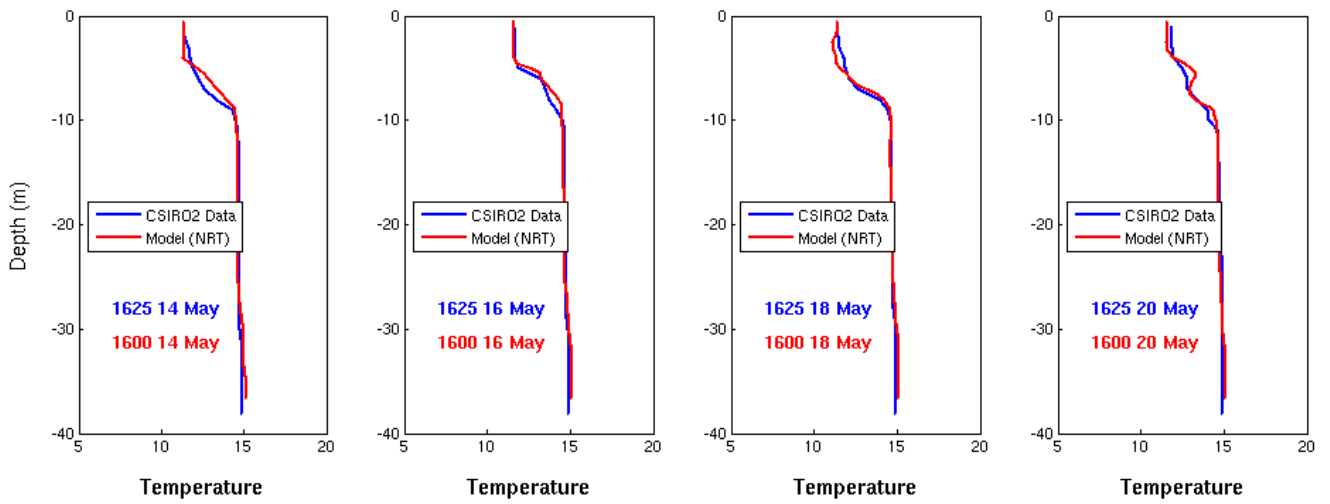


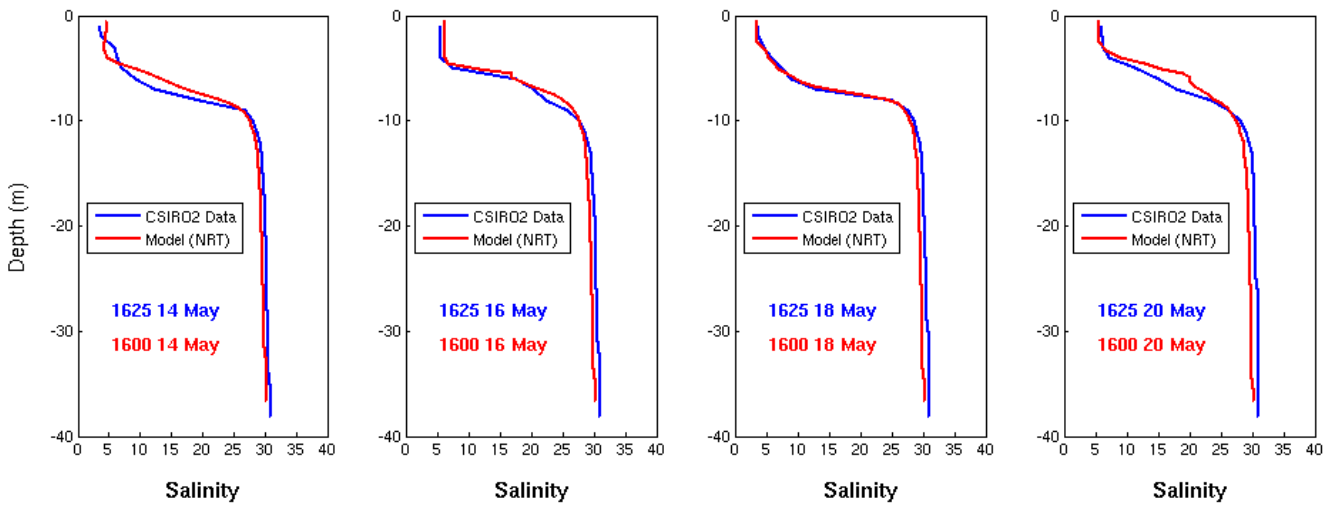
Figure 2.8: Time-series comparison of simulated Oxygen Tracer with observed Dissolved Oxygen, for 7 depths at Site#1 near the CSIRO2 mooring location.

The model simulation of the oxygen tracer agrees very well with observations (Figures 2.7, 2.8, 2.9), especially given the simplified model assumptions i.e. no explicit biological terms. This agreement includes the bottom recharge which initiates in late December 2019. Simulated oxygen tracer at the surface is very accurately reproduced (Figures 2.8, 2.9) and is in the main insensitive to the tuning of model mixing and estimated BOD. Simulated oxygen tracer in the mid and bottom waters is however more sensitive, but is nevertheless well reproduced, except perhaps for some fine-scale variability. The latter could be biologically generated, although there is also similar fine-scale variability within the salinity and temperature data that is not duplicated by the model (not unexpected).

## Water Temperature - CSIRO2 Mooring



## Salinity - CSIRO2 Mooring



## O2 Tracer - CSIRO2 Mooring

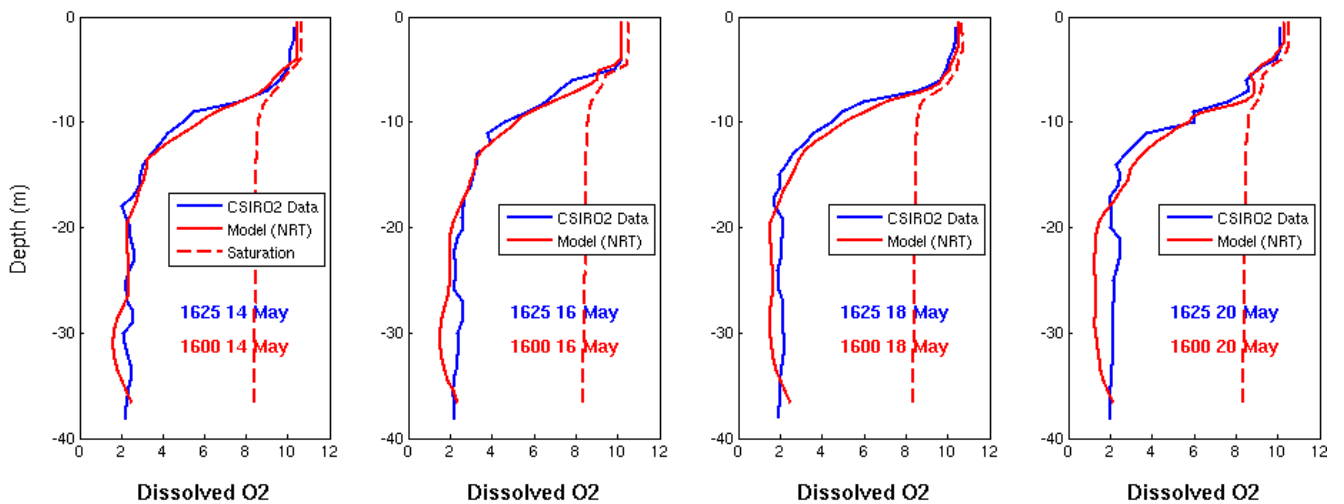


Figure 2.9: Profile comparisons for simulated temperature, salinity and oxygen tracer, with their observed counterparts at the CSIRO2 mooring location.

## 2.3 Harbour Recharge

Illustrations of simulated oceanic oxygen recharge, which occur when incoming ocean water cascades into the harbour from the entrance channel, are given in Figure 2.10. In winter/spring, the halocline is deep and incoming ocean water in the entrance channel mixes strongly with the thick surface layer of fresh water; this water is then of insufficient density to sink to the deeper parts of the harbour (upper plot). In summer/autumn the halocline is thinner and weaker, incoming ocean water passing through the entrance channel retains its density signature and this water is able to sink to greater depths (lower plot).

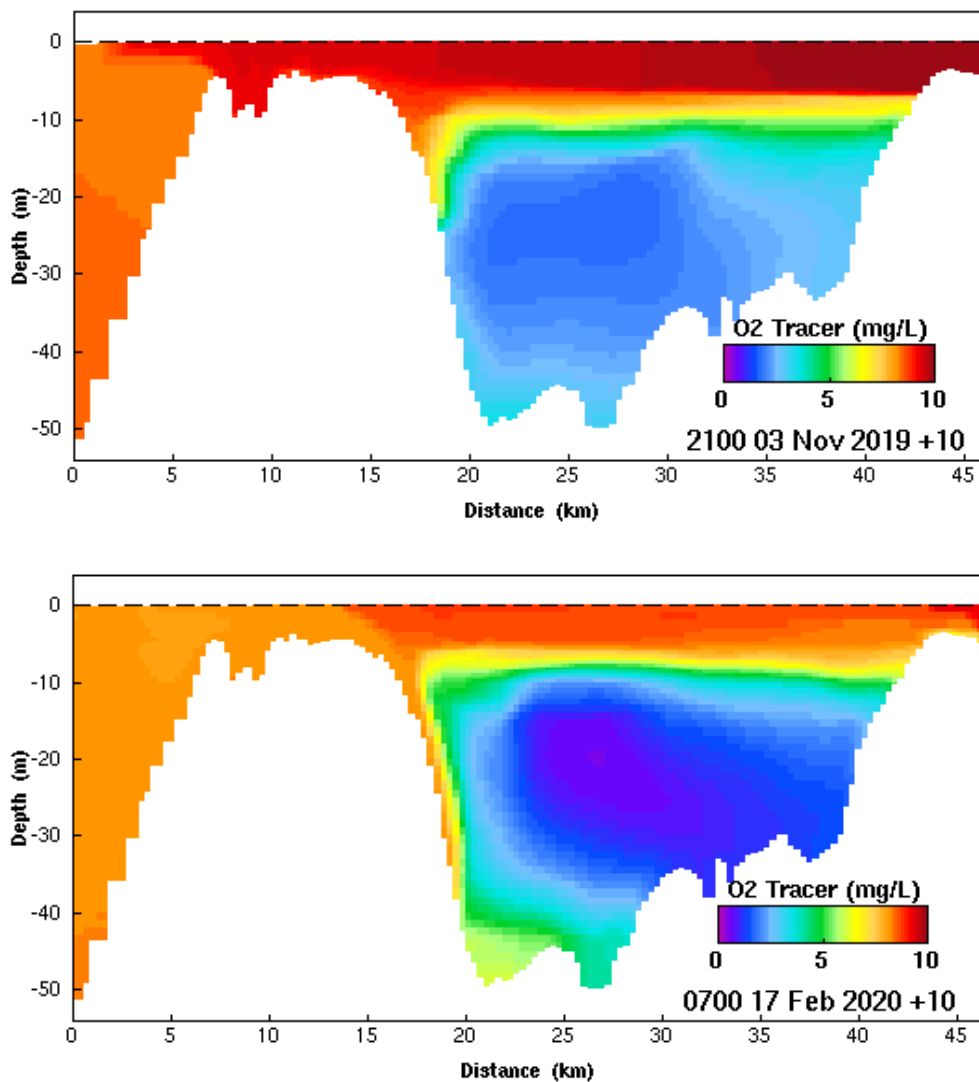


Figure 2.10: Examples of low oceanic recharge in winter/spring (left), and higher recharge in summer/autumn (right).

The predominance of recharge events occurring during the summer/autumn months is evidenced by the frequency of the modelled oxygen tracer spiking over that period at the CSIRO2 mooring location (Figure 2.7). We attribute these spikes to short recharge events (Figure 2.10 lower plot), however these spikes do not appear in the profiling mooring observations. We found that the spikes quickly diminished when the model output point was moved laterally from the CSIRO2 mooring location (Figures 2.8, bottom plot) and the model results then compared more closely with the observations. This finding suggests that the mooring is not located precisely at the mouth of the entrance channel

and is therefore not responding to the recharges to the same extent as the model [and there is a small mis-match in the actual bathymetry and that resolved by the model grid].

The possibility of low oxygenated mid-depth harbour water being upwelled to the surface, is of concern to fish farmers operating in the harbour. One such occurrence was in March 2018 and was described in a previous milestone report (Wild-Allen et al., 2019). On that occasion BoM forewarned stakeholders of an imminent storm system that would bring strong westerly winds to the west coast of Tasmania. Estimated river flows for the same period were low and the CSIRO forecast simulations of dissolved oxygen tracer indicated an intrusion of marine water and uplift of low oxygen mid water to the surface at the northwest end of the harbour. During the actual event, significant oscillations in the halocline were simulated along the length of the harbour and farmers noted strong fluctuations in water quality with a considerable increase in surface salinity and a drop in dissolved oxygen at leases closest to the harbour entrance. After the event, dissolved oxygen was reported to have increased by more than 50% in the bottom water.

Figures 2.11 to 2.15 illustrate a similar, but less intense, event taking place this year. On 27 February 2020 a strong north-westerly was present (Figure 2.11) at a time when the halocline was quite shallow (Figure 2.12) due to low river flows through the summer period. When the wind is aligned along the major axis of the harbour, it readily sets up oscillations in sea-level. Figure 2.13 displays the sea-level modelled for each end of the harbour, where differences of 20cm were predicted for 26-27 February. This would raise and lower the halocline at opposite ends of the harbour. Figure 2.14 shows the thin but uniform halocline prior to the event, followed by a strongly tilted halocline during the event. At this time high saline, low oxygenated water from mid-depths below the halocline, is able to upwell to the surface at the north-western end of the harbour (Figure 2.15 lower plot).

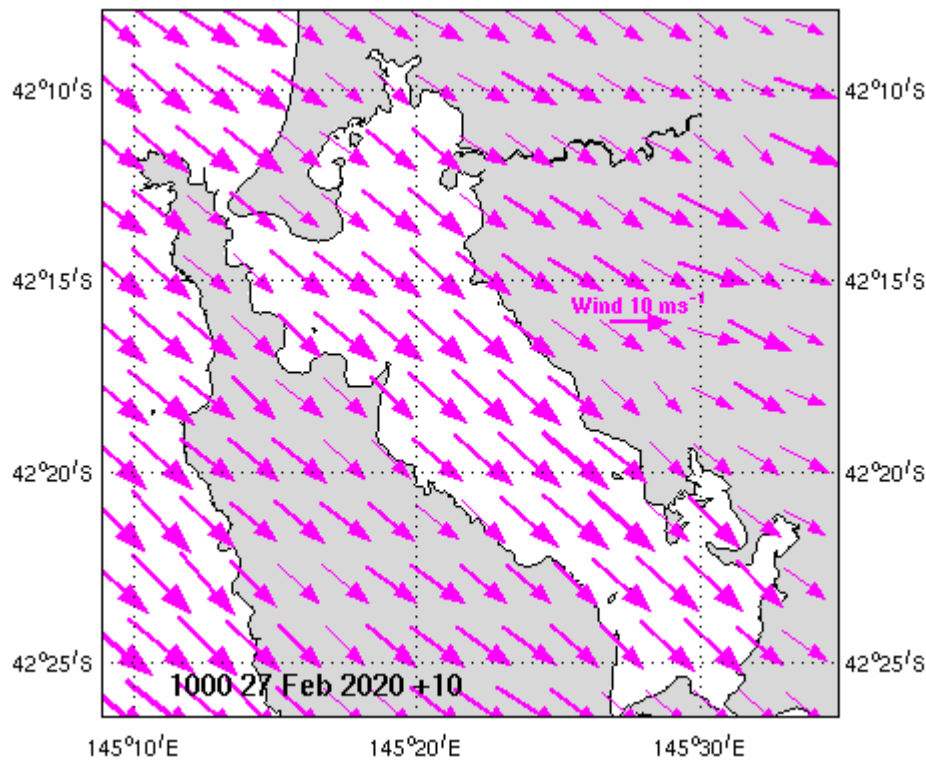


Figure 2.11: BoM ACCESS wind field of strong north-westerly winds across Macquarie Harbour on 27 Feb 2020.

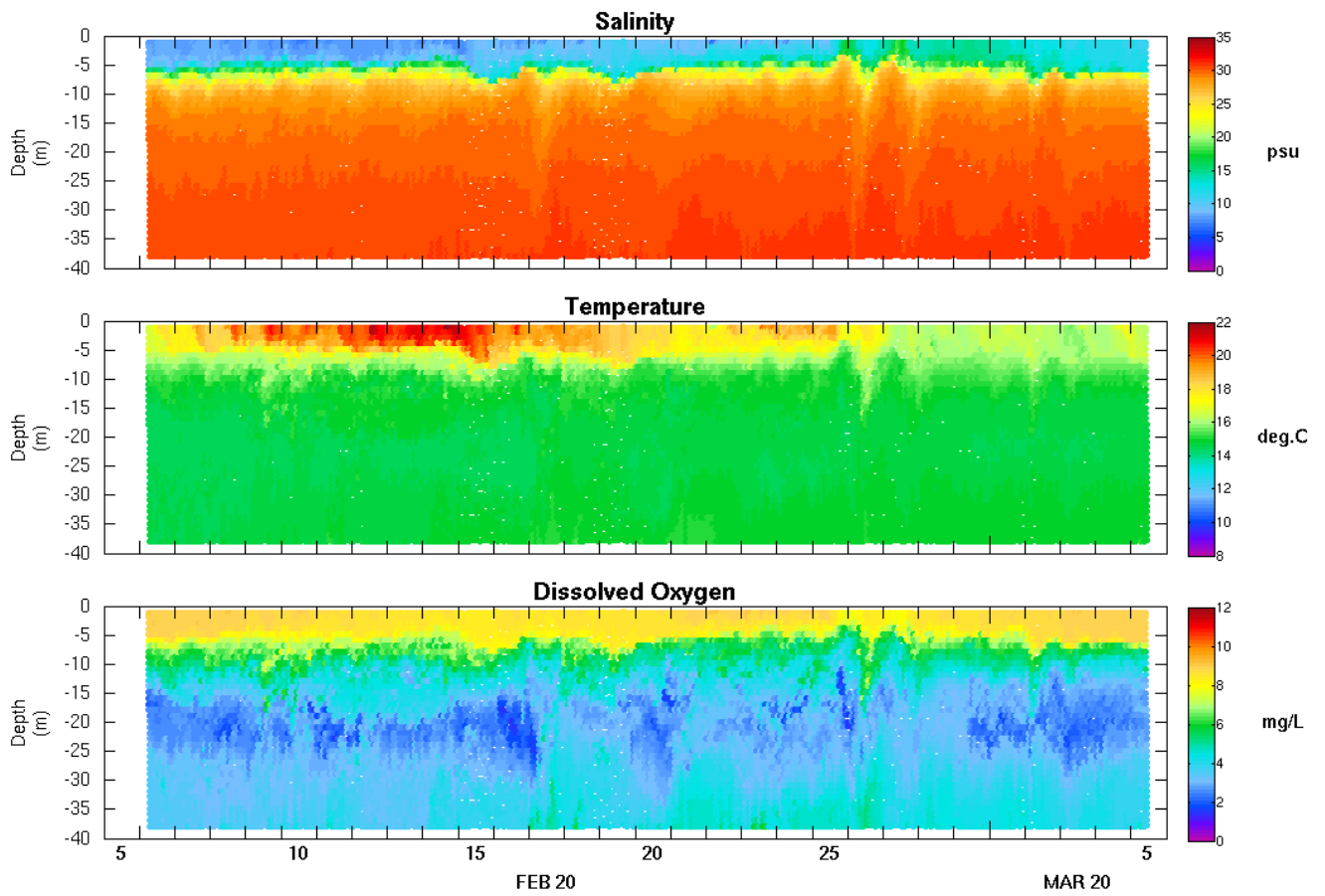


Figure 2.12: Time series of data from the profiling mooring for February 2020.

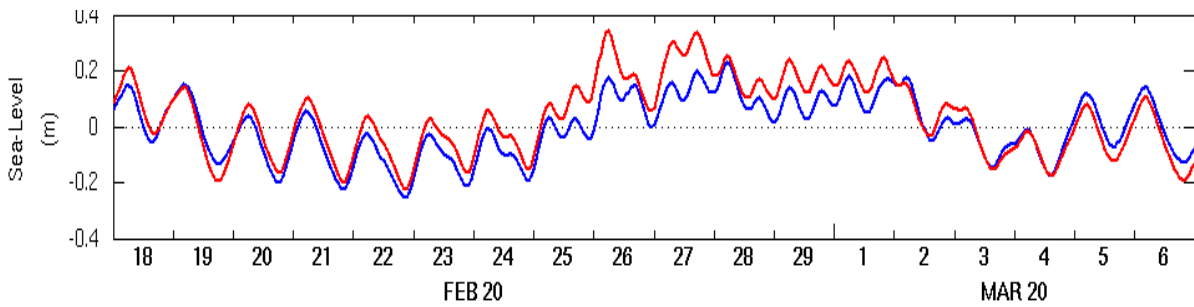


Figure 2.13: Time series of sea-level simulated for NW harbour (blue) and SE harbour (red) for Feb-Mar 2020.

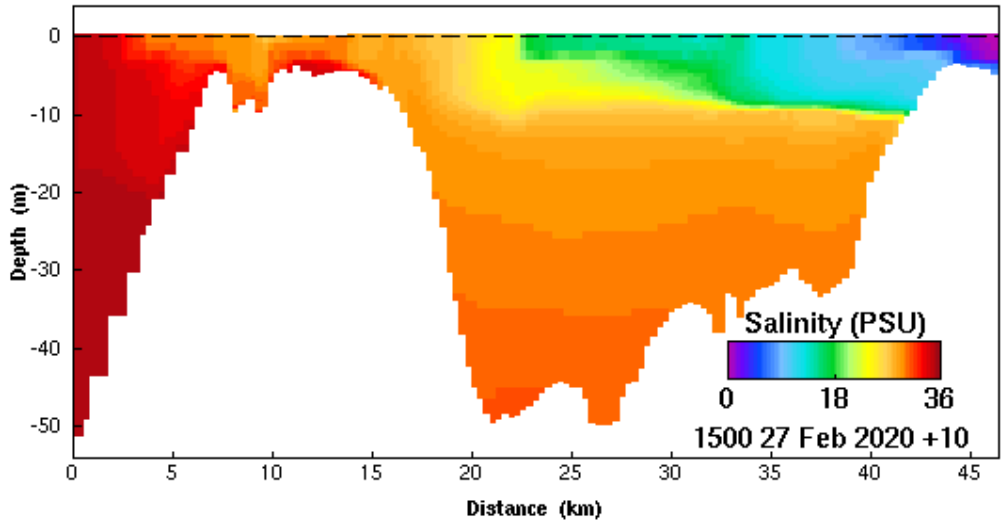
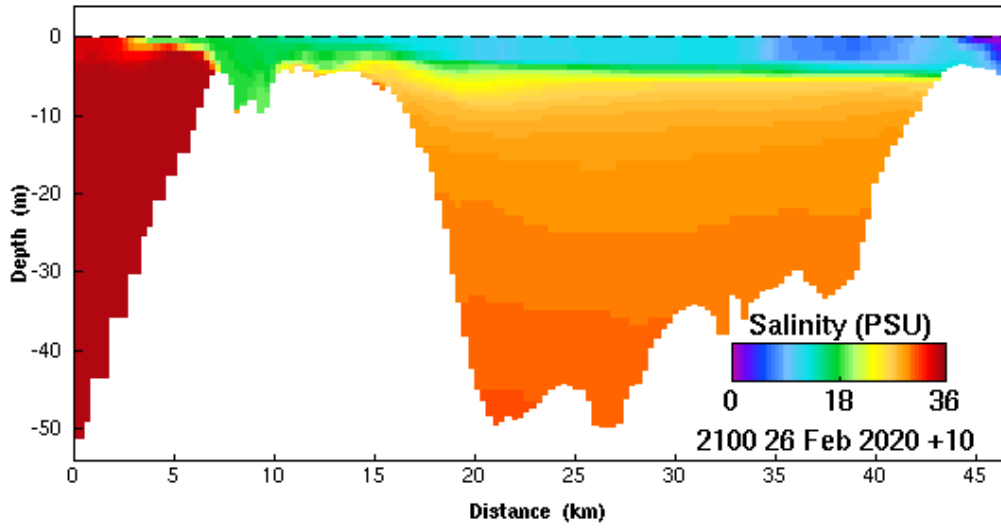


Figure 2.14: Vertical cross-sections of salinity along Macquarie Harbour, as simulated for 26 and 27 February 2020.

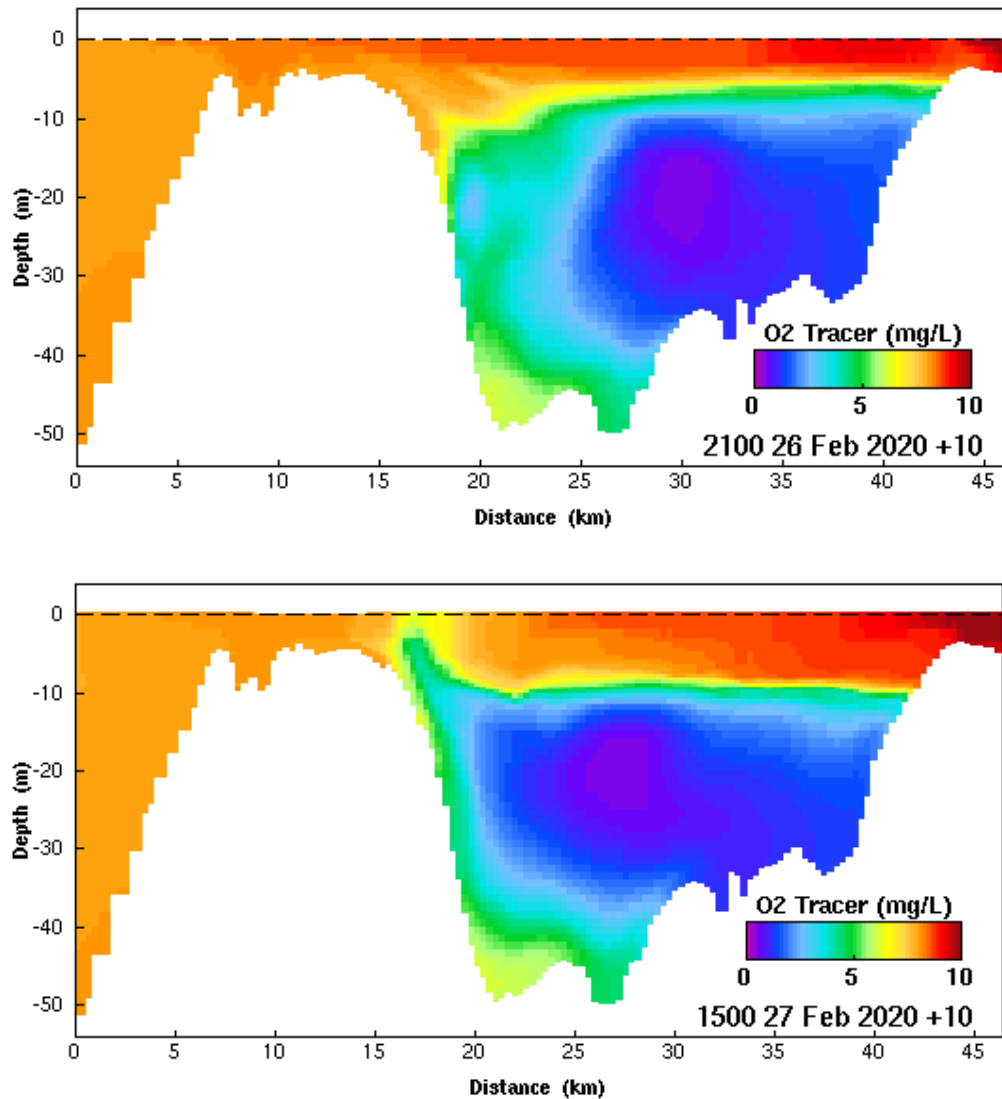


Figure 2.15: Vertical cross-sections of oxygen tracer along Macquarie Harbour, as simulated for 26 and 27 February 2020.

Events similar to those described above are observed to occur throughout the year whenever strong north-westerlies prevail. Although pronounced tilting of the halocline can occur for any of these, the strongest uplift of low-oxygen water to the surface appears to happen predominantly during the summer/autumn period when the halocline is at its thinnest. We also note that according to the model, these upwelling events do not necessarily coincide with an oxygen recharge.

In March 2018, BoM were able to forecast the storm  $\sim 10$  days in advance, and based on our understanding of how the system responds to this combination of predicted wind and seasonally low river flow, fish farmers were able to prepare for the anticipated conditions by moving stock and changing their harvest schedule to reduce stock in the water. At that time, the hydrodynamic and oxygen tracer model was only able to forecast 1-2 days ahead; now with the extended +10 day forecast capability we are better prepared to alert fish farmers of potential low oxygen events.

### 3 Visualisation Dashboard

The CSIRO Macquarie Harbour dashboard continues to operate and display the latest near real time and short term forecast model results at: <https://macqmodelling.csiro.au/> [user login: CSIRO; password: HitchikersGuide]. During the recent low oxygen event stakeholders were directed to the site where they were able to access and explore model products as required.

In recent months, work has focussed on implementing changes based on latest stakeholder feedback. This feedback indicated that complex interactive analysis tools were less useful to often time-poor user groups, who found highly curated, ‘at-a-glance’ information more helpful. As such, recent developments have been focussed largely on improving the usability of the system to target more commonly consumed materials, such updates include:

- Dashboard home page updated to an ‘application directory’ style splash page, with quick links to commonly accessed materials such as ‘Model quick-view’, ‘Meteorological data’, and observation data (Figure 3.1).
- Additional pre-loaded animations for model results
- Improved surface plot animation support within Data Explorer
- Updated user guide
- ‘Share map’ support added to Data Explorer
- Project Reports available as pdf’s

The system has also now been merged with the newer codebase for Storm Bay Modelling Information System prototype, which will enable additional feature updates to be pulled from Storm Bay, into the Macquarie Harbour Visualisation Dashboard without the need for additional development resources for Macquarie Harbour.

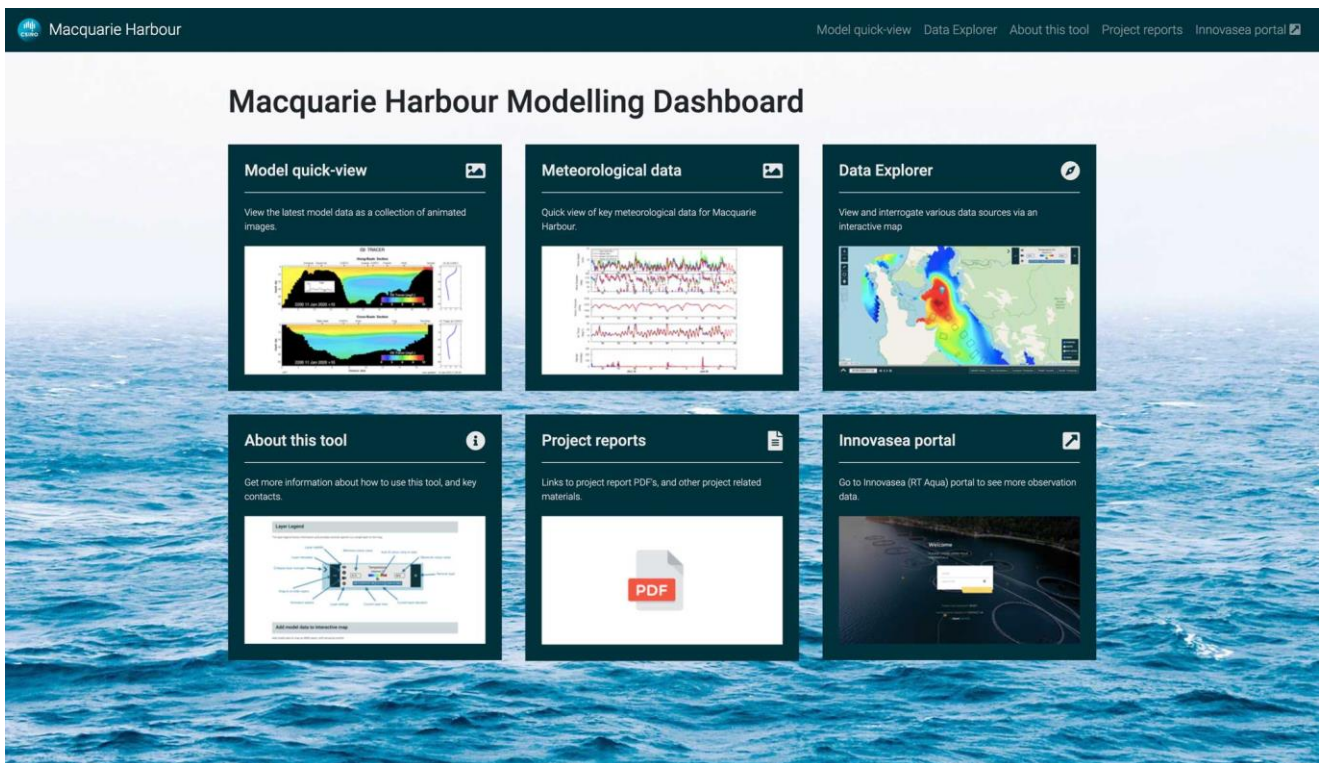


Figure 3.1: Macquarie Harbour modelling dashboard home page.

# 4 Biogeochemical Process Model

## 4.1 Summary of model implementation

The CSIRO Environmental Modelling Suite (EMS) biogeochemical model that simulates carbon, nitrogen, phosphorous and oxygen in pelagic and surface sediment layers has been implemented in Macquarie Harbour (Figure 4.1). The mixing and transport of biogeochemical substances is computed using an offline transport model forced with hourly 3D hydrodynamic model output for the years 2017-2018. Biogeochemical processes resolved by the model include phyto- and zoo-plankton growth and mortality, detrital remineralisation from labile to refractory particulate and dissolved forms, nitrification, denitrification, annamox, air-sea gas exchange for oxygen and carbon dioxide, benthic macroalgae and microphytobenthos. Organic particles sink and are resuspended similar to inorganic sediments and the in-water light field (for accurate calculation of photosynthetic growth) is simulated by a spectrally resolved optical model.

Dissolved nutrients, oxygen and particulate organic matter enter the harbour from the King and Queen rivers, the upper and lower Gordon river catchment and Birches Inlet. In the absence of operational flow gauges on these river systems (particularly in the lower reaches) flow is estimated from rainfall and catchment area [note that this simple approach does not account for variable rainfall or water retention across the catchment, for example in vegetation and soil, and thus could be highly inaccurate at any given time]. Riverine loads are estimated from a synthesis of EPA data, Bell et al., 2018, Knight et al 2015 (Cawthron Report) and observations made by CSIRO in summer 2018.

Anthropogenic nutrients and particulate organic matter enter the harbour from the Strahan wastewater treatment plant and fish farms operating throughout the harbour; monthly data were obtained from Bell et al., (2018) and the Department of Primary Industry, Parks, Wildlife and the Environment, Marine Farming Branch. In the model, the lease specific monthly mean fish farm nutrient load was assumed to be immediately dispersed throughout the model grid cell in which the farm is located, from the surface to a depth of 10 m. Oxygen utilised by farmed salmon respiration was estimated as 50mg O<sub>2</sub> respired per kg fish per hour (EIS 2011 report) with spatial and temporal distribution proportional to feed input and vertical assignment from the surface to a maximum depth of 15 m.

The biogeochemical transport model is very highly resolved (250m spatial resolution, 65 vertical layers) and runs at around 500:1 (500 simulation days to 1 elapsed day) optimised over 24 window partitions on the CSIRO high performance computing infrastructure. A full description of the biogeochemical model, it's parameterisation, forcing and assessment against observations is available in the 4<sup>th</sup> project milestone report (Wild-Allen et al., 2020).

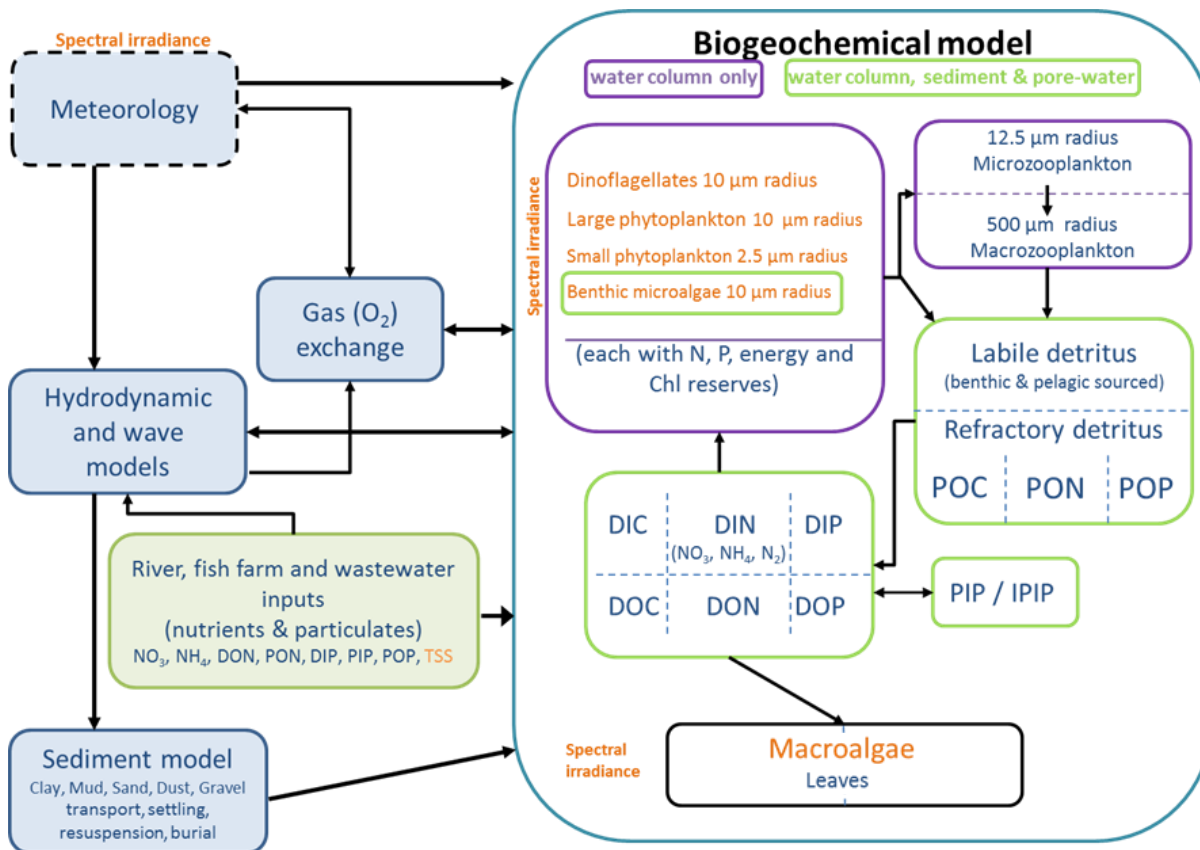


Figure 4.1: Schematic diagram of the CSIRO EMS biogeochemical model components and links.

## 4.2 Summary of model skill compared to observations

The accuracy of the model was assessed by comparison of simulated conditions with observations at the CSIRO1 profiling mooring, 12 continuous logger sites and 32 monitoring locations (Figures 4.2). Moored data included temperature, salinity and dissolved oxygen; monitoring data included temperature, salinity, dissolved oxygen, oxygen saturation, carbon (organic and dissolved organic), nitrogen (nitrate, ammonium, dissolved organic, total, total Kjeldahl, total soluble Kjeldahl), phosphorous (total, dissolved inorganic), chlorophyll, secchi depth and total suspended solids. Full details of the model assessment against observations are included in the previous milestone report (Wild-Allen et al., 2020) and are summarised here including example plots for dissolved oxygen; additional example plots for temperature, salinity, nitrogen, phosphorous, chlorophyll and secchi disk depth are included in the Appendix.

The skill assessment showed that the model accurately simulated the observed vertical structure and seasonal cycle of temperature and salinity throughout the harbour, albeit with slightly less skill at the mouth of the King river, likely due to inaccuracies in the estimates of river flow and river temperature.

The model reproduced the observed vertical gradients in nitrogen and phosphorous and some seasonal variability, although sparse temporal resolution of observations at several stations precluded accurate assessment. Simulated and observed dissolved inorganic nitrogen comprised mostly of nitrate. In surface waters, dissolved inorganic phosphorous concentrations were generally very low with the potential to limit autotrophic phytoplankton growth. The observed spatial gradients and

seasonal variability in secchi depth were well reproduced by the model, with clearer conditions generally present during summer and towards the harbour entrance. The model generally simulated peak chlorophyll concentrations at depth and seasonal variation was consistent with observations in surface waters; additional observations and analysis would provide greater insight and more confident resolution of simulated phytoplankton groups. The model performed best in the main harbour and world heritage area; the model was less accurate at stations influenced by the Gordon and King river systems likely due to inaccurate estimates of river flow, nutrient and particulate loads.

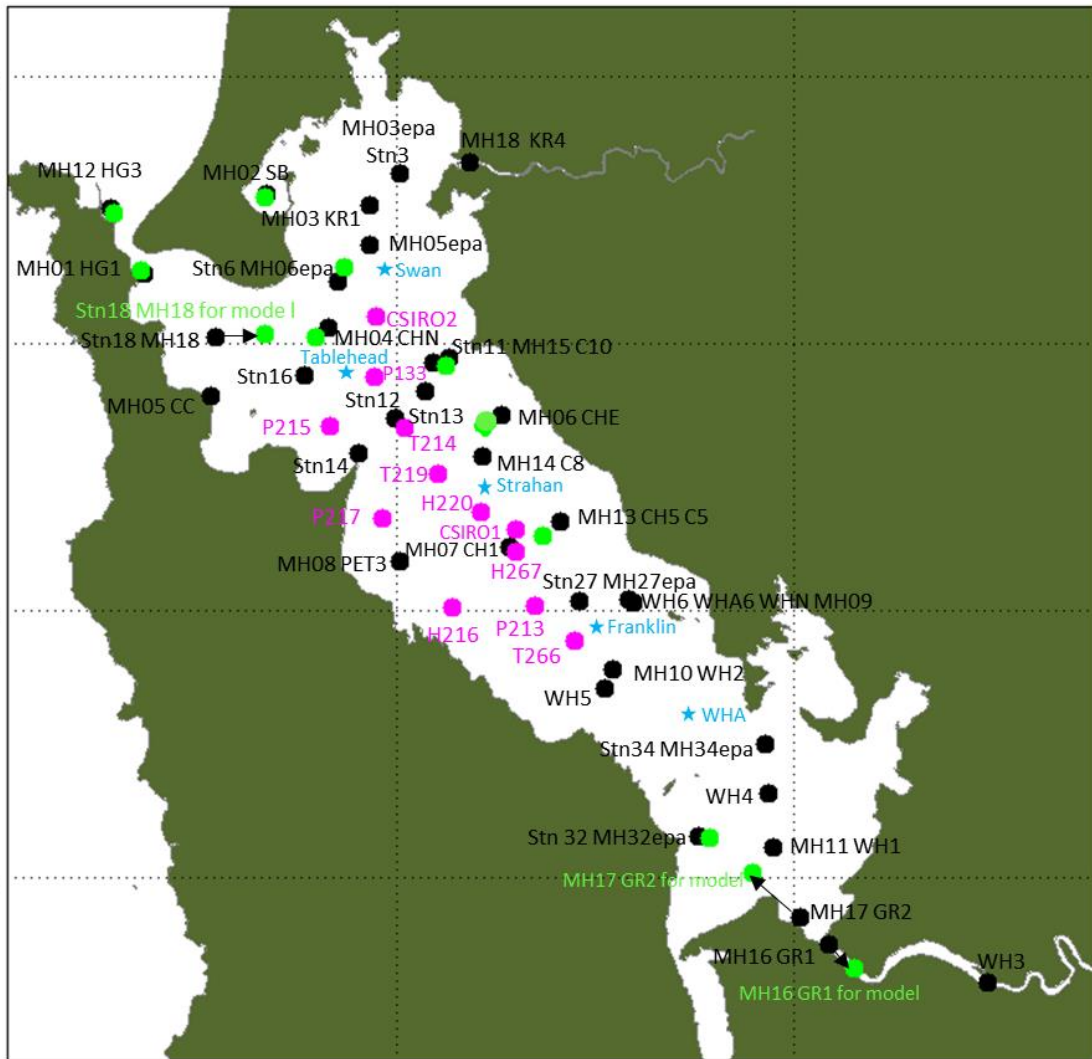


Figure 4.2 Site map for water quality observations and model comparison points in Macquarie Harbour. Black sites are World Heritage Area (WHA), BEMP and EPA sites used to validate against model outputs (all equivalent names are listed for each site location). Green are black sites where some sites have been relocated to a more suitable depth/location in the model grid. The model results and comparison for the sites GR1 GR2 and MH18 must be viewed in this context. Pink sites are farm site loggers. Blue star sites are IMAS and EPA mooring string locations.

Dissolved oxygen (Figure 4.5) was very well simulated at monitoring stations in the main harbour, the northern basin, the world heritage area and the Gordon river estuary; model accuracy was slightly lower at the mouth of the King river and the harbour entrance, likely due to inaccurate estimates of river flow and river oxygen content, and a slight mis-match in simulated and observed tidal phase at the highly variable harbour entrance. Comparison of the model with continuous oxygen loggers showed accurate representation of surface waters, however simulated intrusions of marine water

frequently had insufficient density to displace bottom waters. This is a limitation of the current model that resulted in a positive bias in simulated dissolved oxygen at 15 – 20 m at several stations in the mid-harbour.

Mean Willmott skill metrics are shown in Figures 4.3 and 4.4 and detailed in Table 4.1. Overall the model has a high degree of skill (>60% at the majority of stations; >50% for the majority of substances) in reproducing the observed range of water properties for all times and depths, particularly in the main harbour, northern basin and world heritage area. Simulated properties that have not been validated against observations (e.g. plankton types, denitrification and other microbial remineralisation rates) should only be treated as a hypothesis, albeit consistent with the assessed water properties.

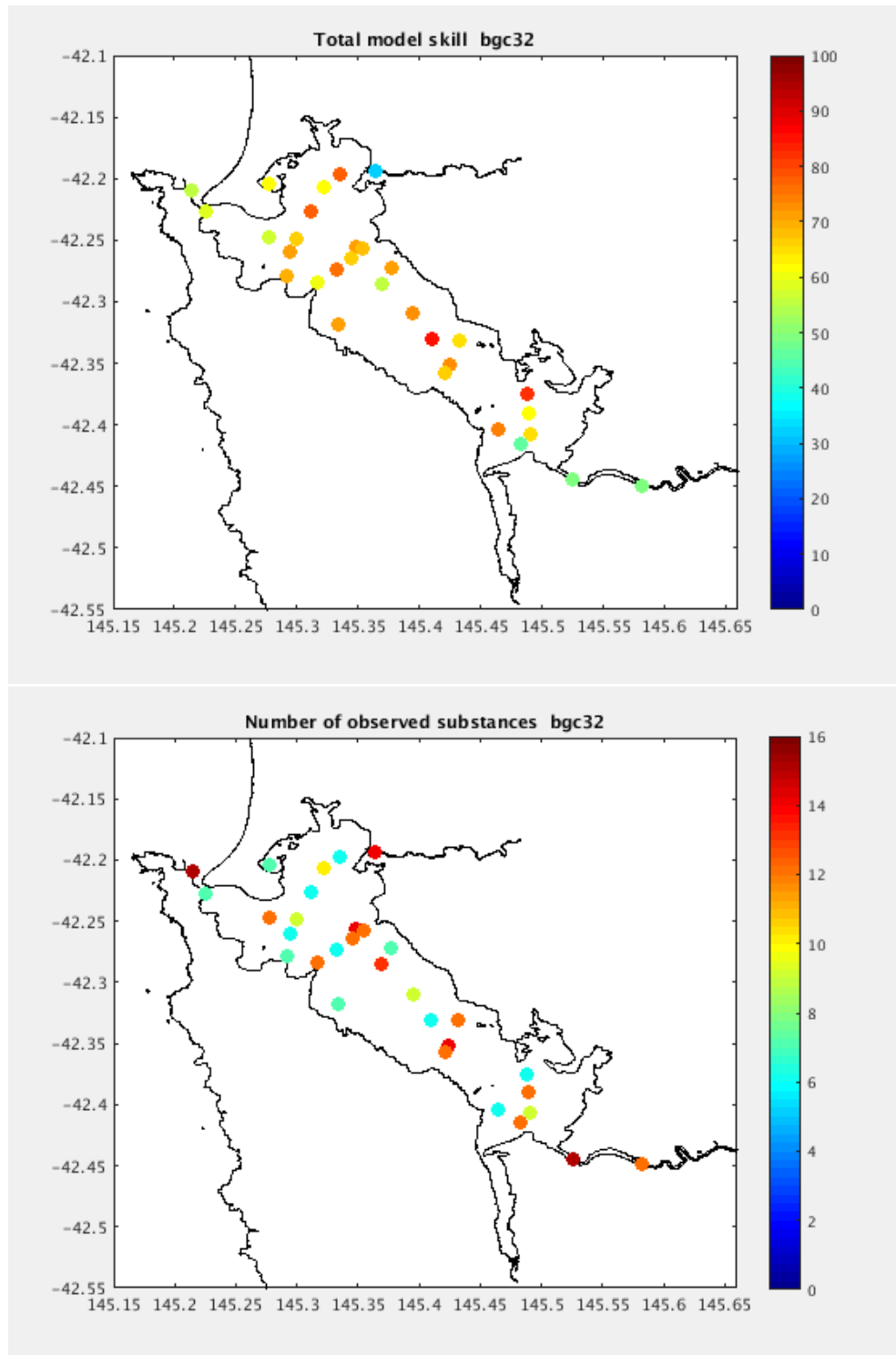


Figure 4.3 Mean model vs observation Willmott skill score (in %; top) and number of observed water properties considered in the analysis (bottom) at 32 monitoring stations in Macquarie Harbour [100% = perfect model skill; 0% = no model skill].

Table 4.1 Mean model vs observation Willmott skill score in % by site (left) and by water property (right).

Mac Harbour Willmott Skill			
Area	Site	Mean Skill %	Number of Observed Substances
Marine Influence	MH12	55	15
	MH01	59	7
	STN18	57	12
	MH05	70	7
	STN16	71	6
	MH04	66	9
	Northern Basin	STN6	78
MH03		62	10
MH02		61	7
STN3		77	6
King River	MH18	33	14
Mid Harbour	STN11	68	12
	MH15	71	14
	STN12	66	12
	STN13	75	6
	STN14	61	12
	MH08	70	7
	MH14	56	13
	MH06	72	7
	MH13	73	9
	STN27	86	6
	World Heritage Area	WHA6	65
MH09		73	9
MH10		73	14
WHA5		66	12
STN34		82	6
WHA4		61	12
STN32		75	6
MH11		65	9
Gordon River	MH17	46	12
	MH16	48	15
	WHA3	49	12

Substance	Mean Skill %	Number of Sites
Temperature	95	32
Salinity	91	32
Oxygen	84	32
Oxygen Saturation	72	32
Organic Carbon	61	20
Dissolved Organic Carbon	58	5
Total Nitrogen	58	15
Total Kjeldahl Nitrogen	44	15
Total Soluble Kjeldahl Nitrogen	54	12
Dissolved Organic Nitrogen	56	12
Nitrate	70	15
Ammonium	25	25
Total Phosphorous	32	8
Dissolved Inorganic Phosphorous	44	8
Chlorophyll-a	37	17
Secchi Depth	65	16
Total Suspended Solids	34	20

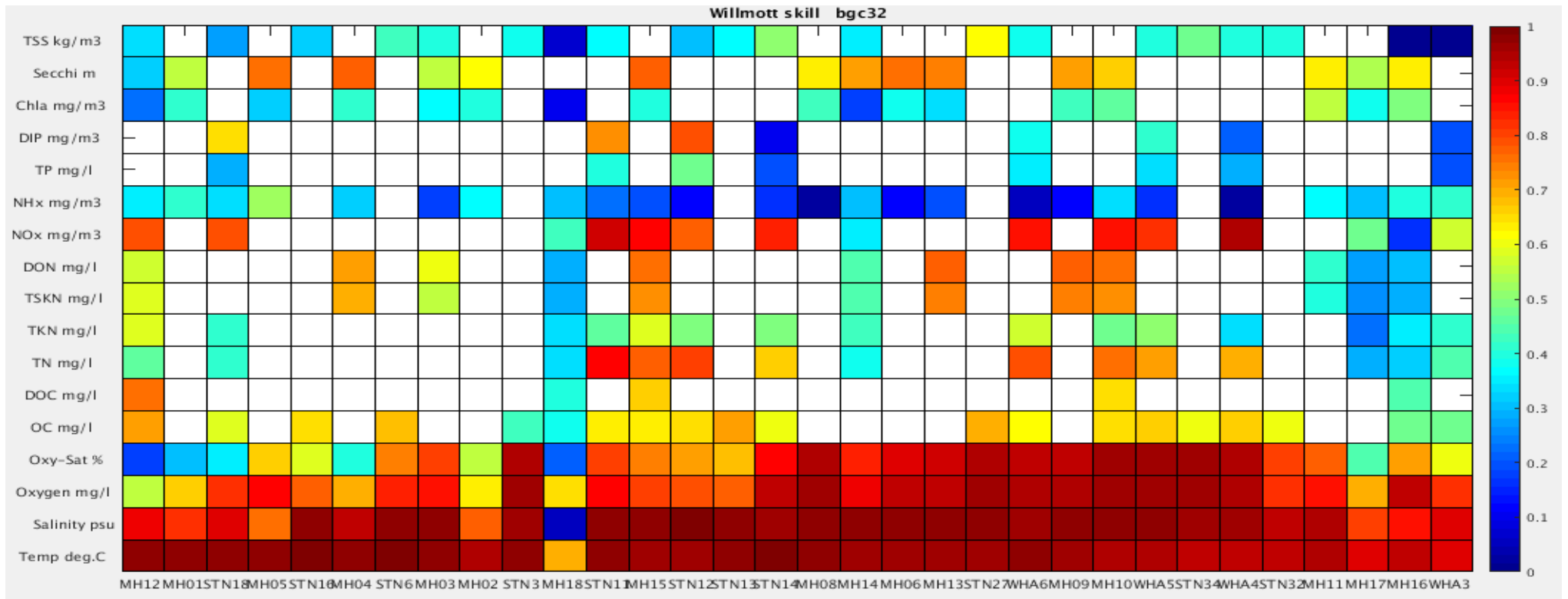


Figure 4.4 Model vs observation Willmott skill score obtained from 2 years of data, often across multiple depths for each station and water property. White squares indicate no observation of that property; 1 = perfect model skill; 0 = poor model skill.

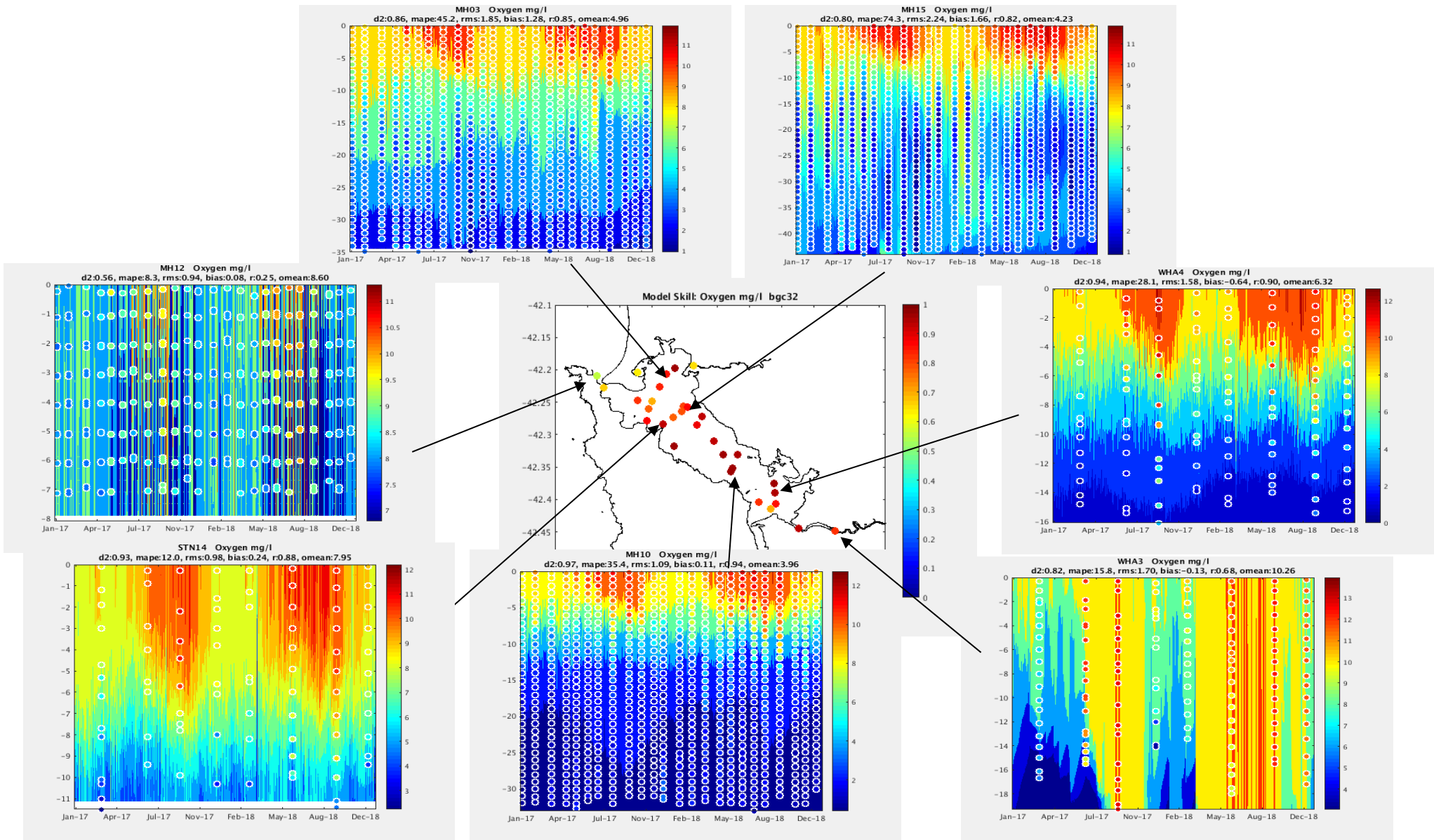


Figure 4.5 Simulated (background) and observed (circles) vertical evolution of dissolved oxygen during 2017-2018 at sites throughout Macquarie Harbour. Skill metrics summarised in subplot titles; Willmott score shown in centre image (1 = best, 0 = poor fit).

## 4.3 Simulated seasonal cycle

### 4.3.1 River flow

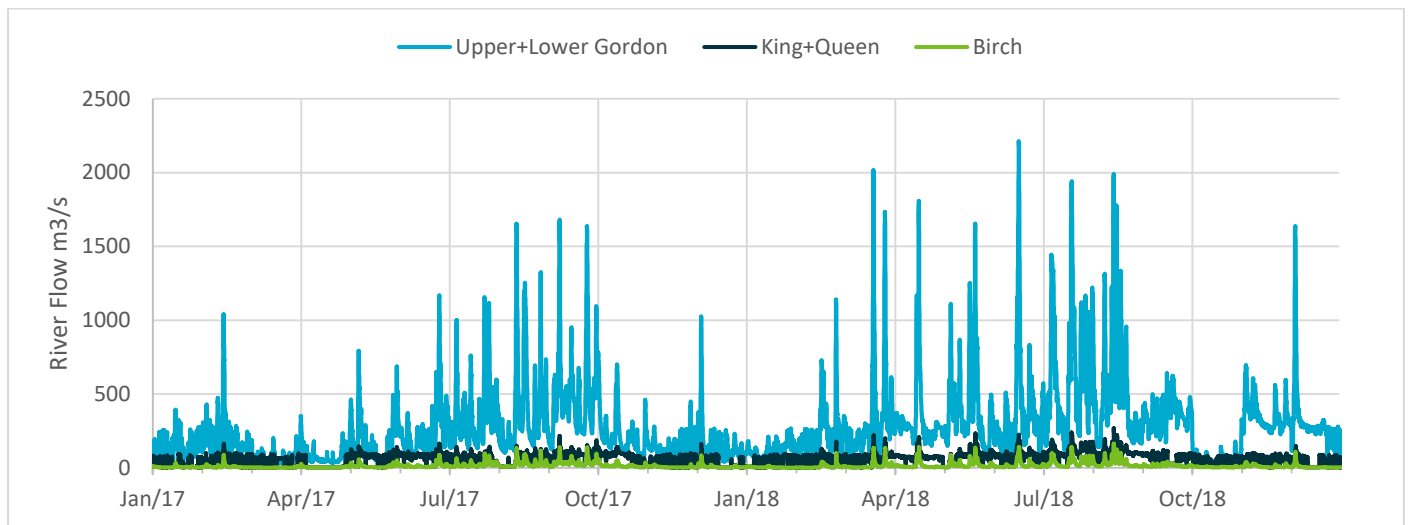


Figure 4.6 Estimated river flow from the 3 main river catchments entering Macquarie Harbour used in the model in 2017 and 2018.

The model includes three rivers contributing freshwater flow: King + Queen, upper + lower Gordon and Birches Inlet (Figure 4.6 & Table 4.2). In the absence of operational flow gauges on these river systems (particularly in the lower reaches) flow was estimated from rainfall and catchment area [note that this simple approach does not account for variable rainfall or water retention across the catchment, for example in vegetation and soil, and thus could be highly inaccurate at any given time].

Table 4.2 Estimated mean annual river flow in  $\text{m}^3\text{s}^{-1}$

River System	2017	2018	Mean
Upper+Lower Gordon	222.2	341.4	281.0
King+Queen	46.9	66.7	56.8
Birches Inlet	12.7	15.3	14.0

The primary source of fresh-water for the harbour is from the Gordon river catchment. For the simulated period there was less fresh-water inflow to the harbour in 2017 compared to 2018 (Table 4.2). In particular, autumn and winter 2018 were wetter than in 2017, whilst spring 2018 experience a month of unusually low river flow (Figure 4.6).

### 4.3.2 Temperature and salinity

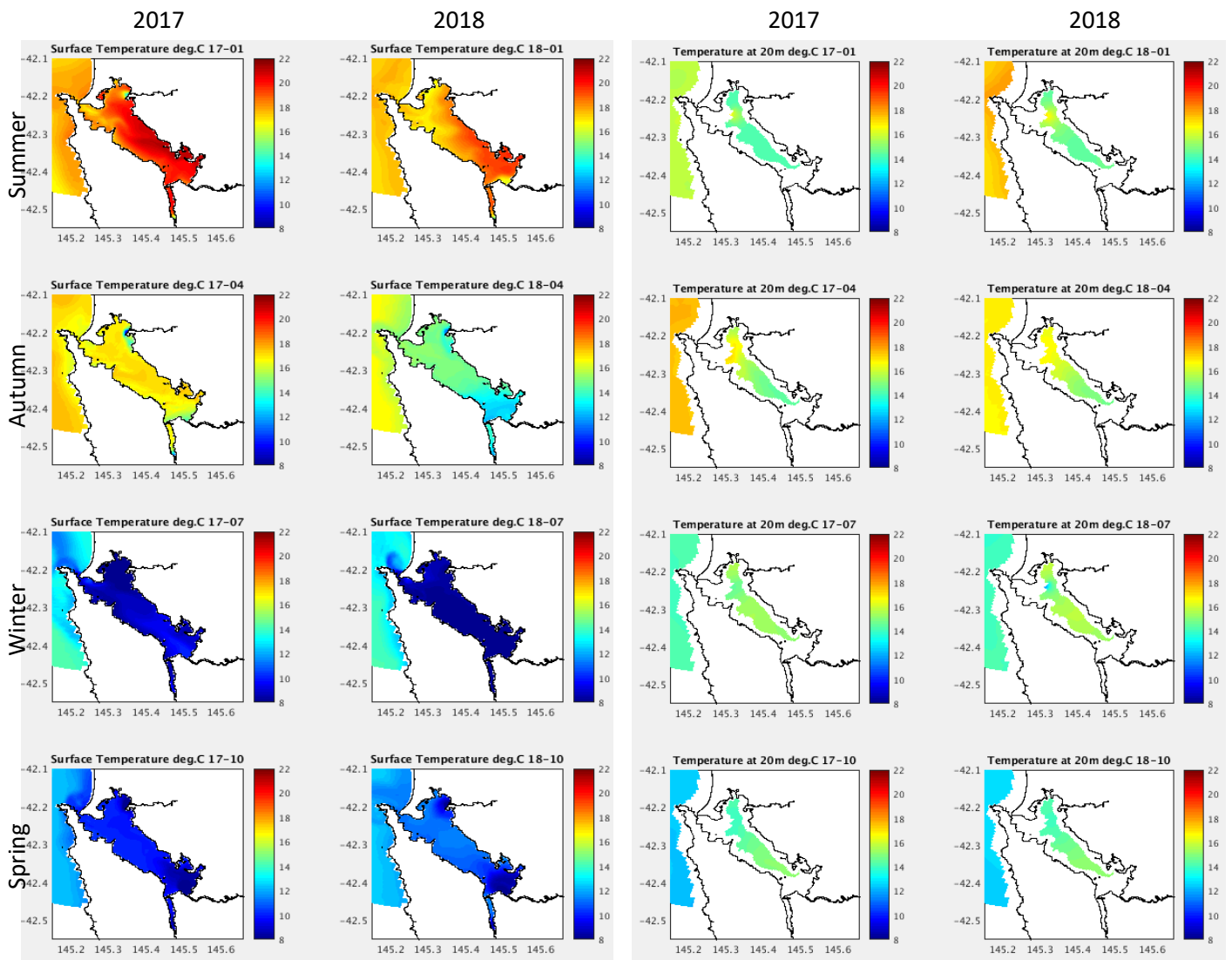


Figure 4.7 Surface (left) and 20m (right) simulated monthly mean temperature in summer (Jan), autumn (Apr), winter (Jul) and spring (Oct) 2017 and 2018 (by row from top to bottom).

Persistent thermal and salinity stratification in Macquarie Harbour constrains fluctuations in water properties over seasonal scales, whilst event scale storms and floods can perturb the system in any season. Monthly mean surface temperature ranges from around 20°C in summer to around 8°C in winter, modulated by river inflow and seasonal atmospheric heat flux (Figure 4.7 & 4.8); at depth temperature remains at around 15°C all year. Monthly mean surface salinity ranges from around 20 PSU in summer/autumn to less than 5 PSU in winter and spring modulated by river flow (Figure 4.9 & 4.10); at depth salinity remains at about 30 PSU all year.

The seasonal cycle in temperature and salinity results in a persistent temperature inversion in winter and spring, which is maintained by the strong salinity driven density gradient [note that low river flow in winter or spring could allow vertical mixing of the water column to re-establish a stable thermal structure]. Comparing 2017 and 2018, higher river flow in spring 2017 and autumn 2018 resulted in a stronger vertical density gradient, thicker fresh-water surface layer and more stable water column (Figure 4.9).

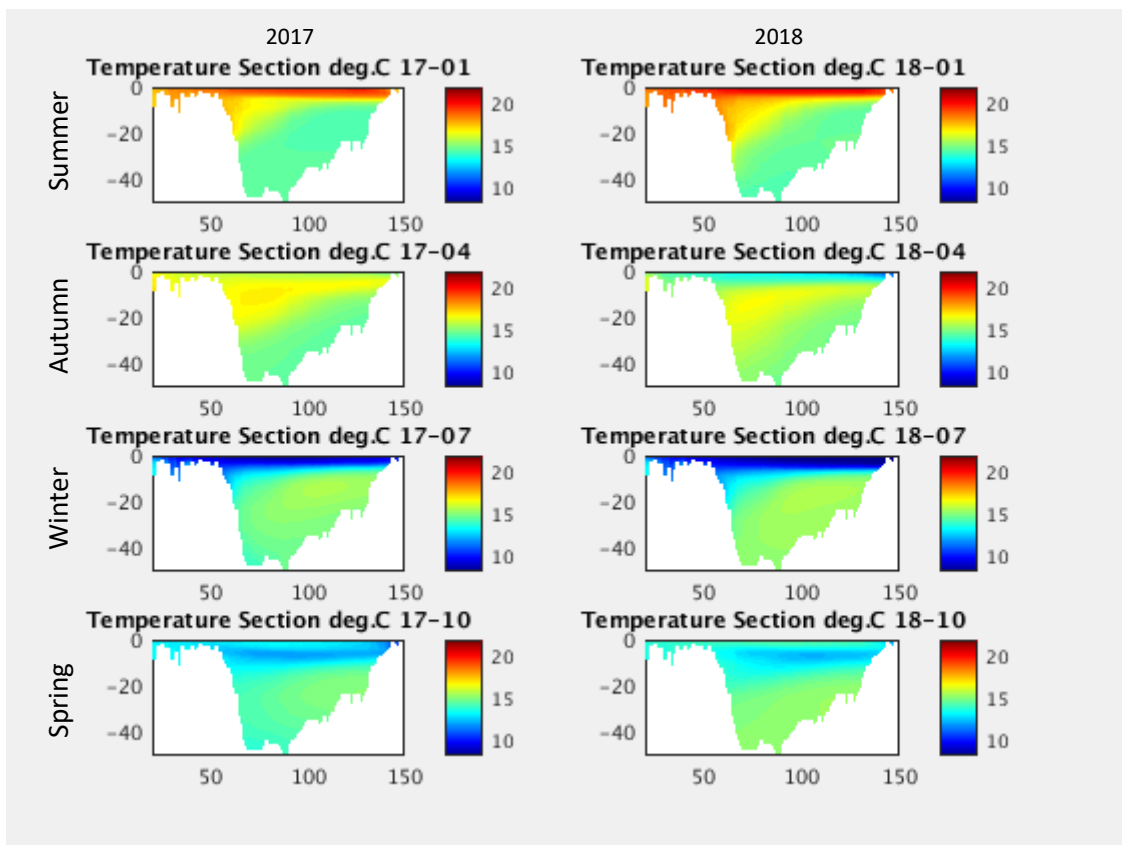


Figure 4.8 Simulated monthly mean temperature in summer (Jan), autumn (Apr), winter (Jul) and spring (Oct) 2017 and 2018.

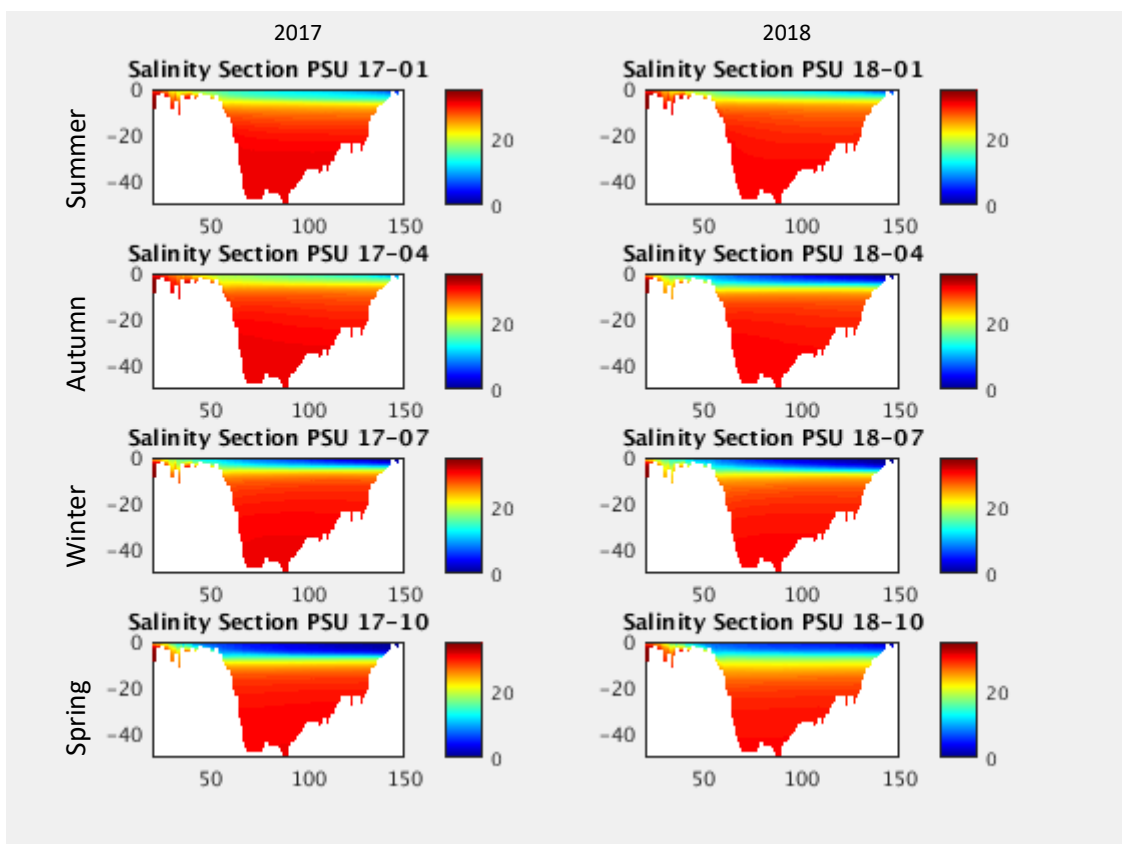


Figure 4.9 Simulated monthly mean salinity in summer (Jan), autumn (Apr), winter (Jul) and spring (Oct) 2017 and 2018.

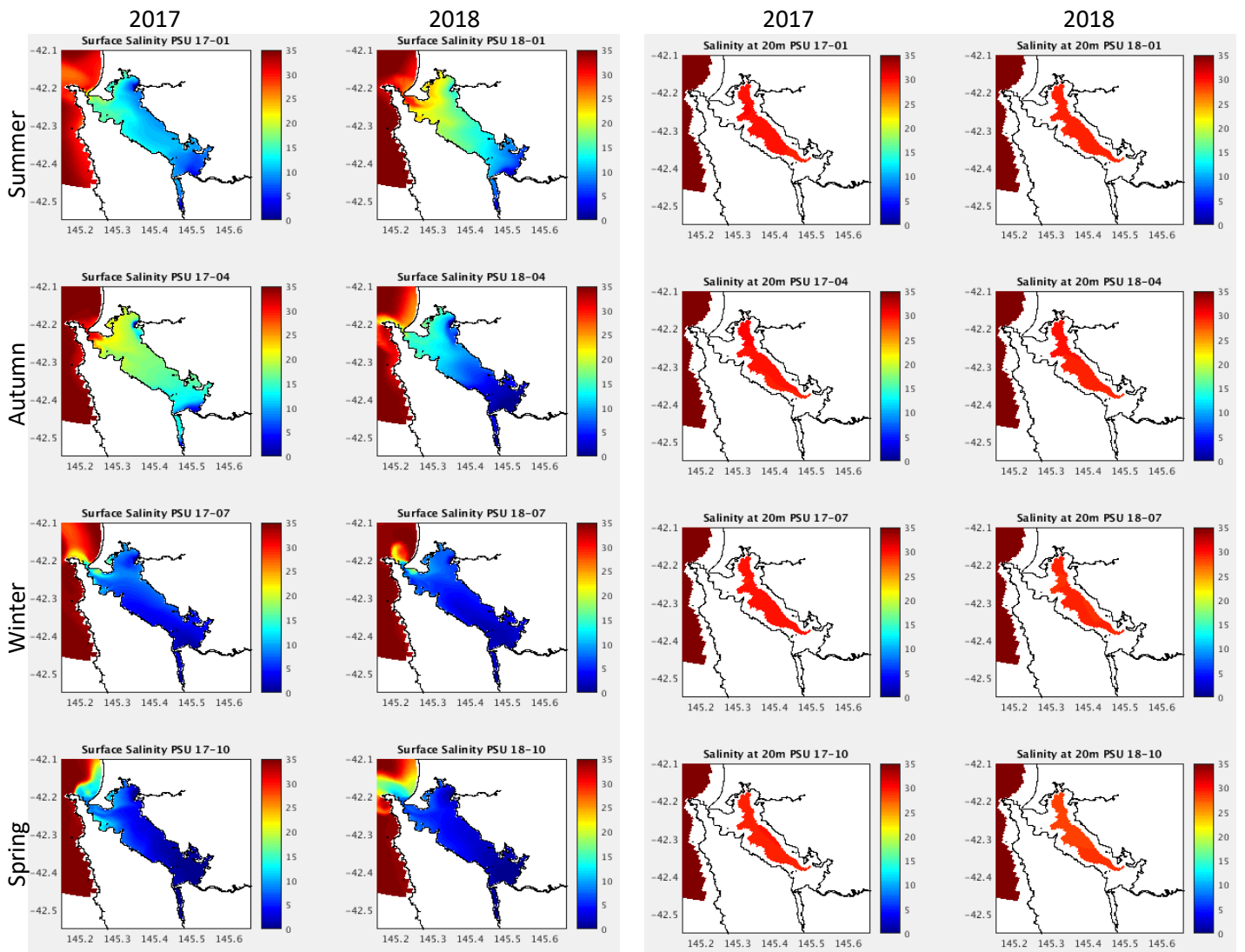


Figure 4.10 Surface (left) and 20m (right) simulated monthly mean salinity in summer (Jan), autumn (Apr), winter (Jul) and spring (Oct) 2017 and 2018 (by row from top to bottom).

### 4.3.3 Nutrients, secchi depth and chlorophyll

Simulated dissolved inorganic nitrogen and phosphorous showed similar spatial and temporal distributions in the harbour. Concentrations were generally low in surface waters and elevated at depth all year (Figures 4.11 – 4.14). Monthly mean surface nitrogen was slightly higher in winter and spring, with locally elevated concentrations at farm lease locations. Monthly mean surface phosphorous concentrations were very low and the ratio of nitrogen to phosphorous in surface waters was very high (Figure 4.15), suggesting a deficit in phosphorous supply for phytoplankton growth (c.f. Redfield 16 mol N : 1 mol P). The potential for phosphorous limitation of phytoplankton growth was first raised by the high resolution spatial nutrient survey conducted in 2017 (Wild-Allen et al., 2017) and has been further explored with a phosphate addition process study (this report - Section 5.4). Simulated nutrient concentrations at depth were generally higher in 2017 and lower in 2018, particularly for nitrogen in winter and spring; this may be due to a corresponding reduction in nitrogen input at fish farm lease sites in 2018 (Table 4.3).

Table 4.3 Annual cumulative fish farm nutrient load into Macquarie Harbour.

Year	Total Nitrogen tN/y	Total Phosphorous tP/y
2016	995	145
2017	975	142
2018	544	79

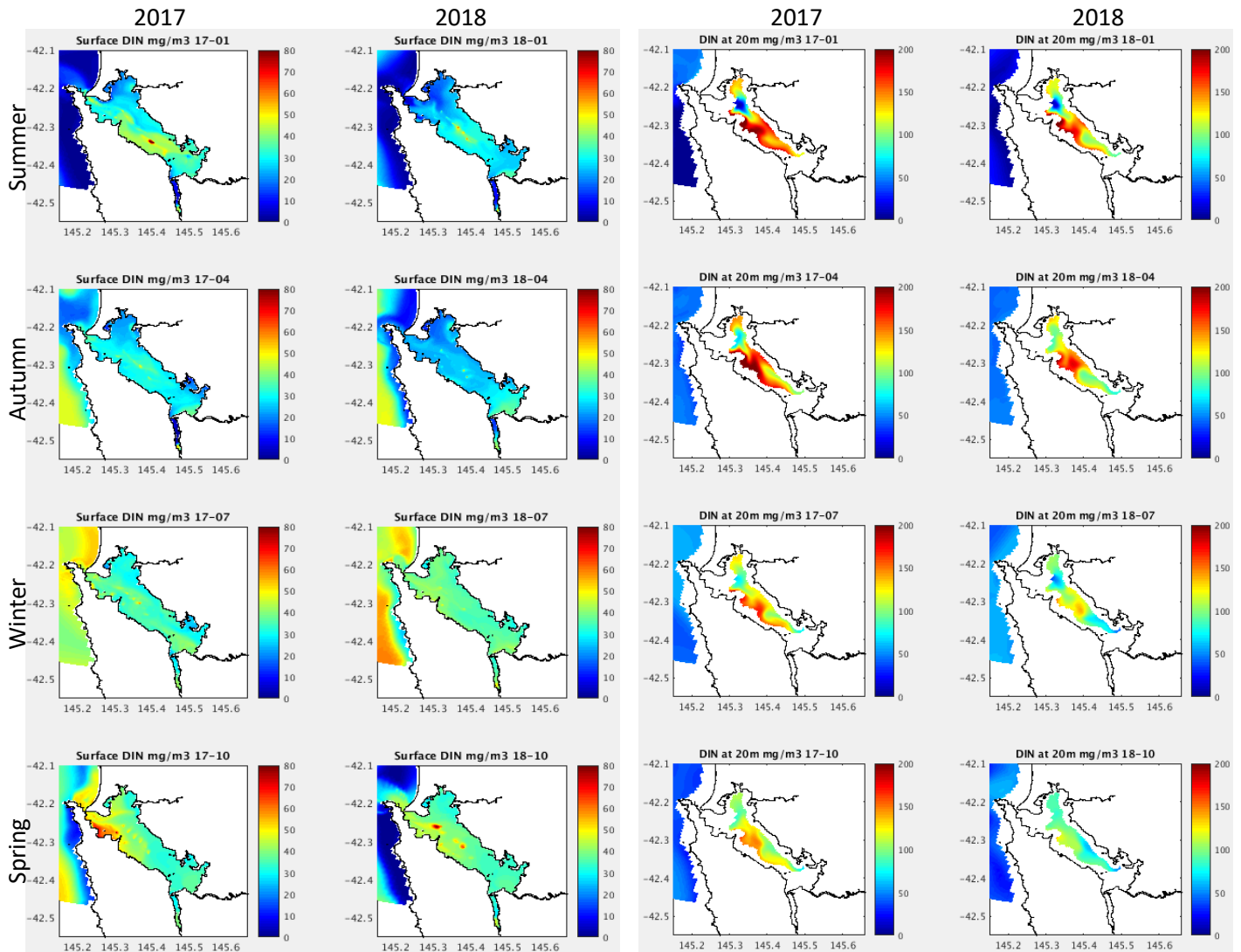


Figure 4.11 Surface (left) and 20m (right) simulated monthly mean dissolved inorganic nitrogen in summer (Jan), autumn (Apr), winter (Jul) and spring (Oct) 2017 and 2018 (by row from top to bottom). Note change in scale from surface to 20m depth.

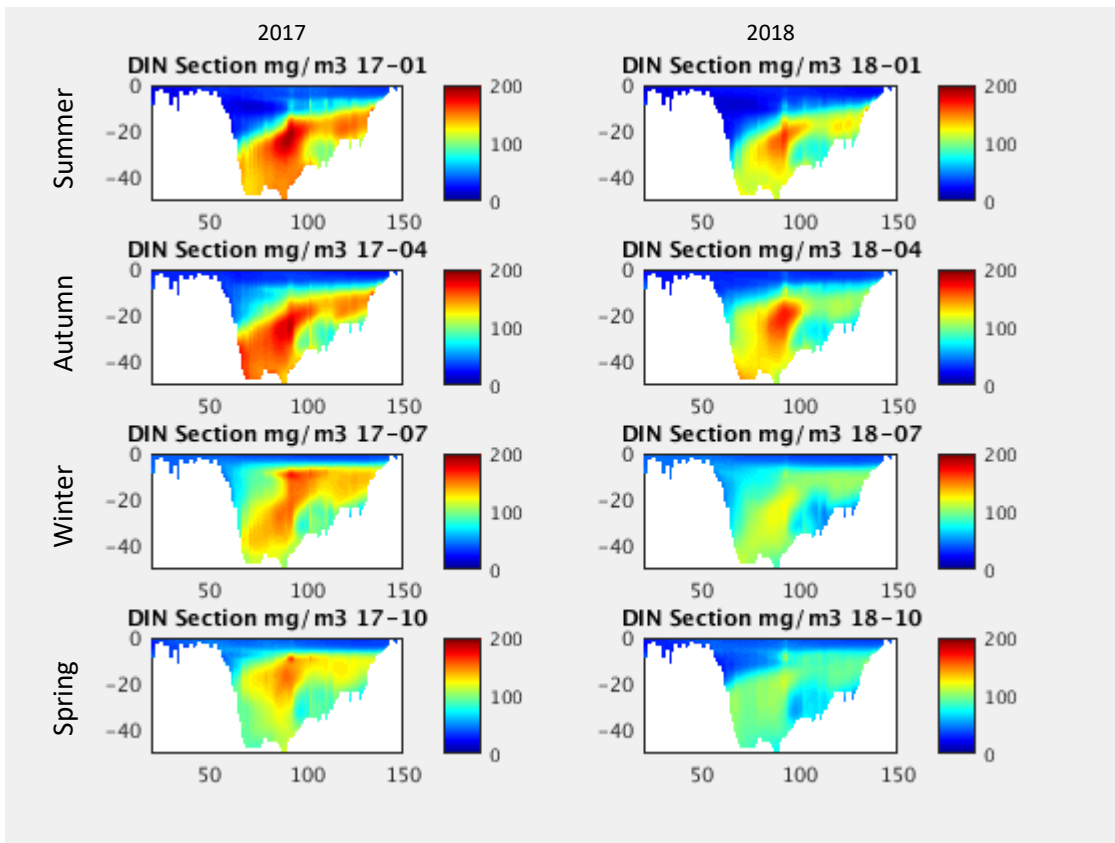


Figure 4.12 Simulated monthly mean dissolved inorganic nitrogen in summer (Jan), autumn (Apr), winter (Jul) and spring (Oct) 2017 and 2018.

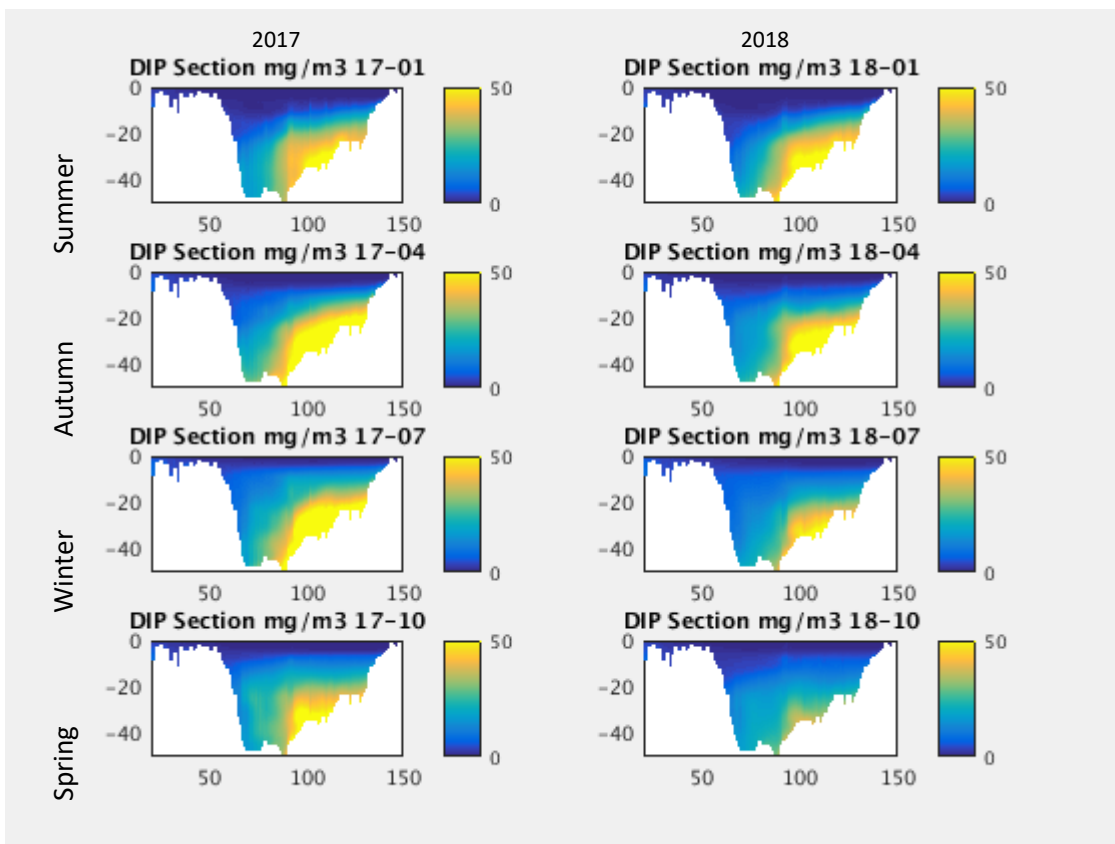


Figure 4.13 Simulated monthly mean dissolved inorganic phosphate in summer (Jan), autumn (Apr), winter (Jul) and spring (Oct) 2017 and 2018.

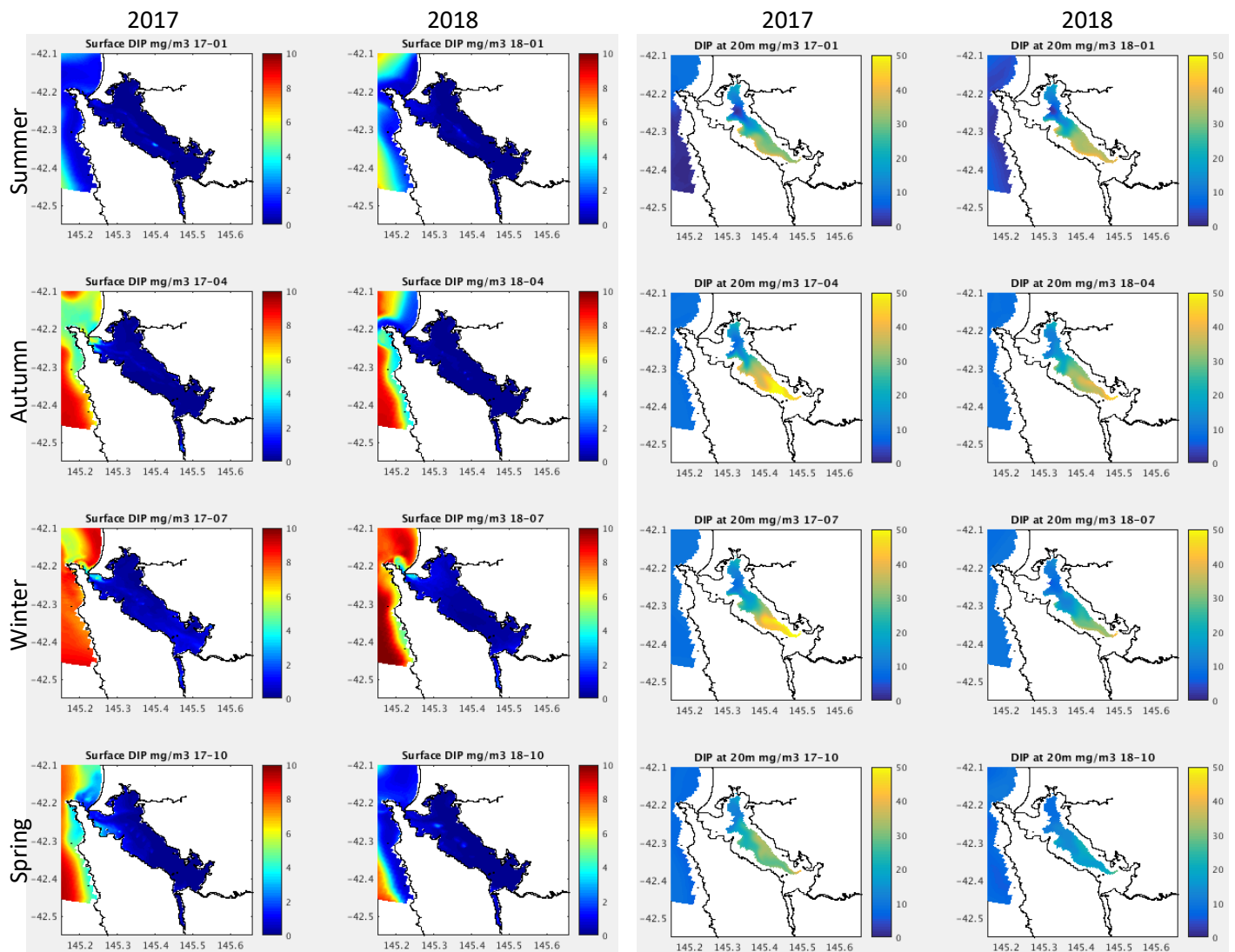


Figure 4.14 Surface (left) and 20m (right) simulated monthly mean dissolved inorganic phosphorous in summer (Jan), autumn (Apr), winter (Jul) and spring (Oct) 2017 and 2018 (by row from top to bottom). Note change in scale from surface to 20m depth.

Simulated secchi depth was greatest when river flow was low, consistently in summer, but also in autumn 2017 (Figure 4.17); this is due to the strong light attenuation of CDOM in river water in other seasons. Dark river water with low nutrient content limits phytoplankton growth in surface layers throughout the harbour. Peak concentrations of chlorophyll were simulated at around 15m depth towards the northern end of the harbour which was subject to greater marine nutrient supply and more transparent water, particularly in summer but also in autumn 2017 and during the lower flow period in autumn 2018. The correlation between lower river flow, increased secchi depth and elevated chlorophyll concentration indicates that phytoplankton respond quickly to even a small increase in available light. It should be noted, however, that the model allows phytoplankton to vary their chlorophyll content to optimise photosynthesis according to ambient light and nutrient levels (as shown in observational studies). Phytoplankton typically have greater pigment concentration under low light conditions to maximise the opportunity for photosynthesis, and chlorophyll concentration therefore may not directly correspond to phytoplankton biomass. Correlations in the simulated distribution of chlorophyll and nutrients in the harbour indicates that phytoplankton assimilation is drawing down dissolved inorganic nitrogen and phosphorous in the northern part of the harbour, particularly in summer (Figures 4.16, 4.12 & 4.13).

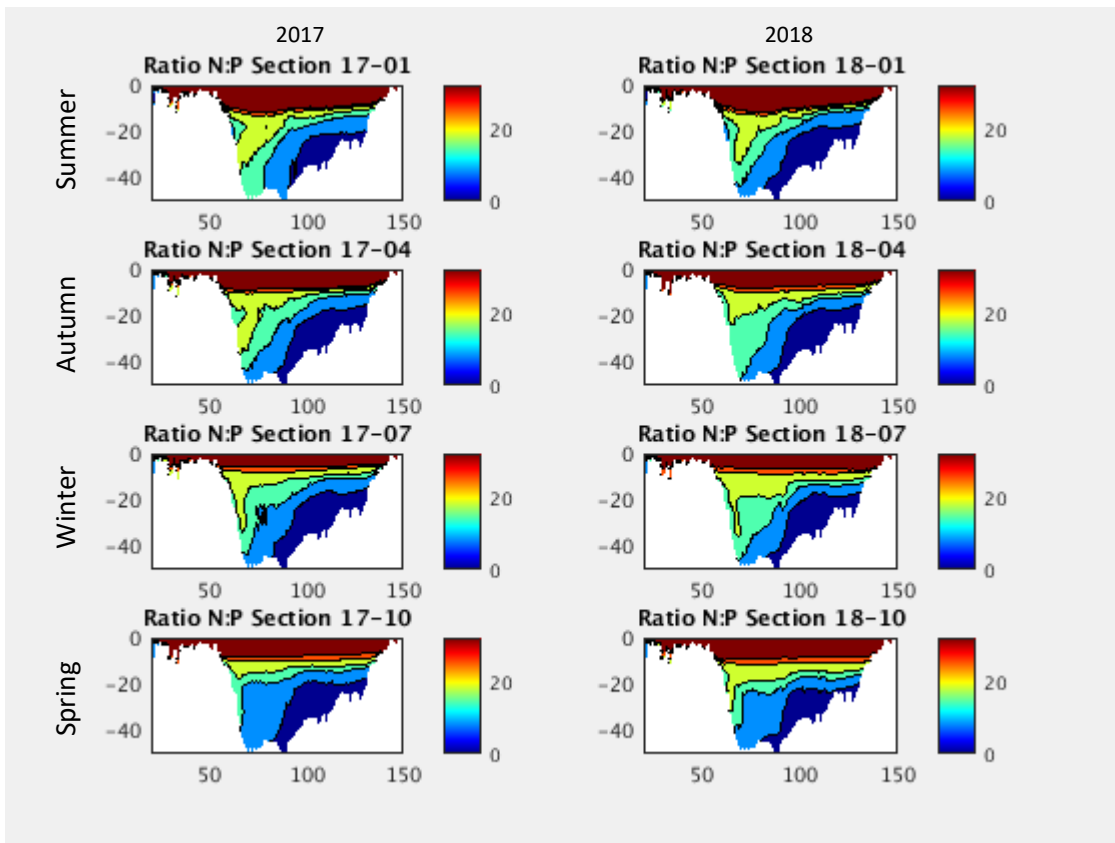


Figure 4.15 Monthly mean simulated molar ratio of dissolved inorganic nitrogen to phosphorous in summer (Jan), autumn (Apr), winter (Jul) and spring (Oct) 2017 and 2018; Redfield ratio is 16N : 1P for balanced phytoplankton growth.

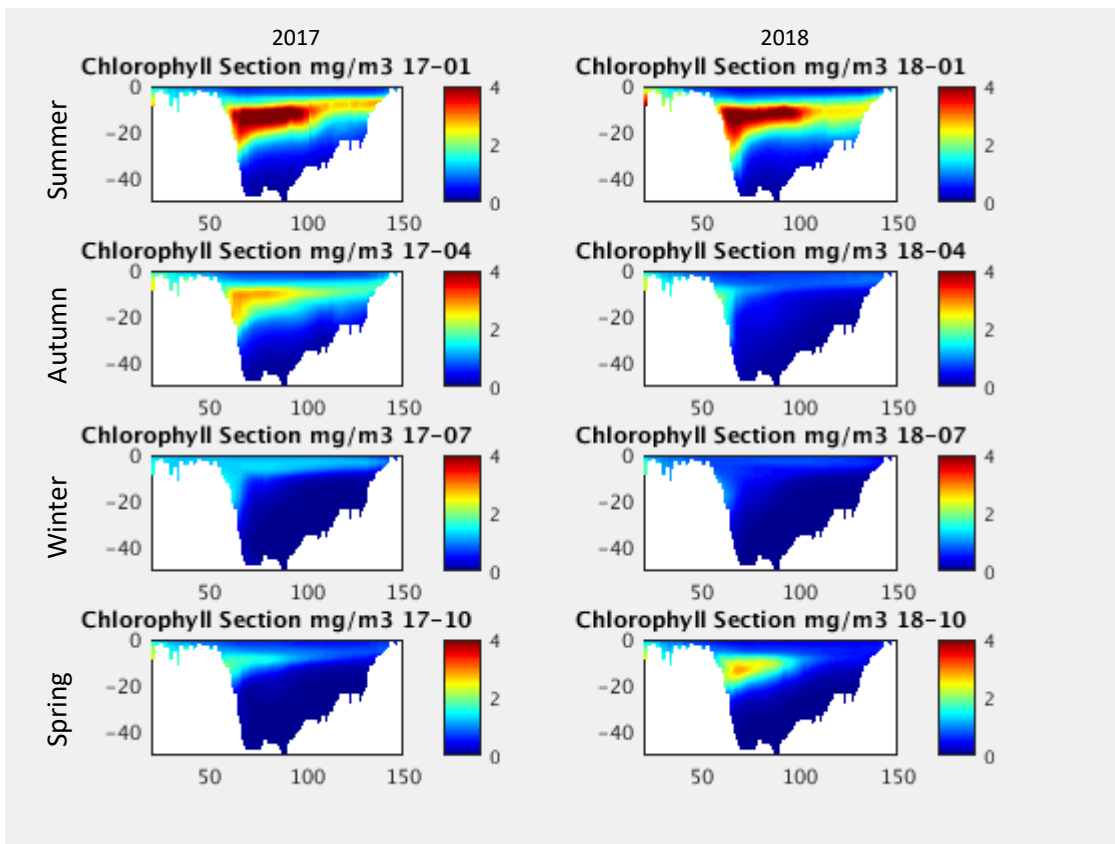


Figure 4.16 Simulated monthly mean chlorophyll in summer (Jan), autumn (Apr), winter (Jul) and spring (Oct) 2017 and 2018.

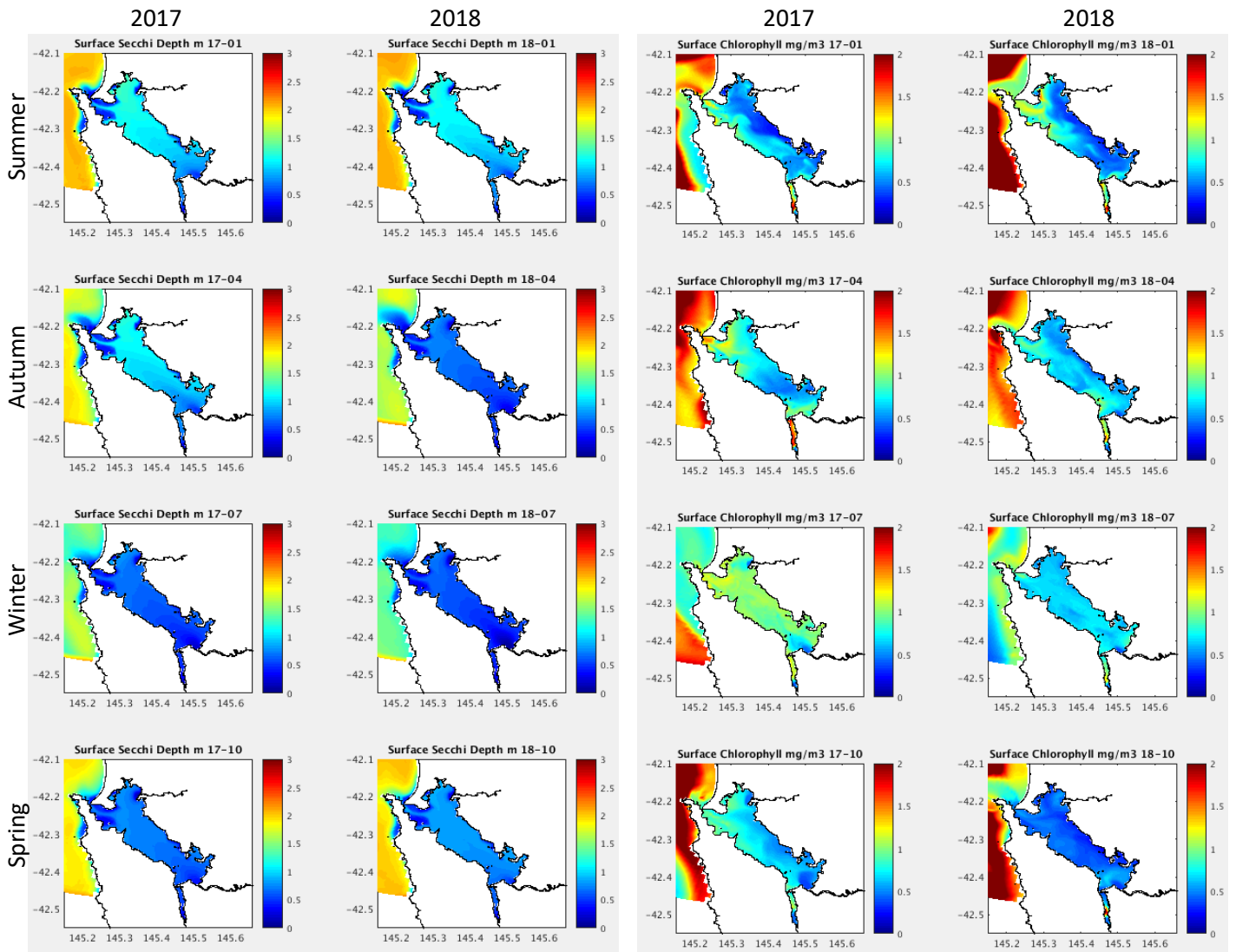


Figure 4.17 Simulated monthly mean secchi depth (left) and surface chlorophyll (right) in summer (Jan), autumn (Apr), winter (Jul) and spring (Oct) 2017 and 2018 (by row from top to bottom).

### 4.3.4 Dissolved Oxygen

Simulated dissolved oxygen concentrations throughout the harbour show persistent high concentrations of oxygen in surface waters and reduced concentrations at depth, particularly at the southern end of the harbour and more generally in spring (Figures 4.18 & 4.19). Monthly mean concentrations were similar in 2017 and 2018, although there was slightly greater drawdown of midwater oxygen in 2018 that correlates with greater river flow and associated reduced ocean influx and midwater flushing.

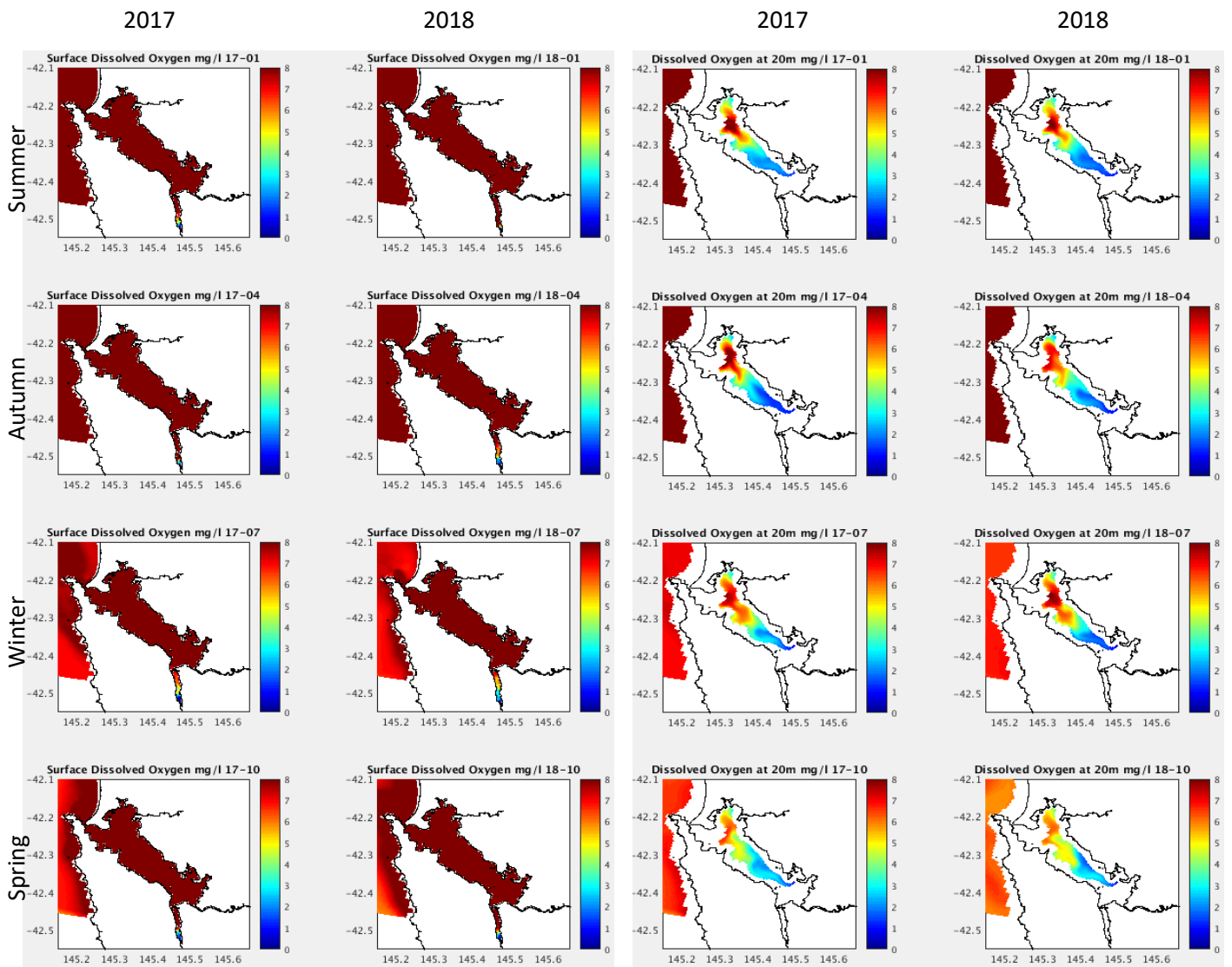


Figure 4.18 Surface (left) and 20m (right) simulated monthly mean dissolved oxygen in summer (Jan), autumn (Apr), winter (Jul) and spring (Oct) 2017 and 2018 (by row from top to bottom).

To characterise dissolved oxygen conditions in the harbour further we calculated the simulated water volume and surface sediment area with anoxic (< 1%), hypoxic (1-30%), intermediate (30-80%) and healthy (>80%) oxygen saturation. This analysis was done for the Strahan Basin, the World Heritage Area (WHA), the Northern Harbour Basin and the whole harbour according to the areas delineated in Figure 4.20.

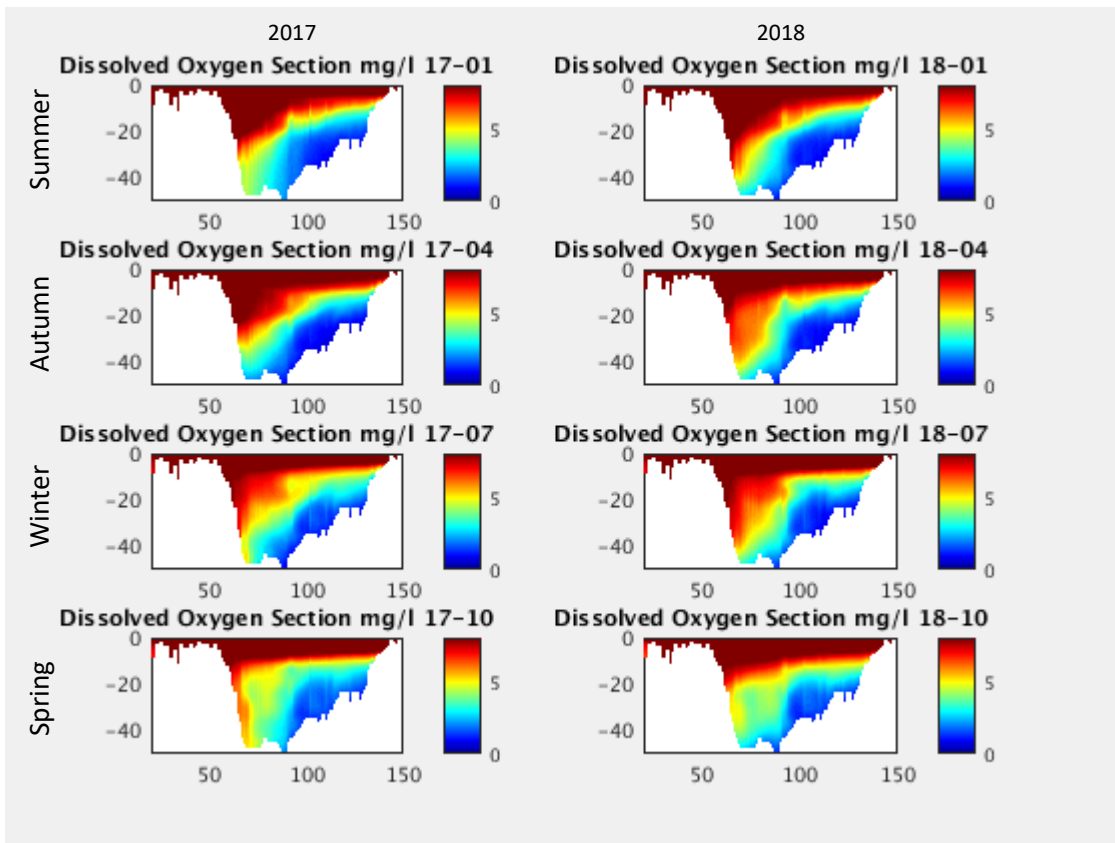


Figure 4.19 Simulated monthly mean dissolved oxygen in summer (Jan), autumn (Apr), winter (Jul) and spring (Oct) 2017 and 2018.

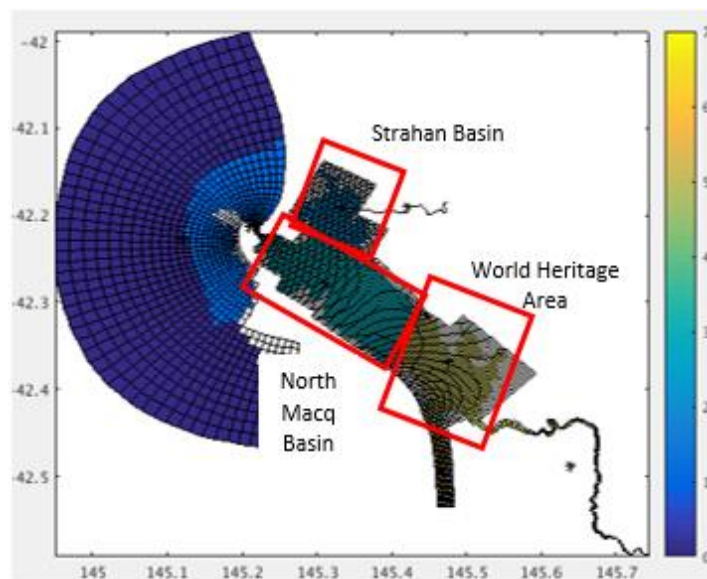


Figure 4.20 Three sub-regions of Macquarie Harbour used in the analysis of model results; these 3 subregions are summed for whole of harbour metrics.

No anoxic water or sediment areas were simulated by the biogeochemical model (Figure 4.21). Hypoxic water (1-30% oxygen saturation) was simulated persistently throughout the harbour with greatest proportional volume found in the WHA and the least volume found in the Strahan Basin. Mean conditions for 2017-18 for the whole harbour showed that 14% of the water was found to be hypoxic. The volume of water similarly classified with 'healthy' oxygen content (>80% oxygen saturation) was 44% of the whole harbour. The Strahan Basin had the greatest (53%) and the WHA had the least (41%) proportion of

'healthy' water. Seasonal variation in conditions was small, although there was a slight increase in hypoxic water in summer and autumn; the volume of 'healthy' water was also slightly greater in autumn.

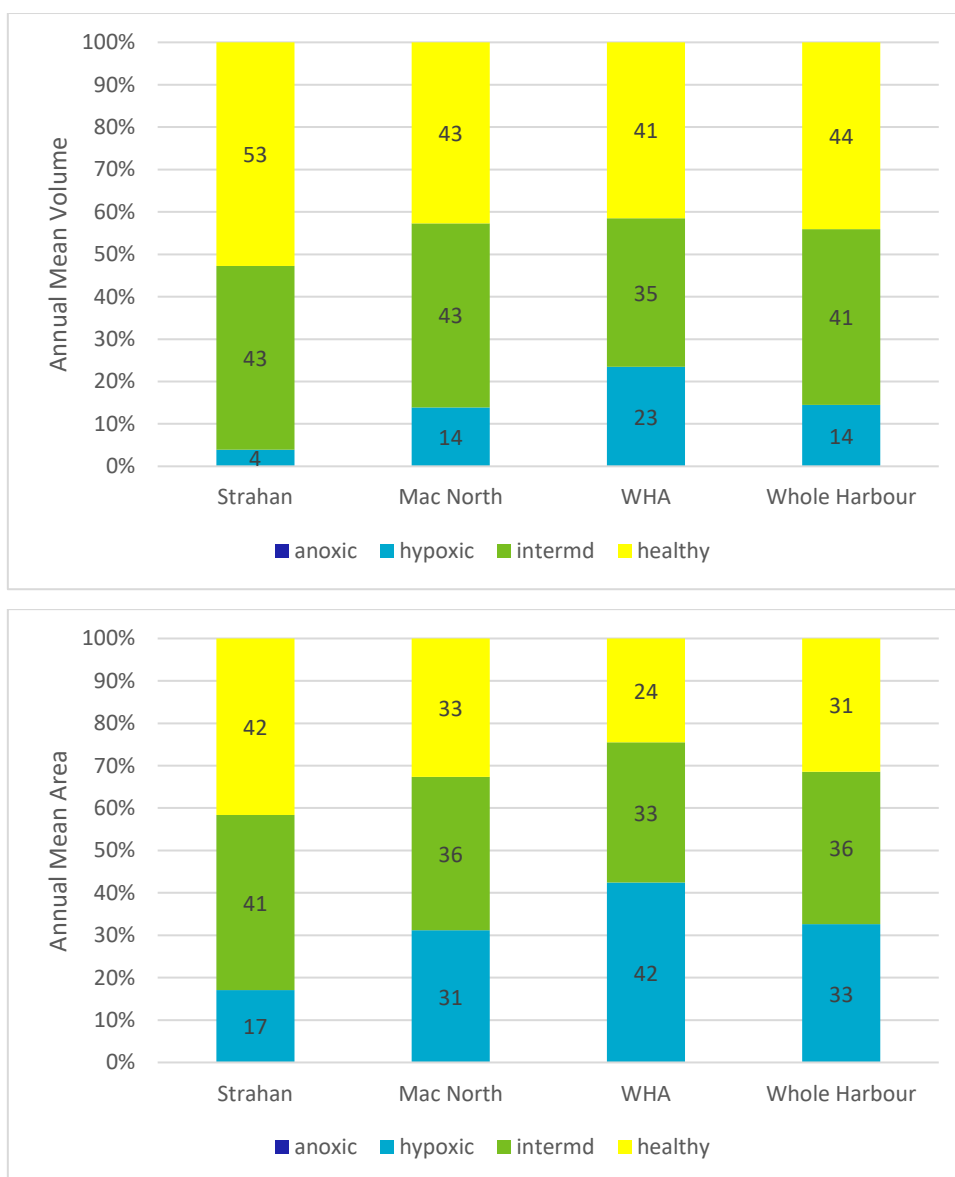


Figure 4.21 Annual mean water volume (top) and sediment area (bottom) with anoxic (<1%), hypoxic (1-30%), intermediate (30-80%) and healthy (>80%) dissolved oxygen saturation.

Analysis of simulated surface sediment conditions showed that the WHA had the largest (43%) and the Strahan Basin the smallest (17%) proportional area of hypoxia. Of the whole harbour area, mean conditions for 2017-18 showed 33% of the sediment was hypoxic. The sediment area classified as healthy ranged from 42% for Strahan Basin to 24% for the WHA; overall, 31% of the whole harbour was found to have healthy sediment oxygen conditions. There was some seasonal variation in hypoxic area with a small increase in summer and autumn. The area of 'healthy' sediment showed little seasonal variation in most of the harbour except for in the WHA which had an increased area of healthy sediment in late winter and early spring. These differences in oxygen saturation between basins are due to the depth of each basin, the stratification and flushing regime for each basin and local biogeochemical (including sediment) source and sink terms.

## 4.4 Oxygen and nitrogen budget analysis

### 4.4.1 Oxygen Budget

An oxygen budget was calculated for the whole harbour based on the area shown in Figure 4.20. Inputs to the harbour and losses from the harbour are summarised in Figures 4.22 and 4.23 for 2017 and 2018; differences between years are largely due to the change from a drier year (2017) to wetter conditions (in 2018) and associated differences in river flow, hydrodynamic circulation, marine intrusions and residence time, and fish farm loads (larger in 2017; reduced in 2018).

The largest input of dissolved oxygen to the harbour is from rivers with the Gordon catchment providing on average 66% of the total input. Marine input of oxygen varied from 7-13%, whilst air sea flux provided 6% of the total input. Net ecological input to the harbour (from photosynthesis less remineralisation), provided a small ~2% addition of oxygen to the water column. The largest loss term for dissolved oxygen from the harbour is export of oxygen rich surface water to the ocean (87%). The 2<sup>nd</sup> largest loss term is from biogeochemical remineralisation processes in the sediment (8%). Estimated fish respiration at farm sites accounted for a further 3% of the total loss with the remaining contributions from air sea flux, water column biogeochemistry and a small flux into the Birch Inlet (not included in the harbour budget area).

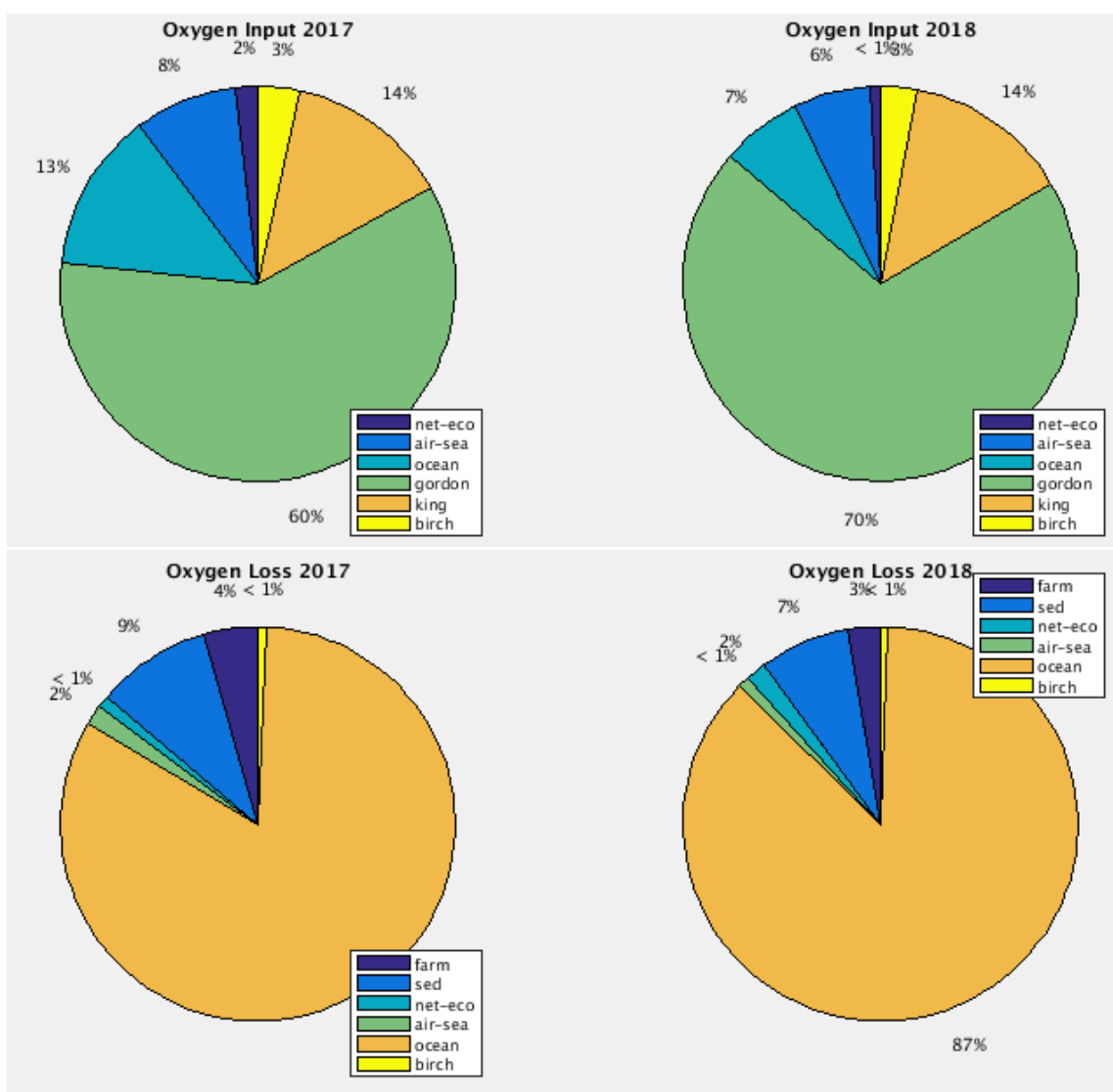


Figure 4.22 Relative contribution of modelled inputs and losses of dissolved oxygen for Macquarie Harbour in 2017 and 2018.

The net sum of the modelled oxygen input and loss terms (Figure 4.23 & 4.24) shows that the simulated harbour oxygen budget is very close to balanced, being in deficit by only around -2900tO/y. Given the large fluxes of oxygen into and out of the harbour, the significance of this small net sum should be treated with caution as any minor inaccuracies in, for example river flow or harbour entrance bathymetry, could change this small net sum. Notwithstanding this context, in both 2017 and 2018 the harbour was found to have a small oxygen deficit.

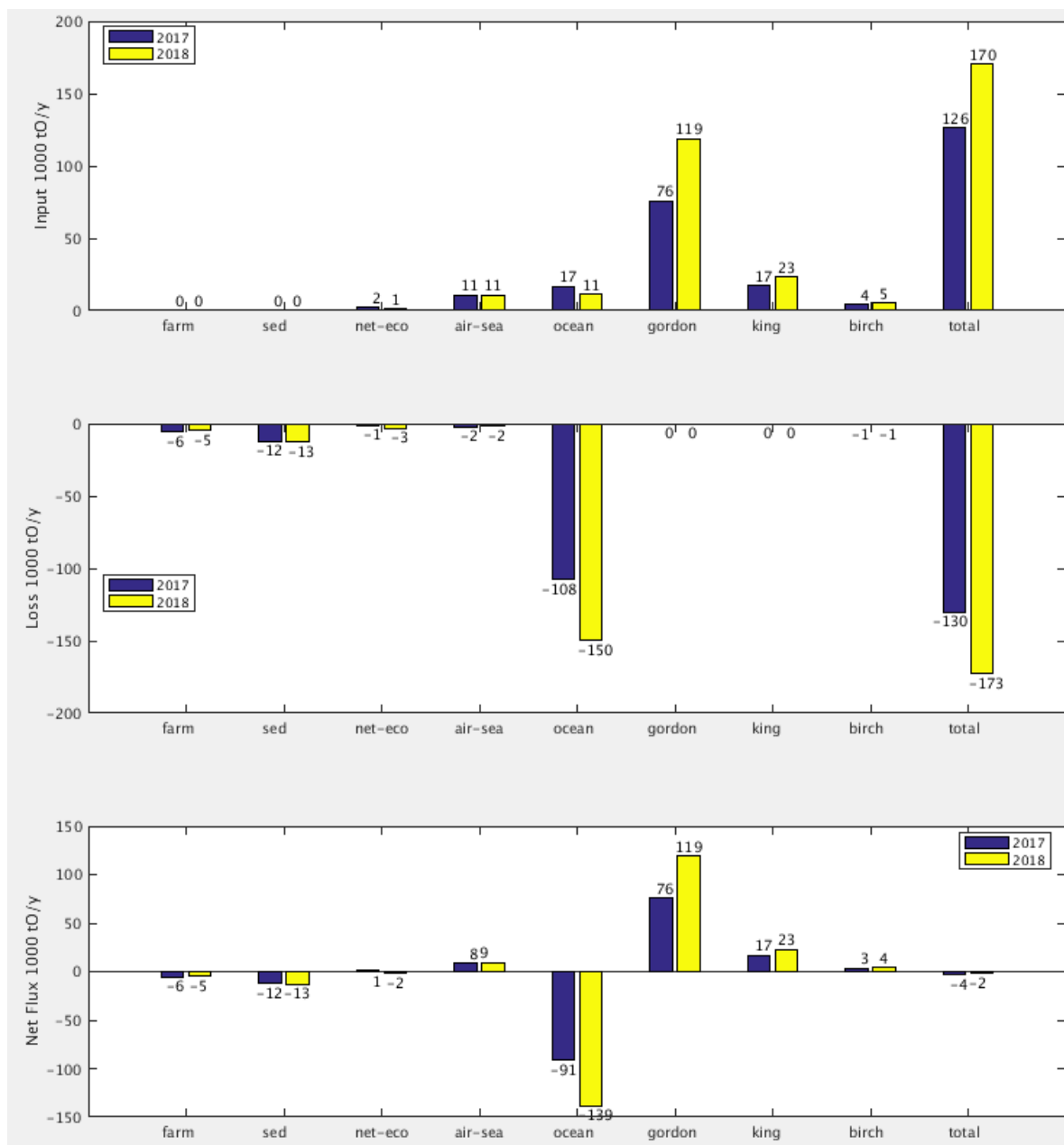


Figure 4.23 Modelled inputs (top), losses (middle) and net flux (bottom) of dissolved oxygen for Macquarie Harbour in 2017 and 2018 (in 1000tO/y).

Analysis of the oxygen budget by month (Figure 4.25) shows how the seasonal variation in inputs and outputs are closely matched. Greatest influx and export of oxygen to the harbour occurs in winter, from river input and ocean outflow, and fluxes were larger in 2018 which was a wetter year. In contrast, the input of oxygen from marine intrusions is greatest in summer, when river flows are reduced. The net balance in oxygen flux is small compared to the magnitude of the input and loss terms and should be treated with caution as a small inaccuracy in the modelled fluxes (as mentioned previously) could change this net sum. Within this context general trends in the net flux suggest an increase in harbour oxygen in winter, and less consistently in autumn, whilst there is a net loss of oxygen in spring.

### 2017-18 Mean Annual Oxygen Budget 1000 tO/y

Net Flux -2,900 tO/y

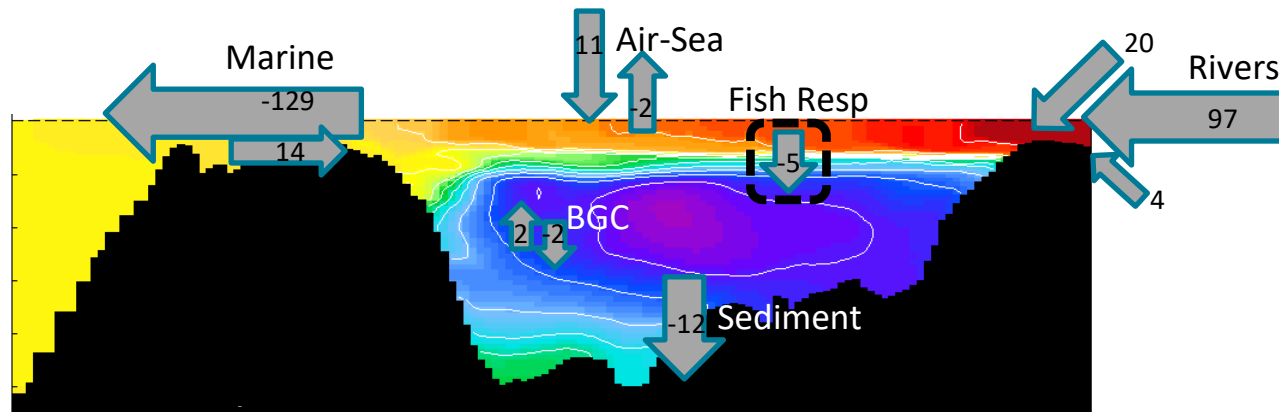


Figure 4.24 Schematic showing mean annual modelled inputs and loss terms for dissolved oxygen in Macquarie Harbour in 2017 and 2018 (in 1000tO/y).

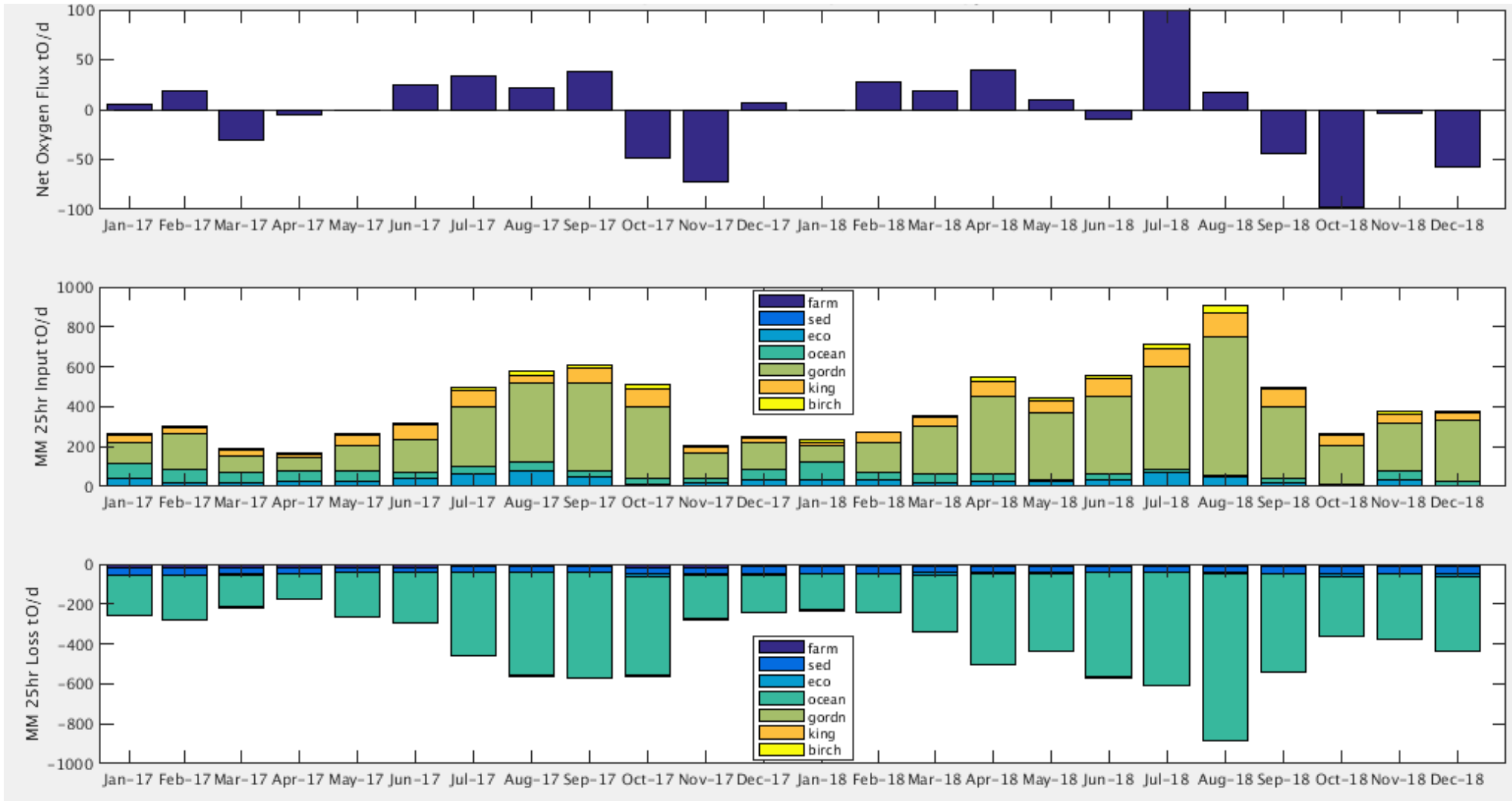


Figure 4.25 Simulated monthly mean net oxygen budget (top), inputs (middle) and loss terms (bottom) for Macquarie Harbour in 2017 and 2018 (in tO/d).

#### 4.4.2 Nitrogen Budget

A total nitrogen budget was calculated for the whole harbour for the area shown in Figure 4.20, in a similar way to the oxygen budget. Inputs to the harbour and losses from the harbour are summarised in Figures 4.26 and 4.27 for 2017 and 2018; differences between years are largely due to the change from a drier year (2017) to wetter conditions (in 2018) and associated differences in river flow, hydrodynamic circulation, marine intrusions and residence time, and fish farm loads (larger in 2017; reduced in 2018).

The largest input of nitrogen to the harbour is from rivers with the Gordon catchment providing on average 45% of the total input. Fish farms and sewerage treatment plant loads accounted for 33% and 18% of the total nitrogen load into the harbour in 2017 and 2018, respectively. Although the fish farm contribution of nitrogen to the harbour was reduced in 2018, elevated river flow resulted in a slightly greater total input of nitrogen to the system than in 2017 [however it is important to note that for the Gordon river only 30% of the nitrogen load is labile (reactive) material c.f. 100% of fish farm and sewerage treatment plant waste]. Marine input of nitrogen was on average 23% of the total influx with atmospheric deposition contributing around 1%. The greatest loss term for nitrogen from the harbour was by export of harbour water to the ocean (80% of the total flux). Sediment and water column denitrification (including annamox) accounted for 14% and 6% of nitrogen loss respectively, with the remainder comprised of minor fluxes into the Birch Inlet, and the lower estuarine reaches of the King and Gordon river systems (these were modelled but excluded from the harbour budget – see Figure 4.20).

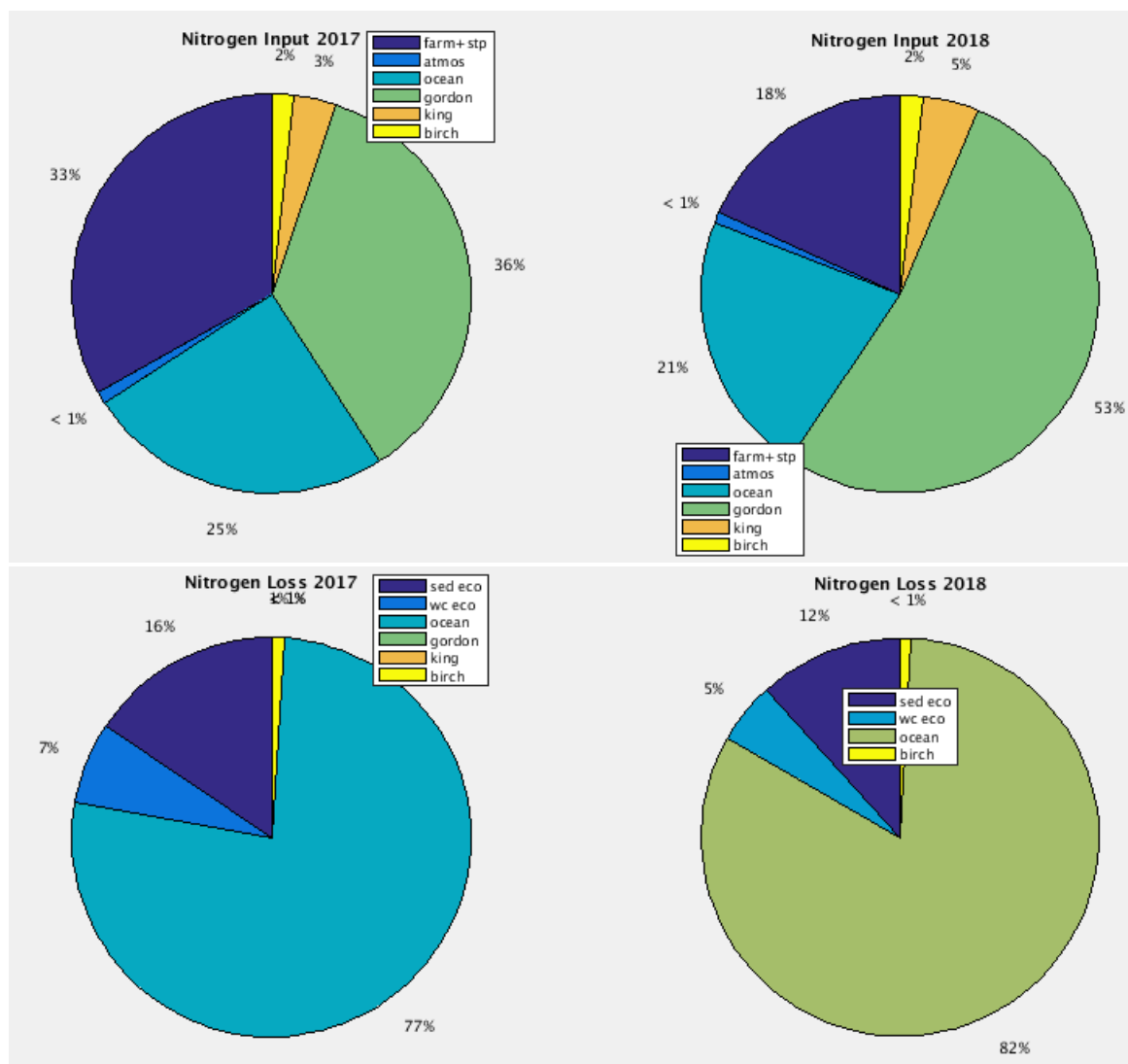


Figure 4.26 Relative contribution of modelled inputs and losses of nitrogen for Macquarie Harbour in 2017 and 2018.

The net sum of the simulated nitrogen input and loss terms (Figure 4.27 & 4.28) shows that the simulated harbour nitrogen budget has a small net deficit of -50 tN/ty in 2017 and -150 tN/y in 2018. Similar to the oxygen budget, these small net sums should be treated with caution given the relatively large fluxes of nitrogen into and out of the system. Whilst specification of the nutrient concentrations in the initial condition, at the marine boundary and for each river system were based on the best available data they are at best indicative of likely conditions for the simulated period. The net deficit in simulated nitrogen indicates that the modelled harbour is not in steady state but is eroding nitrogen to the surrounding environment; this loss of nitrogen is greater in 2018 under wetter conditions.

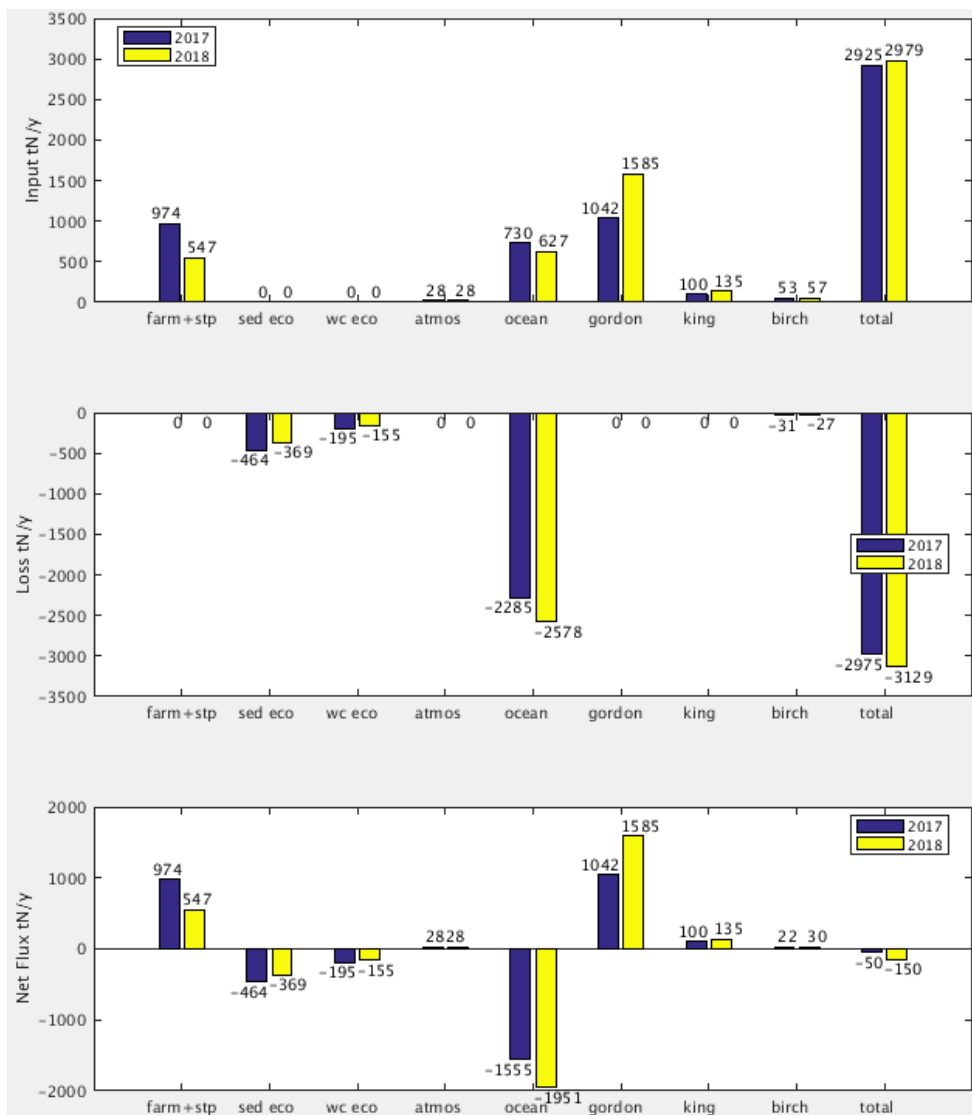


Figure 4.27 Modelled inputs (top), losses (middle) and net flux (bottom) of nitrogen for Macquarie Harbour in 2017 and 2018.

Analysis of the nitrogen budget by month (Figure 4.29) shows how the seasonal variation in inputs and outputs are closely matched. Greatest influx and export of nitrogen in the harbour occurs in winter from river input and ocean outflow respectively. Whilst oxygen fluxes were significantly larger in 2018 which was a wetter year, nitrogen fluxes were comparable in both years, as the increased riverine nutrient load was largely offset by the simultaneous decline in fish farm loads. Input of nitrogen from marine intrusions was greatest in summer, and during periods of reduced river flow. The net balance in nitrogen flux is small compared to the magnitude of the input and loss terms and should be treated with caution as a small inaccuracy in the modelled fluxes (as mentioned previously) could change this net sum. Within this context general trends in the net flux suggest a loss of harbour nitrogen in winter and an accumulation of nitrogen in summer with some variability in spring and autumn between years.

## 2017-18 Mean Annual Nitrogen Budget tN/y

Net Flux -100 tN/y

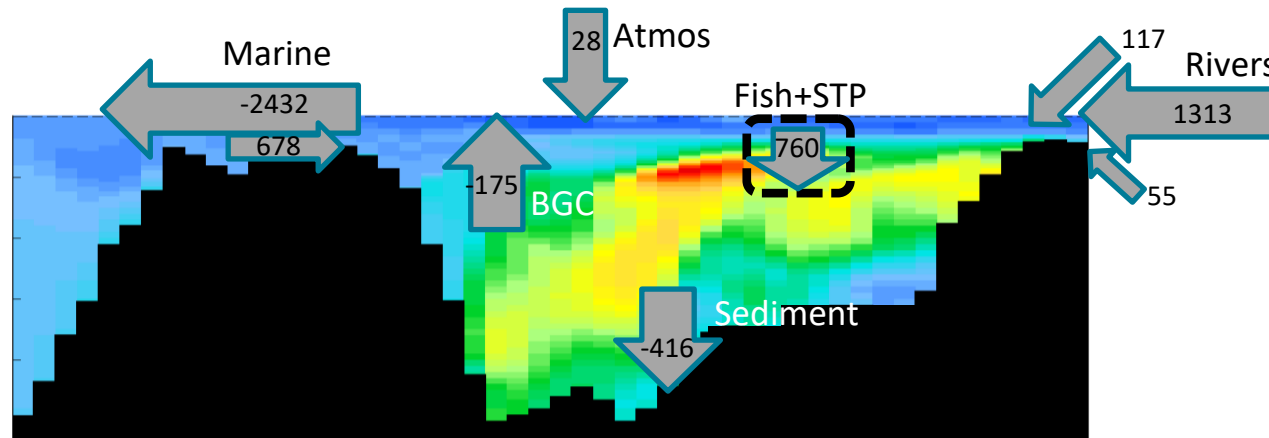


Figure 4.28 Schematic showing mean annual modelled inputs and loss terms for total nitrogen in Macquarie Harbour in 2017 and 2018 (in tN/y).

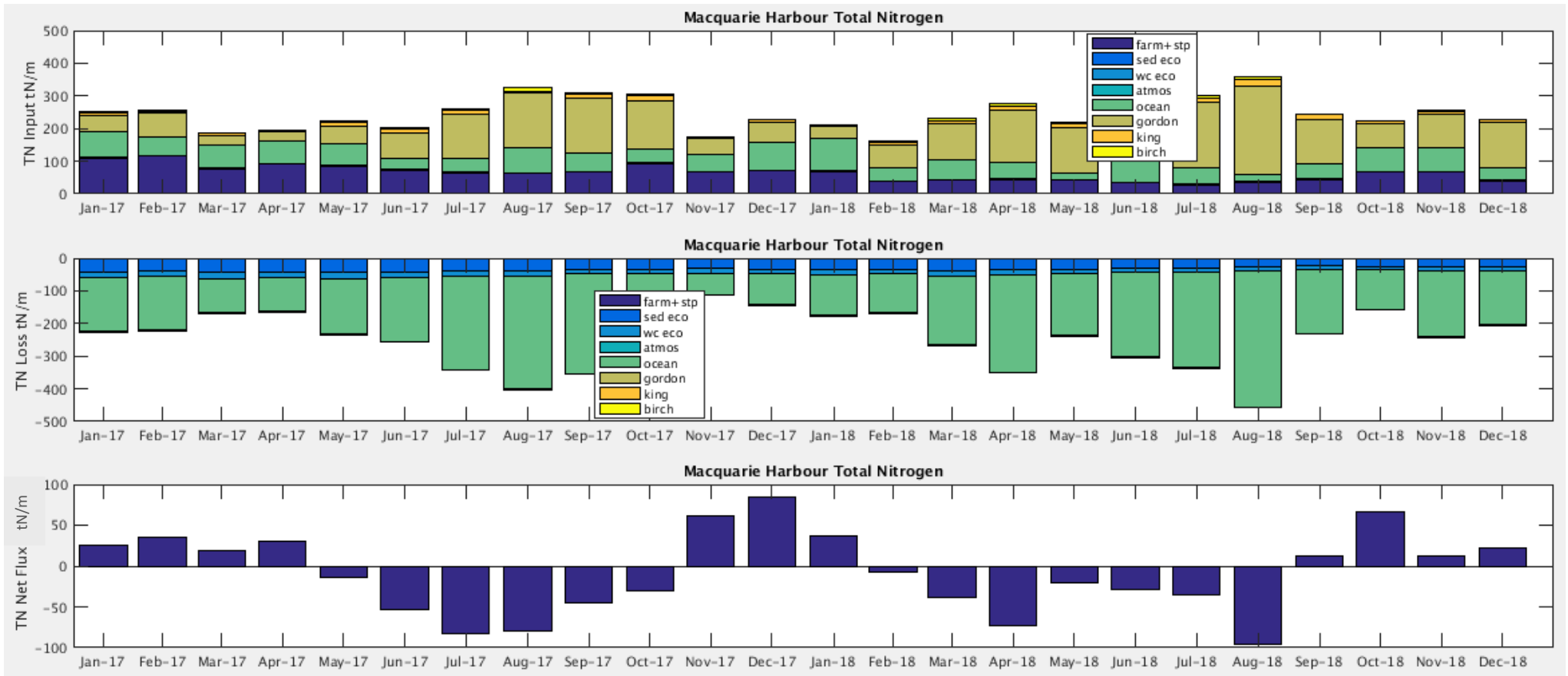


Figure 4.29 Simulated monthly mean nitrogen inputs (top), loss terms (middle) and net budget for Macquarie Harbour in 2017 and 2018 (in tN/month).

## 4.5 Model scenario simulations

Following a meeting on 25<sup>th</sup> September 2019 attended by EPA, DPIPW marine farming, Huon Aquaculture, Tassal and Petuna, a number of 'no regrets' scenarios were identified to explore the sensitivity of Macquarie Harbour water quality to contrasting fresh water input. These scenarios will provide insight into potential future harbour conditions under systematically wetter, or drier west coast weather. Scenarios that contrast wet vs dry years were hypothesised to correspond to worst vs best case situations with respect to ocean flushing and pelagic dissolved oxygen concentrations.

To investigate drier conditions the hydrodynamic model was run for 2017-18 with 10% less river flow in all rivers, and 20% less river flow in all rivers. Output from these hydrodynamic model runs was then used to force the biogeochemical transport model to simulate water quality and surface sediment conditions under reduced fresh water flow [note that these simulations were parameterised, initialised and forced with the same anthropogenic nutrient loads as the calibration model run].

To investigate the impact of wetter west coast conditions on harbour water quality, the hydrodynamic model was run for 2017-18 with 10% more river flow in all rivers and 20% more river flow in all rivers. Output from these hydrodynamic model runs was then used to force the biogeochemical transport model as for the drier weather scenarios.

A further scenario to explore the impact of a reduction in anthropogenic nutrient load on water quality in the harbour was also completed. In this scenario the model was run for 2017-18 conditions as for the calibration run, but omitting all fish farm waste loads and fish farm oxygen respiration; sewerage treatment plant wastewater was still included in the scenario.

In addition to these scenario investigations, stakeholders were interested in the impact of persistent conditions over a longer timeframe than 2 years. All model runs were therefore extended by a nominal further 2 years by repeating the weather and hydrodynamic forcing of 2017-18.

The full set of model runs completed are detailed in Table 4.2.

Table 4.2 Details of all model runs completed including the calibration model run and scenario variations.

Scenario	River Flow	Farm Load	Purpose	Metrics
2017-18	2017-18	2017-18	Calibration run	Monthly mean DO, Chl, N, P, at 0m, 20m, bottom, transect, DO budget, ocean influx
2017-18 Extension	2017-18	2017-18	Persistent 'normal' conditions	Focus on Oxygen reporting incl. ocean influx
-10%	- 10%	2017-18	Drier conditions	Focus on Oxygen reporting incl. ocean influx
-10% Extension	- 10%	2017-18	Persistent drier conditions	Focus on Oxygen reporting incl. ocean influx
-20%	- 20%	2017-18	Much drier conditions	Focus on Oxygen reporting incl. ocean influx
-20% Extension	- 20%	2017-18	Persistent much drier conditions	Focus on Oxygen reporting incl. ocean influx
+10%	+ 10%	2017-18	Wetter conditions	Focus on Oxygen reporting incl. ocean influx
+10% Extension	+ 10%	2017-18	Persistent wetter conditions	Focus on Oxygen reporting incl. ocean influx
+20%	+ 20%	2017-18	Much wetter conditions	Focus on Oxygen reporting incl. ocean influx
+20% Extension	+ 20%	2017-18	Persistent much wetter conditions	Focus on Oxygen reporting incl. ocean influx
NF 2017-18	2017-18	No Farms	Reduced anthropogenic load	Focus on Oxygen reporting incl. ocean influx
NF 2017-18 Extension	2017-18	No Farms	Persistent reduced anthropogenic load	Focus on Oxygen reporting incl. ocean influx

## 4.6 Analysis of scenario simulations

### 4.6.1 Harbour Oxygen Levels During Drier or Wetter Conditions

Under drier conditions monthly mean simulated concentrations of dissolved oxygen in Macquarie Harbour were shown to increase in deep water (Figure 4.30). The increase was greatest in winter but occurred in all seasons, with the much drier scenario (-20% river flow) showing the larger increase (>2mg/l). Under wetter conditions dissolved oxygen concentrations in deep water were reduced with the largest decline simulated in the much wetter scenario (+20% river flow) in winter. Differences in deep water dissolved oxygen concentration between scenarios were largely driven by differences in the marine influx of oxygen, which these scenarios show to be modulated by river flow; greatest influx of marine oxygen occurs under low river flow, particularly in winter and spring.

In surface waters there was a small reduction in dissolved oxygen concentration (~0.5 mg/l) under drier conditions and a similar increase in dissolved oxygen under wetter conditions (Figure 4.30). This was predominantly driven by systematic variation in the thickness of the surface layer (c.f. the 2017-18 condition) determined by the influx of river water.

Oxygen conditions in the harbour were classified as anoxic (<1% oxygen saturation), hypoxic (1-30% oxygen saturation), intermediate (30-80% oxygen saturation) and healthy (>80% oxygen saturation) for each scenario and compared with conditions in 2017-18 (Figure 4.31). Anoxic conditions were not simulated by the biogeochemical model under any of the scenarios. Under drier conditions the model simulated a small reduction in the volume of hypoxic water and a small increase in the volume of healthy water. The converse was found under wetter conditions with a small increase in hypoxic volume and a similar decrease in the volume of healthy water. The analysis of surface sediment oxygen showed a similar pattern in hypoxic area albeit with greater magnitude; the simulated annual mean area of hypoxic sediment was reduced by 5% in the much drier scenario, but increased by 4% in the much wetter scenario. In contrast, the area of healthy sediment remained unchanged at 32% for all scenarios.

Healthy water and sediments were generally simulated in the upper water column and in shallow waters and these areas were less impacted by changes in river flow. Hypoxic water and sediments were generally simulated in the deeper reaches of the harbour which were most impacted by differences in the supply of marine oxygen between scenarios. Under reduced river flow, there was greater influx of marine water into the deeper parts of the harbour and reduced hypoxia; with increased river flow, marine influx was suppressed, deep water residence time increased and hypoxia increased (Figure 4.32). Whilst the strong linear relationship between simulated hypoxia and total river flow into the harbour suggests that river flow could be used as an indicator for water quality, confounding factors (such as anthropogenic load) should also be investigated.

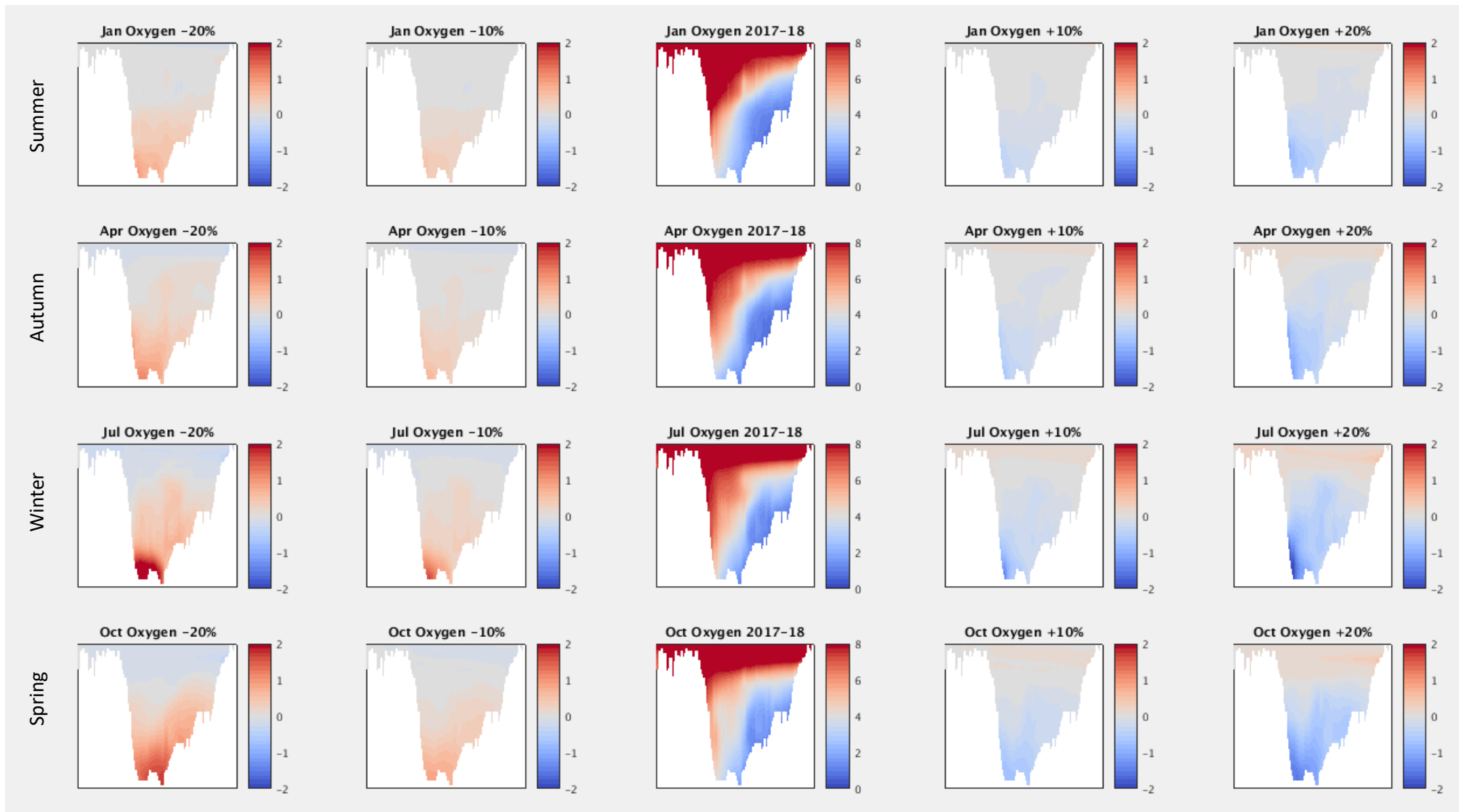


Figure 4.30 Monthly mean dissolved oxygen concentration (centre column) with drier scenario dissolved oxygen anomalies (to the left) and wetter scenario oxygen anomalies (to the right). Note that the centre plot shows the actual mean condition in 2017-18, whilst all other plots are anomalies from this condition. All units are mg/l.

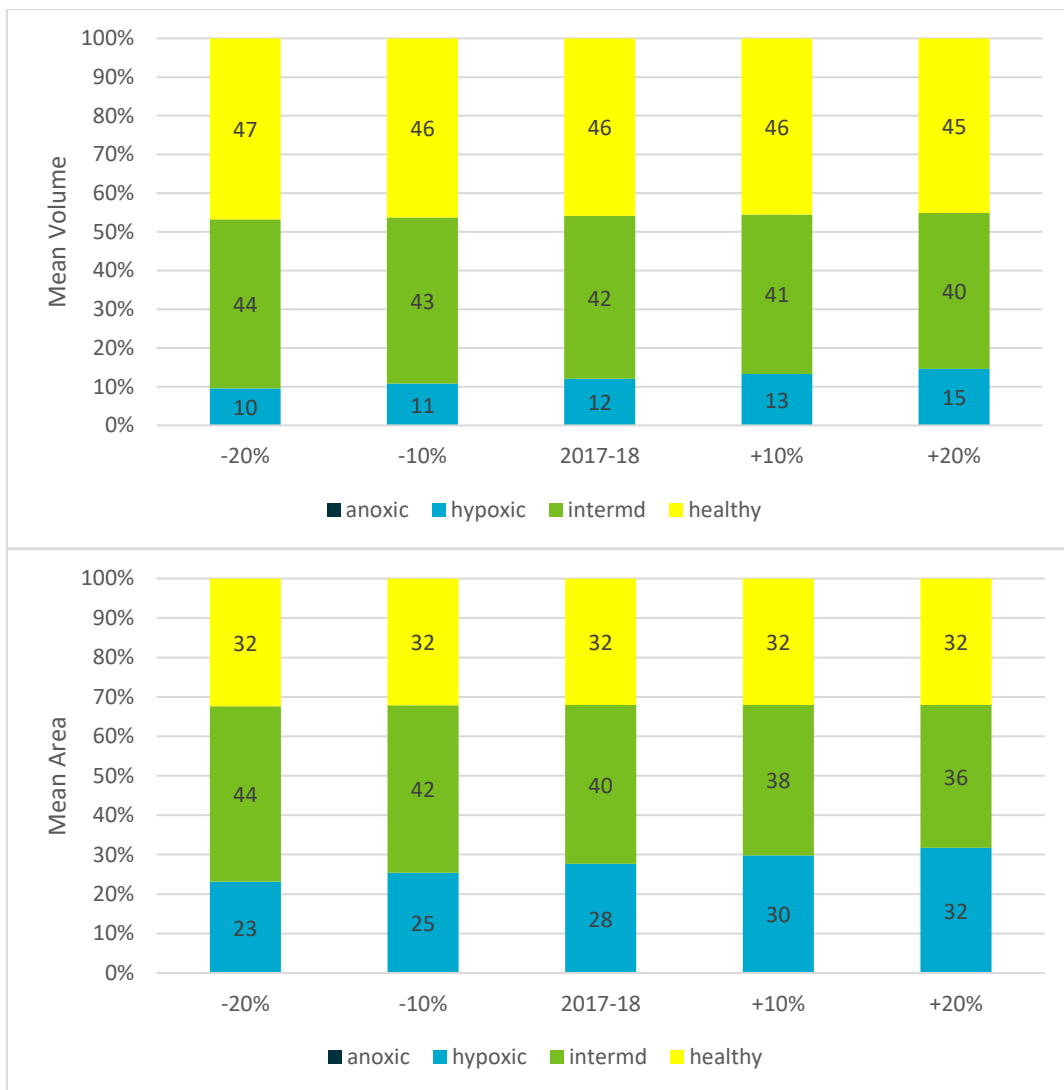


Figure 4.31 Simulated annual mean pelagic volume (top) and surface sediment area (bottom) with hypoxic (1-30% oxygen saturation), intermediate (30-80% oxygen saturation) and healthy (>80% oxygen saturation) status for each scenario. Drier scenarios are shown on to the left of the 2017-18 condition (central) and wetter scenarios are shown to the right.

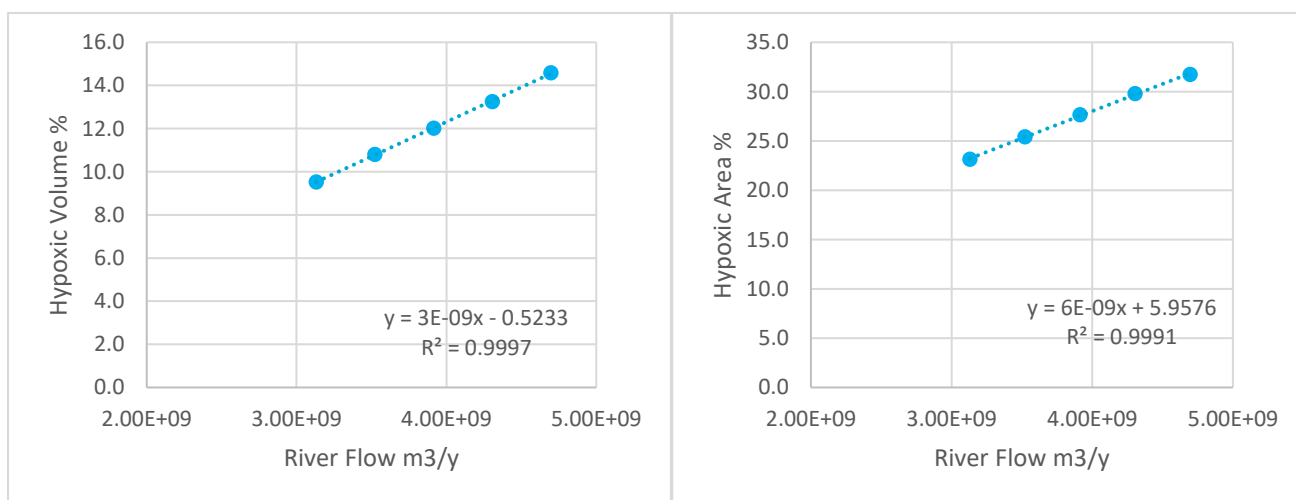


Figure 4.32 Simulated annual mean hypoxic pelagic volume (left) and hypoxic surface sediment area (right) variation with total river inflow for each scenario.

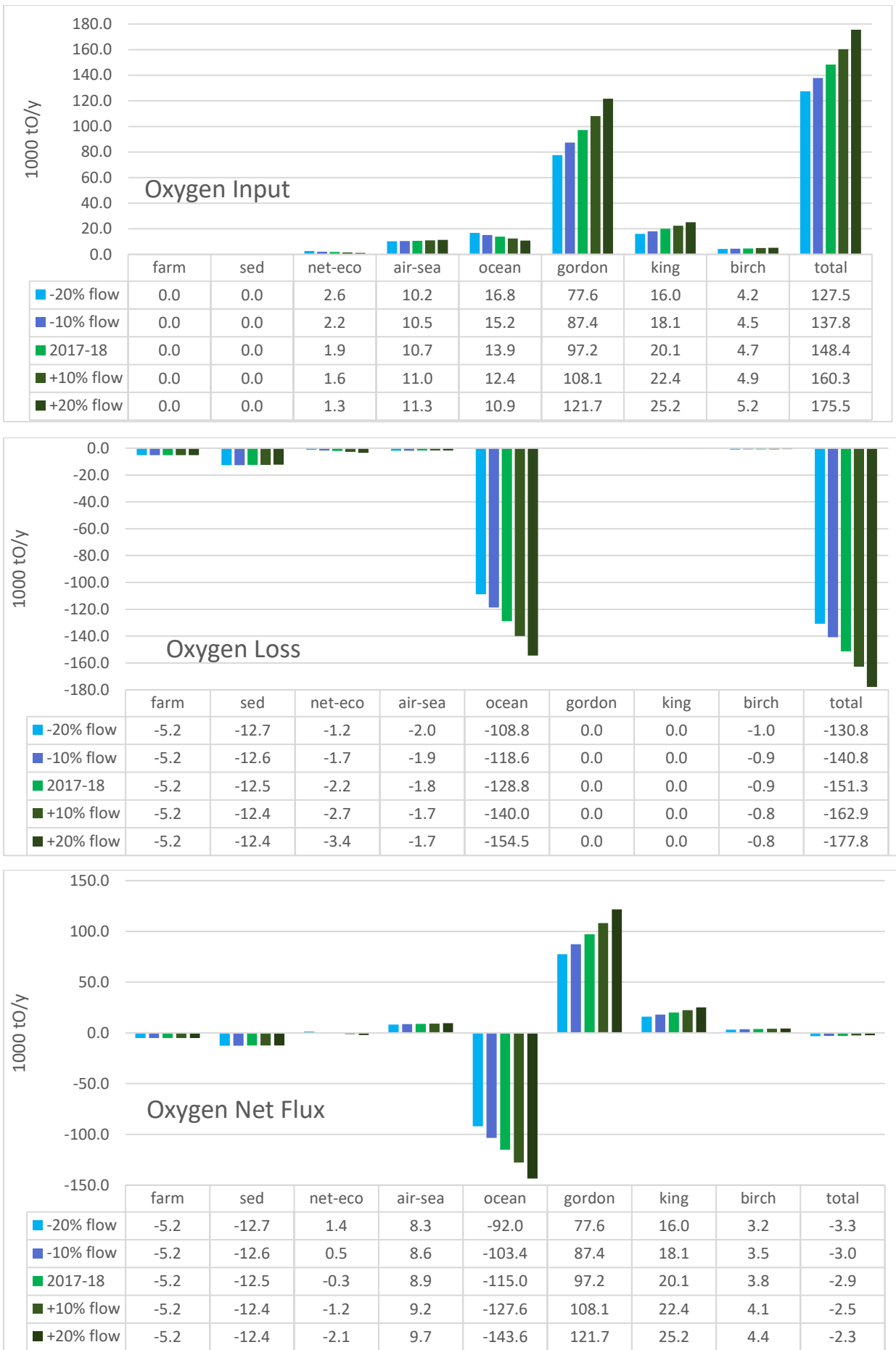


Figure 4.33 Simulated dissolved oxygen input (top), loss (middle) and net flux (bottom) in Macquarie Harbour for all scenarios. Drier scenarios are shown on to the left of the 2017-18 condition (central green bar) and wetter scenarios are shown to the right.

The simulated oxygen budgets for each scenario (Figure 4.33) show the magnitude of variation in each oxygen flux with changes in river flow. The greatest change in oxygen supply to the harbour between scenarios was from differences in river input; increased river flow provided more dissolved oxygen to the harbour, but also resulted in greater loss to the ocean due to the larger throughput of water. Ocean influx of oxygen varied inversely with river flow such that much drier conditions resulted in ~20% increase in marine oxygen influx whilst much wetter conditions suppressed the flux by ~20% (c.f. 2017-18 conditions).

Ecological inputs were smaller by comparison but showed systematic variation across the river flow scenarios with greatest net input under drier conditions. This was largely due to reduced CDOM and increased photosynthetic production of oxygen under the low flow scenarios, but also potentially due to a reduction in nitrification and denitrification in the water column c.f. the higher river flow scenarios. Simulated sediment oxygen demand (for detrital remineralisation) was very slightly larger under low flow scenarios, whilst air-sea flux was slightly greater with the high flow scenarios.

Overall the simulated net oxygen budget was small compared to the magnitude of fluxes through the harbour and its absolute value should be considered with caution given the uncertainty in river flow estimates and harbour entrance bathymetry. Notwithstanding this context there was a small but systematic variation in the net oxygen budget between scenarios with drier conditions resulting in a slightly greater drawdown in oxygen of wetter scenarios. This indicates that the additional influx of river oxygen in the wetter scenarios outweighs the increased oxygen supply from marine and ecological sources which were favoured in the drier scenarios.

Whilst the whole of harbour oxygen budget is useful, it does not distinguish the rapidly flushed surface layers from the deep waters which have much longer residence times (Andrewartha & Wild-Allen 2017); from an ecological perspective, the flux of oxygen into these deep waters is of much greater significance. Figure 4.34 shows that there is a strong linear relationship between river flow and marine influx of oxygen across the scenario simulations, and a similar relationship between hypoxia in the harbour and ocean influx of oxygen. These scenarios show that hypoxia in the harbour is consistently reduced by increasing marine input of oxygen [note that this relationship will vary with confounding factors such as contrasting anthropogenic load].

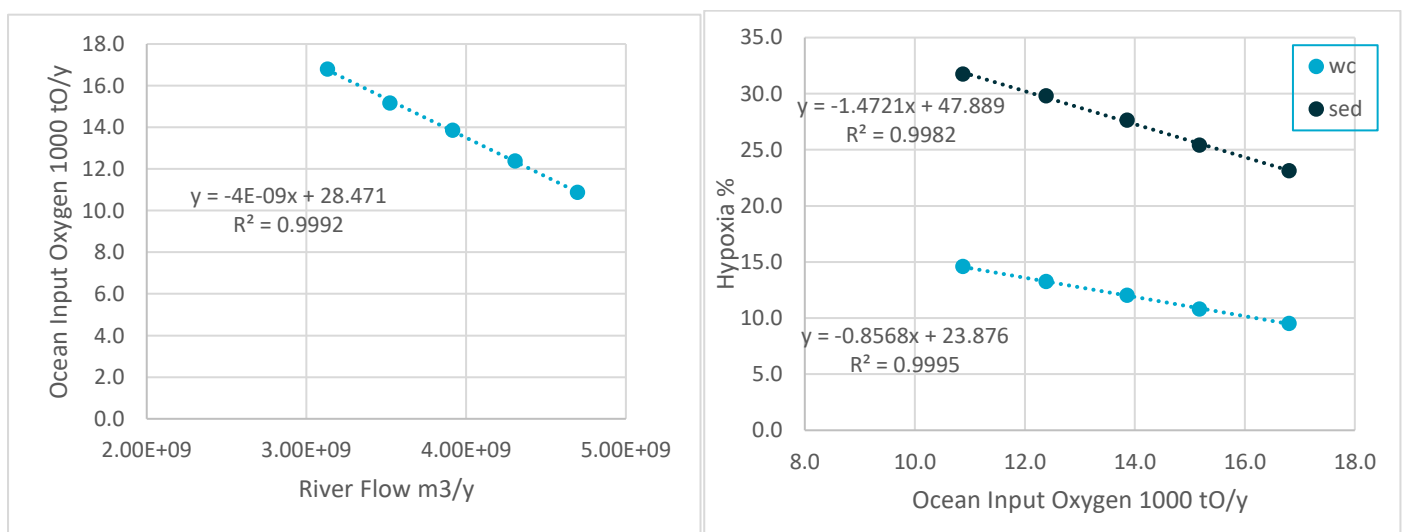


Figure 4.34 Relationship between marine influx of dissolved oxygen and river flow (left) and the relationship between hypoxia and marine influx of dissolved oxygen (right) [for water column hypoxic volume (blue) and sediment hypoxic area (black)].

## 4.6.2 Harbour Oxygen Under Persistent Drier or Wetter Conditions

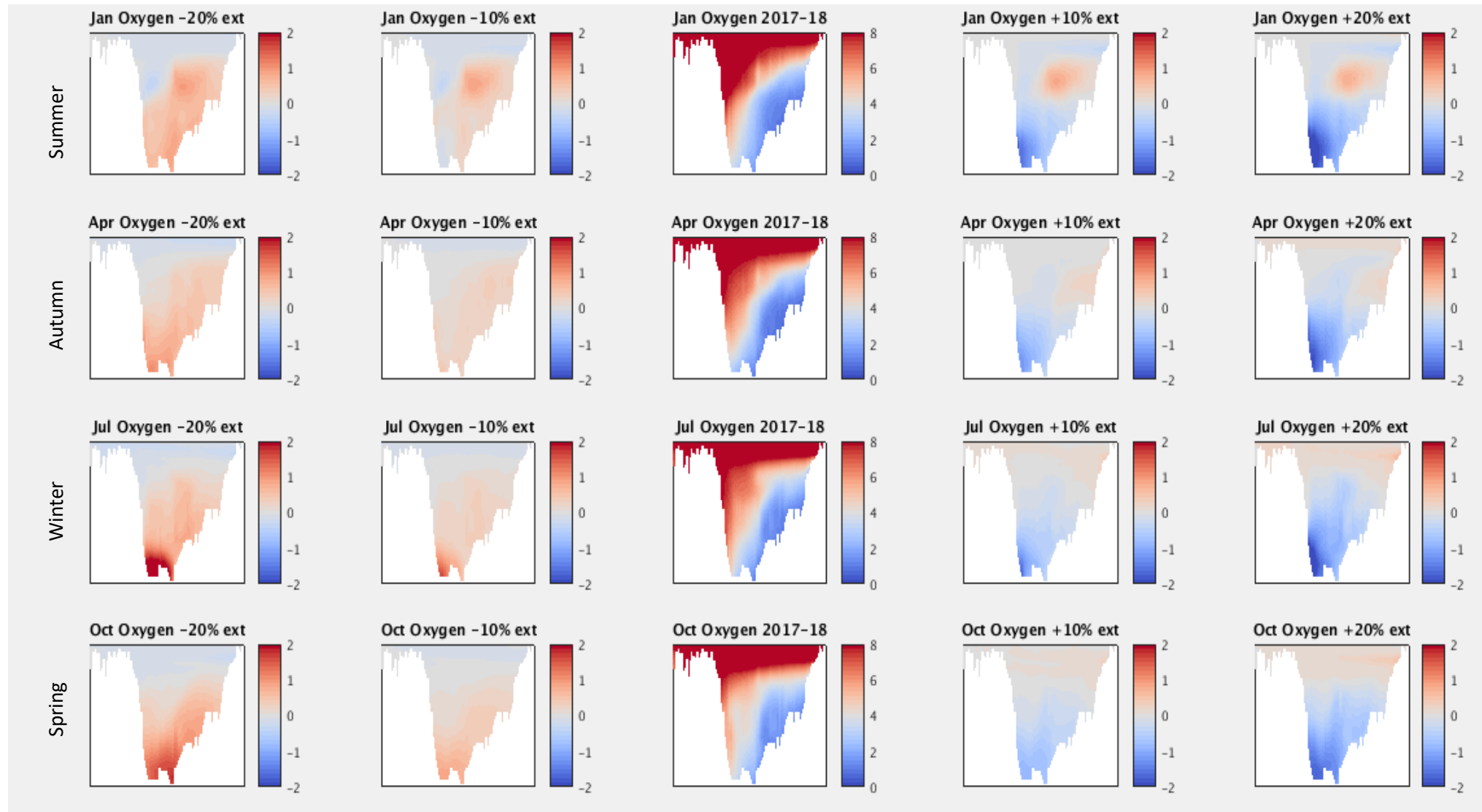


Figure 4.35 Monthly mean dissolved oxygen concentration (centre column) with oxygen anomalies for the drier scenarios extended for a 2 further years (to the left) and oxygen anomalies for the wetter scenarios extended for a 2 further years (to the right). Note that the centre plot shows the actual mean condition in 2017-18, whilst all other plots are anomalies from this condition. All units are mg/l.

Under persistent drier or wetter conditions, patterns noted in the initial 2 years of scenario simulation became more established (Figure 4.35). Persistent drier conditions led to increased oxygen concentrations at depth in all seasons (c.f. 2017-18), with greatest increase in the very dry (-20% river flow) scenario. Persistent wetter conditions led to a reduction in dissolved oxygen at depth with greatest reduction in the very wet scenario (-20% river flow). In summer, midwater oxygen concentrations in the central harbour were slightly higher (+1 mg/l) than in the initial scenario simulations; this reflects the evolution of the persistent scenarios initial condition (c.f. the original scenario simulations) following a reduction in 2018 fish farm oxygen respiration. The persistence of this anomaly demonstrates the impact of the long residence time of deep water in the harbour; under wetter conditions deep water residence time increases and this positive anomaly can still be seen in autumn.

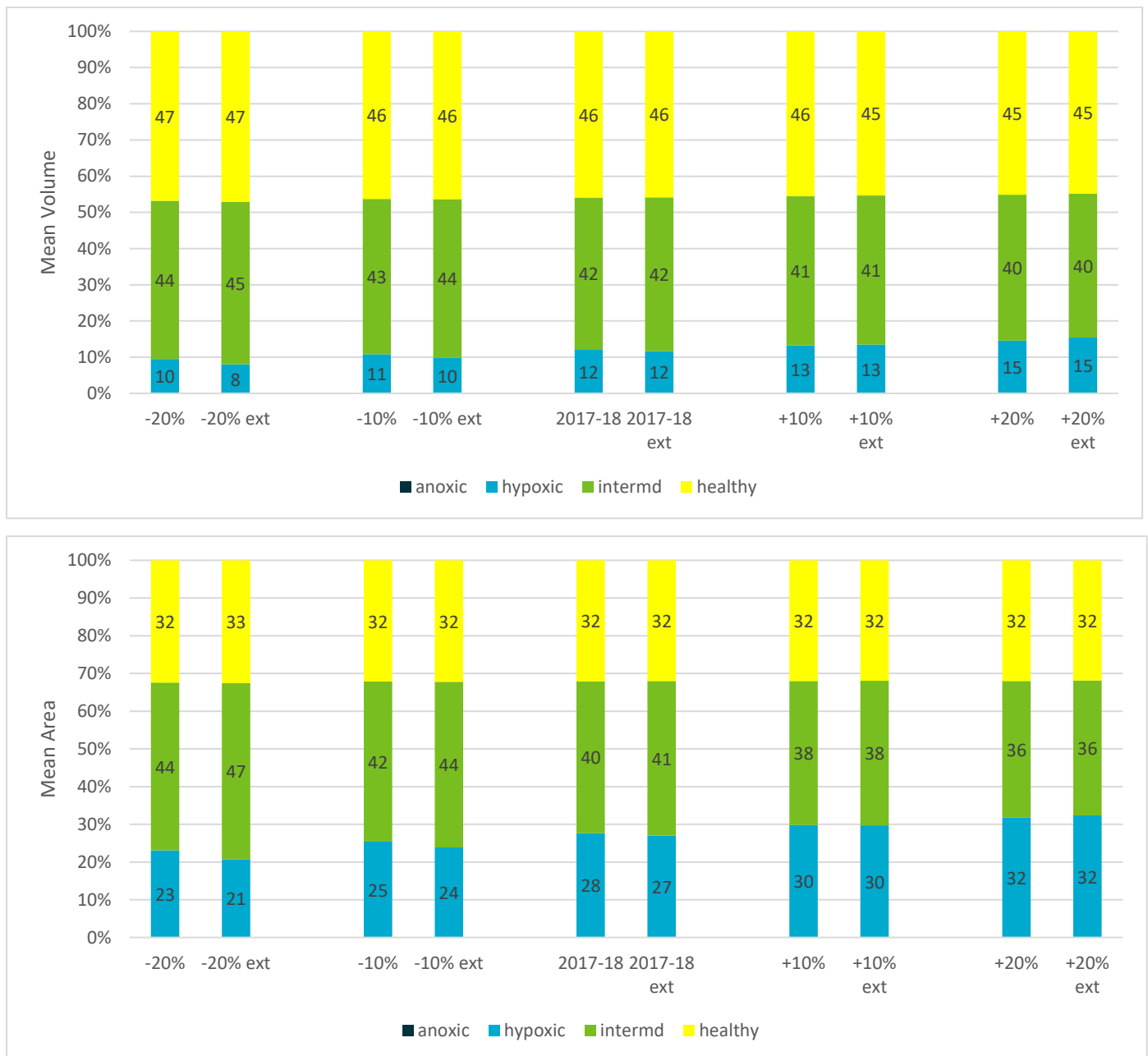


Figure 4.36 Simulated annual mean pelagic volume (top) and surface sediment area (bottom) with hypoxic (1-30% oxygen saturation), intermediate (30-80% oxygen saturation) and healthy (>80% oxygen saturation) status for each scenario. Drier scenarios are shown on to the left of the 2017-18 condition (central) and wetter scenarios are shown to the right as pairs of columns for the original and extended scenario simulations.

Oxygen conditions (with respect to hypoxic, intermediate and healthy classification of the harbour), under persistently drier and wetter conditions were similar to the original simulations in most cases (Figure 4.36). The exception was in the slight reduction in volume and area of hypoxia under persistently drier conditions; this was matched by a small but corresponding increase in the volume of water and area of sediment classified with >30% oxygen saturation. The largest impact was seen in the very dry scenario (-20% river flow) with a 2% reduction in annual mean hypoxic volume and hypoxic sediment area. The relationship between hypoxia in the harbour and river volume (Figure 4.37) shows the consistent decrease in hypoxia under reduced river flow and a very slight (<1%) increase in hypoxia under very wet (+20% river flow).

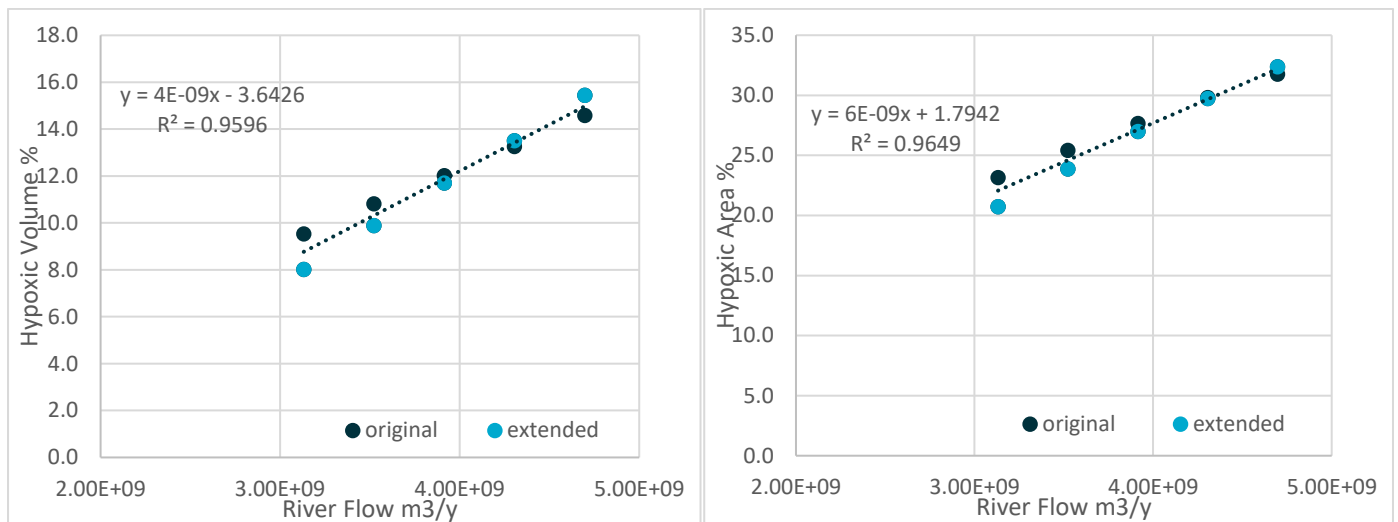


Figure 4.37 Simulated annual mean hypoxic pelagic volume (left) and hypoxic surface sediment area (right) variation with total river inflow for each scenario [original 2 year simulation shown in black, extended 2 year simulation shown in blue].

The oxygen budgets calculated for the persistent scenarios show comparable results to the original simulations (Figure 4.38). As before the greatest influx of oxygen to the harbour was from river input which was matched by a proportional discharge to the ocean for each flow scenario. Marine influx to the harbour was greatest for the drier scenarios and the input of oxygen from ecological processes was slightly greater for the drier scenarios. Where very slight differences were noted in the fluxes these were due to the difference in initial condition for the persistent scenario (which was generated by the former model runs in each case).

Overall the net budget for the persistent scenario simulations varied in a similar pattern to the original scenarios with drier conditions resulting in a slightly greater drawdown in oxygen c.f. the wetter scenarios. The very slight differences in fluxes from the original to the extended scenario simulations were systematic, and resulted in a small reduction in the net oxygen deficit for each scenario. In all cases the persistent scenario simulations had a smaller oxygen deficit than the original scenario runs, with the very wet (+20% river flow) scenario having the smallest oxygen deficit.

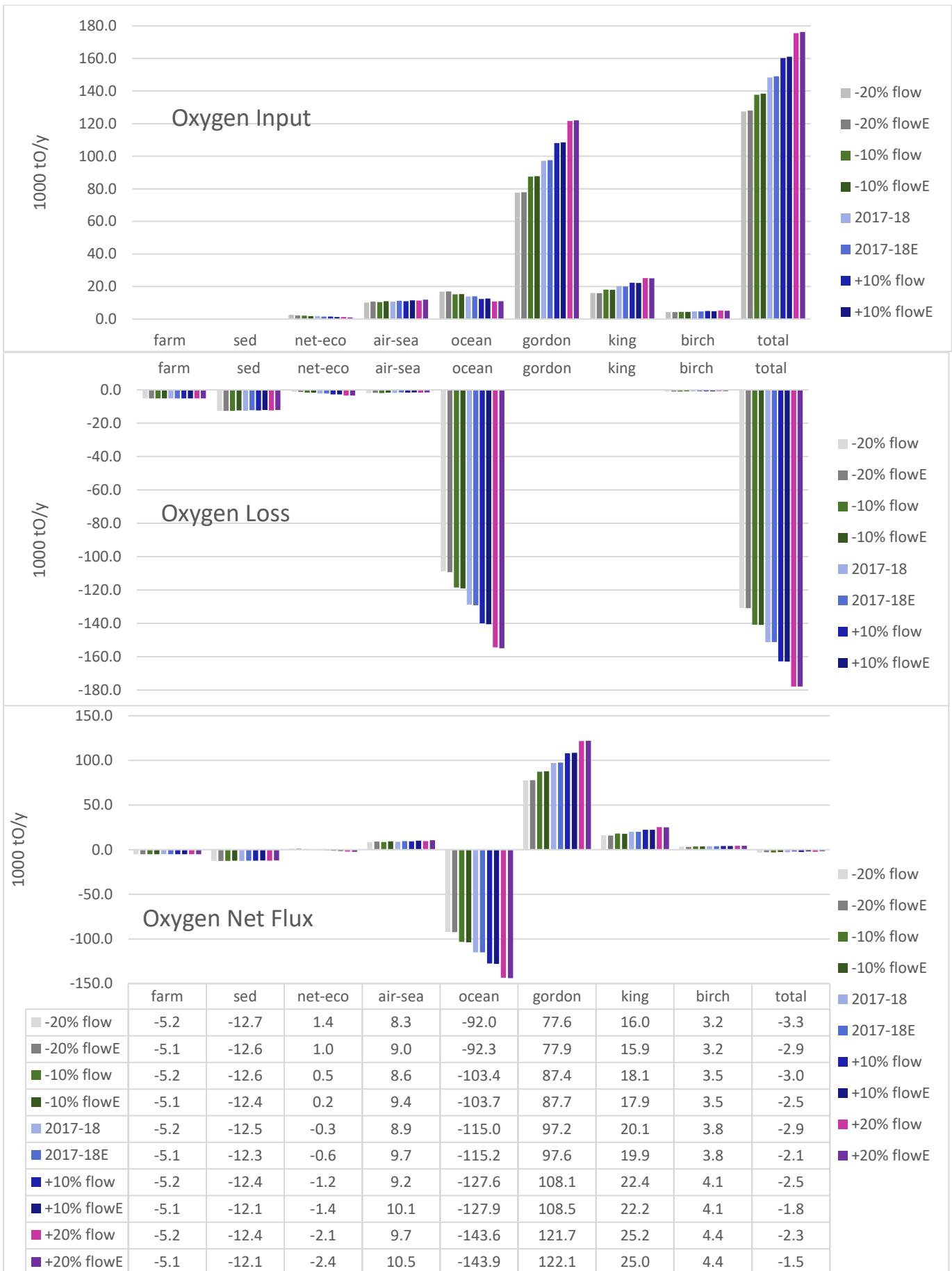


Figure 4.38 Simulated dissolved oxygen input (top), loss (middle) and net flux (bottom) in Macquarie Harbour for all scenarios. Drier scenarios are shown on to the left of the 2017-18 condition (central pale blue bar) and wetter scenarios are shown to the right, in pairs of columns for each original and extended (E) scenario simulation.

For the original scenario simulations we showed that there was a strong linear relationship between river flow and marine influx of oxygen across the scenario simulations, and a similar relationship between hypoxia in the harbour and ocean influx of oxygen (Figure 3.34). Analysis of the persistent scenario simulations shows that this relationship is robust over extended timescales (Figure 4.39). Hypoxia in the harbour is consistently reduced by increasing marine input of oxygen [note that this relationship will vary with confounding factors such as contrasting anthropogenic load].

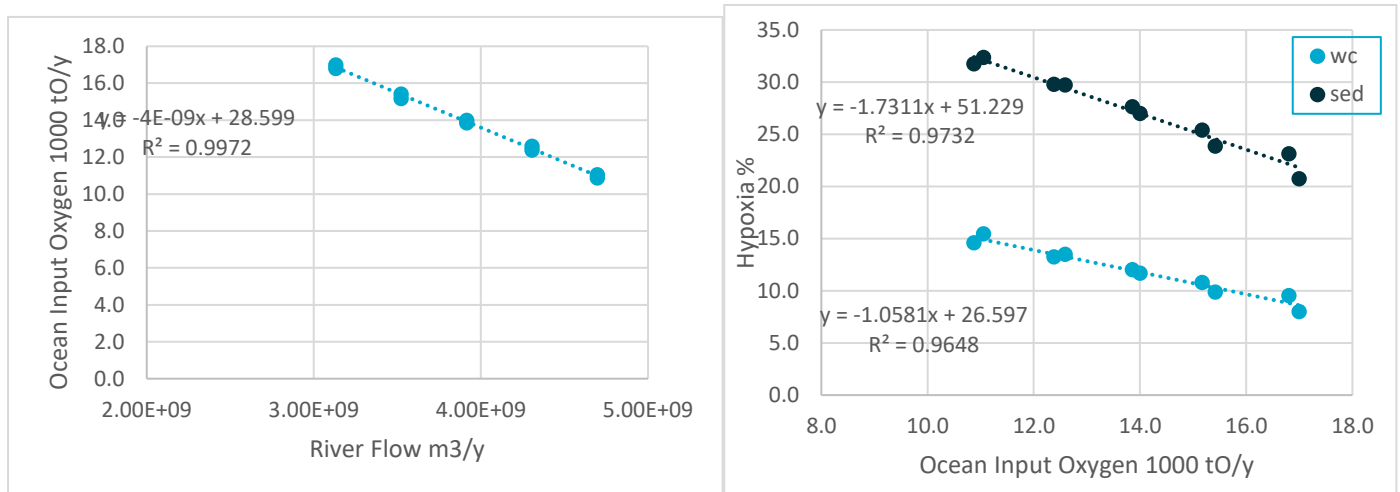


Figure 4.39 Relationship between marine influx of dissolved oxygen and river flow (left) and the relationship between hypoxia and marine influx of dissolved oxygen (right) for all original and extended model scenarios [right figure - water column hypoxic volume is shown in blue; sediment hypoxic area is shown in black].

### 4.6.3 Harbour Water Quality Under Reduced Anthropogenic Load

To explore the impact of anthropogenic loads on dissolved oxygen conditions in the harbour, a scenario simulation was run omitting fish farm oxygen drawdown and dissolved and particulate waste. [Note that the small amount of waste from Strahan sewerage treatment plant remained in the simulation.] To investigate persistent changes in the environment the simulation was also extended for a further 2 years by repeating the 2017-18 hydrodynamic conditions.

Monthly mean distributions of dissolved oxygen (Figure 4.40) show an increase in dissolved oxygen in all seasons, particularly in mid water for the simulation with reduced anthropogenic load. The extended model scenario showed a greater increase in dissolved oxygen (>2mg/l) in a similar pattern throughout the harbour in particular in the mid and southern part of the harbour.

Classification of oxygen conditions as anoxic (<1% oxygen saturation), hypoxic (1-30% oxygen saturation), intermediate (30-80% oxygen saturation) and healthy (>80% oxygen saturation) showed a 50% reduction in hypoxic volume and a 40% reduction in hypoxic sediment area under reduced anthropogenic loads c.f. conditions in 2017-18 (Figure 4.41). For the extended scenario run hypoxia was further reduced; healthy water volume increased from 46% in 2017-18 to 56% and healthy sediment area increased from 32% in 2017-18 to 36% of the total harbour area.

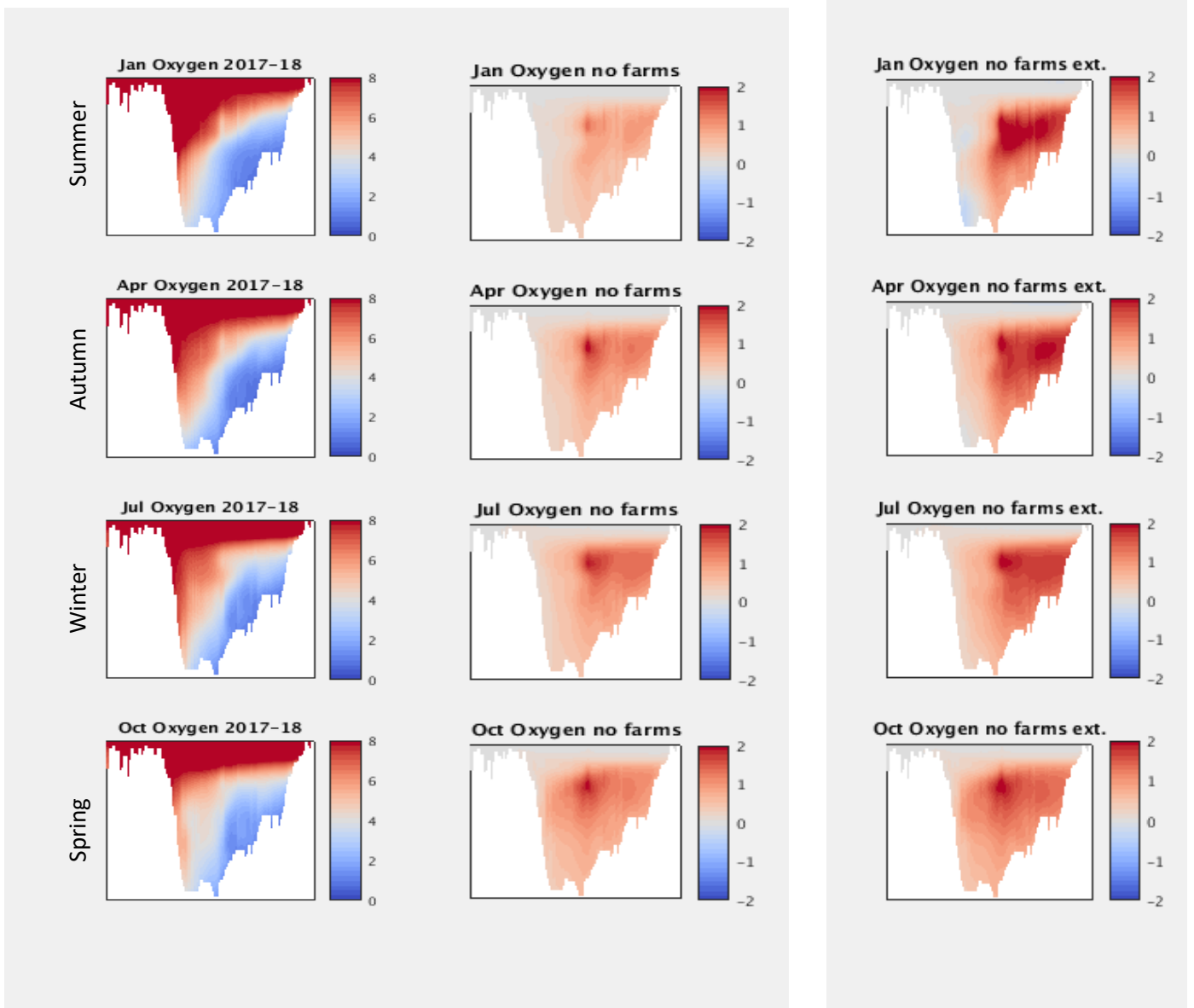


Figure 4.40 Monthly mean dissolved oxygen concentration in 2017-18 (left), oxygen anomaly simulated in the no fish farm scenario (centre) and in the no fish farm scenario extended for a further 2 years (right). Note that the left hand plots show the actual mean condition, whilst the right hand plots are anomalies from this condition. All units are mg/l.

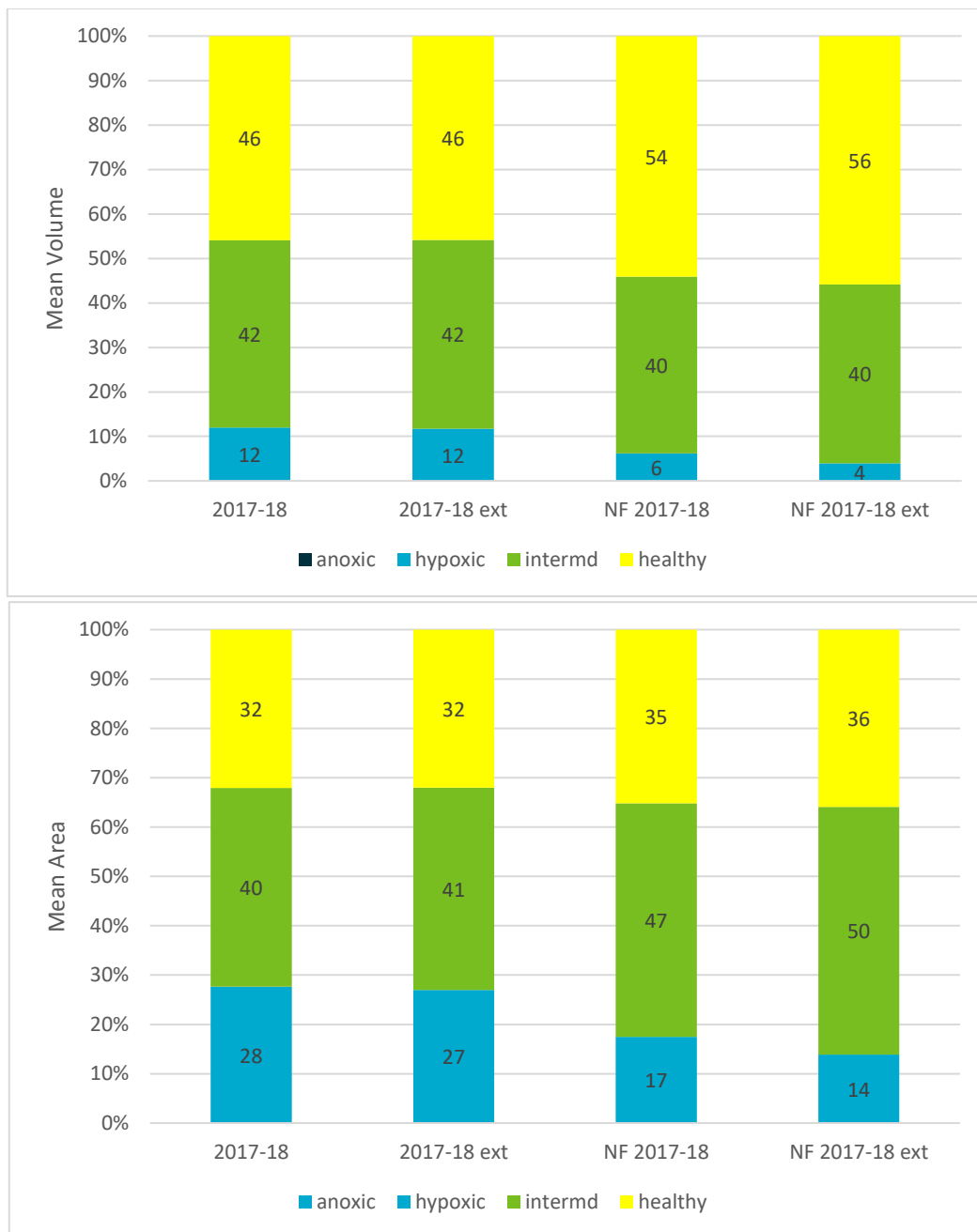


Figure 4.41 Simulated annual mean pelagic volume (top) and surface sediment area (bottom) with hypoxic (1-30% oxygen saturation), intermediate (30-80% oxygen saturation) and healthy (>80% oxygen saturation) status for the 2017-18 condition (left pair) and the reduced anthropogenic load scenarios (right pair) for the original and extended scenario simulations.

The oxygen budget analysis (Figure 4.42) shows that under reduced anthropogenic loads, river and marine oxygen fluxes remained similar to conditions in 2017-18. Differences in the net oxygen flux to the harbour were primarily due to the omission of fish farm oxygen drawdown, a very slight reduction in sediment oxygen demand (for detrital remineralisation and denitrification) and a small increase in pelagic oxygen demand, likely due to a reduction in anthropogenic nutrient fuelled photosynthesis.

The net budget is small relative to the large river and marine fluxes and should be considered in the context of potential uncertainty in the estimated river flow or harbour entrance bathymetry. Nevertheless the reduced anthropogenic load scenario and persistent reduced anthropogenic load scenario suggest that the net oxygen deficit would be reduced by >50% compared to 2017-18 conditions.

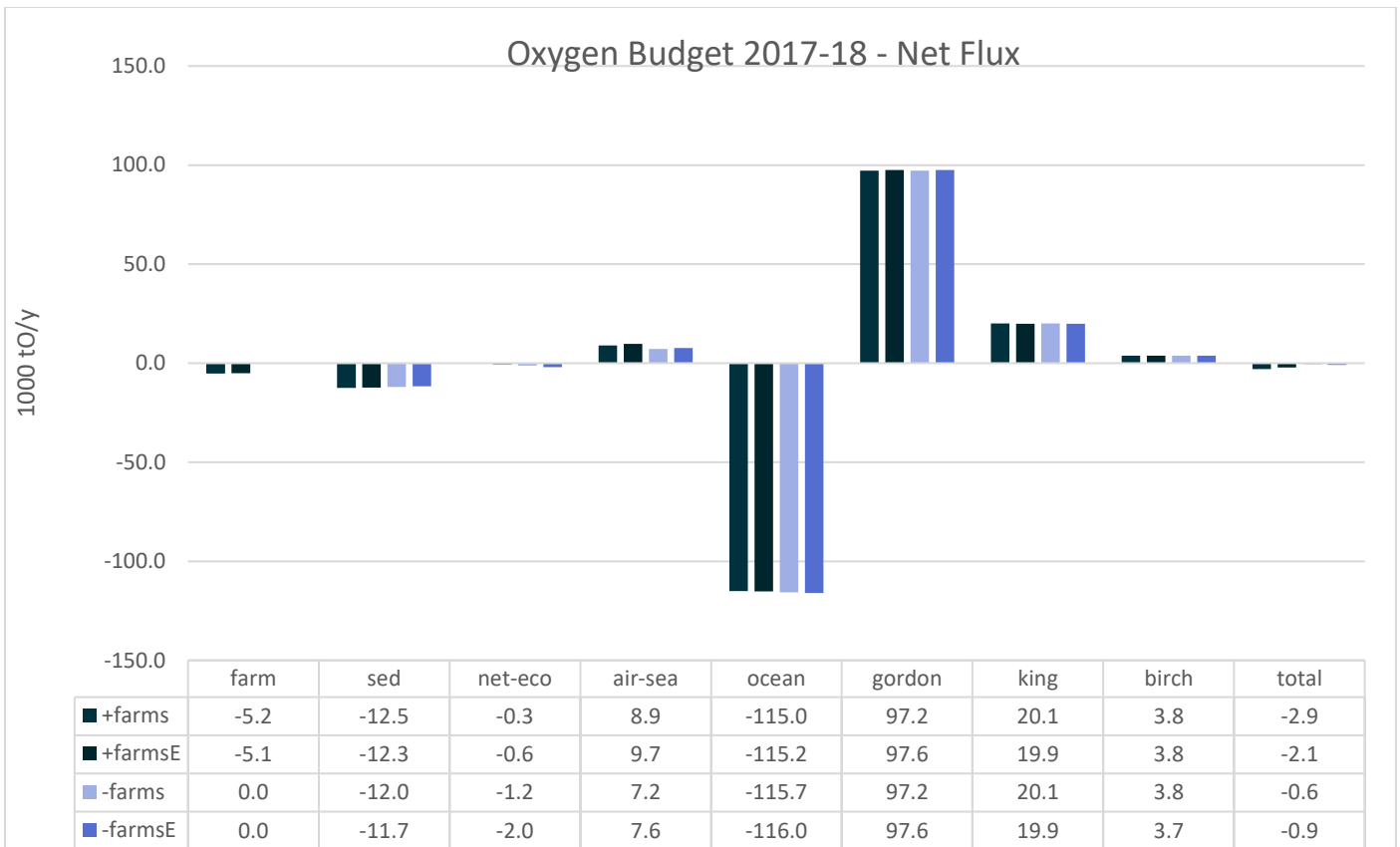


Figure 4.42 Simulated net flux of dissolve oxygen in Macquarie Harbour for the 2017-18 condition (left pair) and the reduced anthropogenic load scenarios (right pair) for the original and extended scenario simulations.

With the multiple wetter and drier river flow scenarios it was possible to characterise the systematic oxygen response associated with variations in annual drier or wetter conditions. For similar understanding with respect to anthropogenic loads, a range of load scenarios should be considered. In Figure 4.43 we have plotted hypoxia vs ocean oxygen input for all scenarios; the reduced anthropogenic load scenarios show a significant reduction in hypoxia under comparable ocean oxygen influx c.f. all other scenarios.

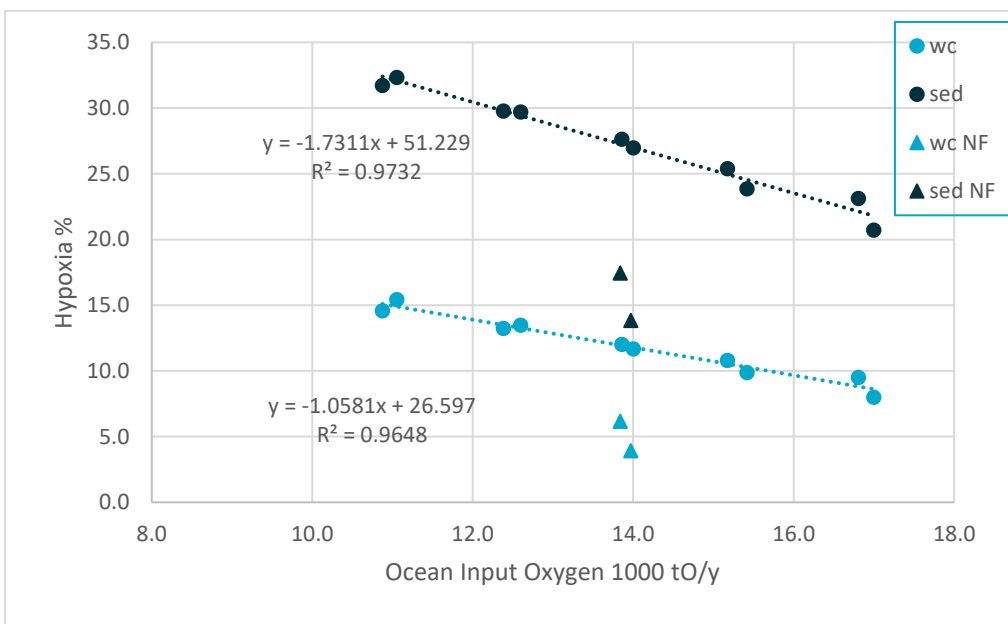


Figure 4.43 Relationship between hypoxia and marine influx of dissolved oxygen for all original and extended model scenarios [water column hypoxic volume is shown in blue; sediment hypoxic area is shown in black; triangles denote analysis from the scenario with reduced anthropogenic loads].

# 5 New Observations

## 5.1 Optical properties

The waters of Macquarie Harbour are optically complex due to the high levels of coloured dissolved organic matter (CDOM) in surface waters overlying clearer, more saline waters at depth. The high levels of colour in the surface waters influence light penetration and thus the growth of phytoplankton species that rely on photosynthesis for nutrition. The phytoplankton community observed (see later discussion) is thus one that can adapt to the specific light and nutrient conditions observed in the harbour. The spectral properties of the water column can be assessed by measuring the optical properties of water samples collected at a range of depths. Total absorption of the sample can be calculated as:

$$a(\lambda) = a_{ph}(\lambda) + a_d(\lambda) + a_{CDOM}(\lambda) + a_w(\lambda)$$

where  $a_{ph}$ ,  $a_d$ ,  $a_{CDOM}$  and  $a_w$  are absorption coefficients ( $m^{-1}$ ) due to phytoplankton, detrital or non-algal matter, CDOM and water respectively (Clementson et al 2004) at a specific wavelength  $\lambda$ .

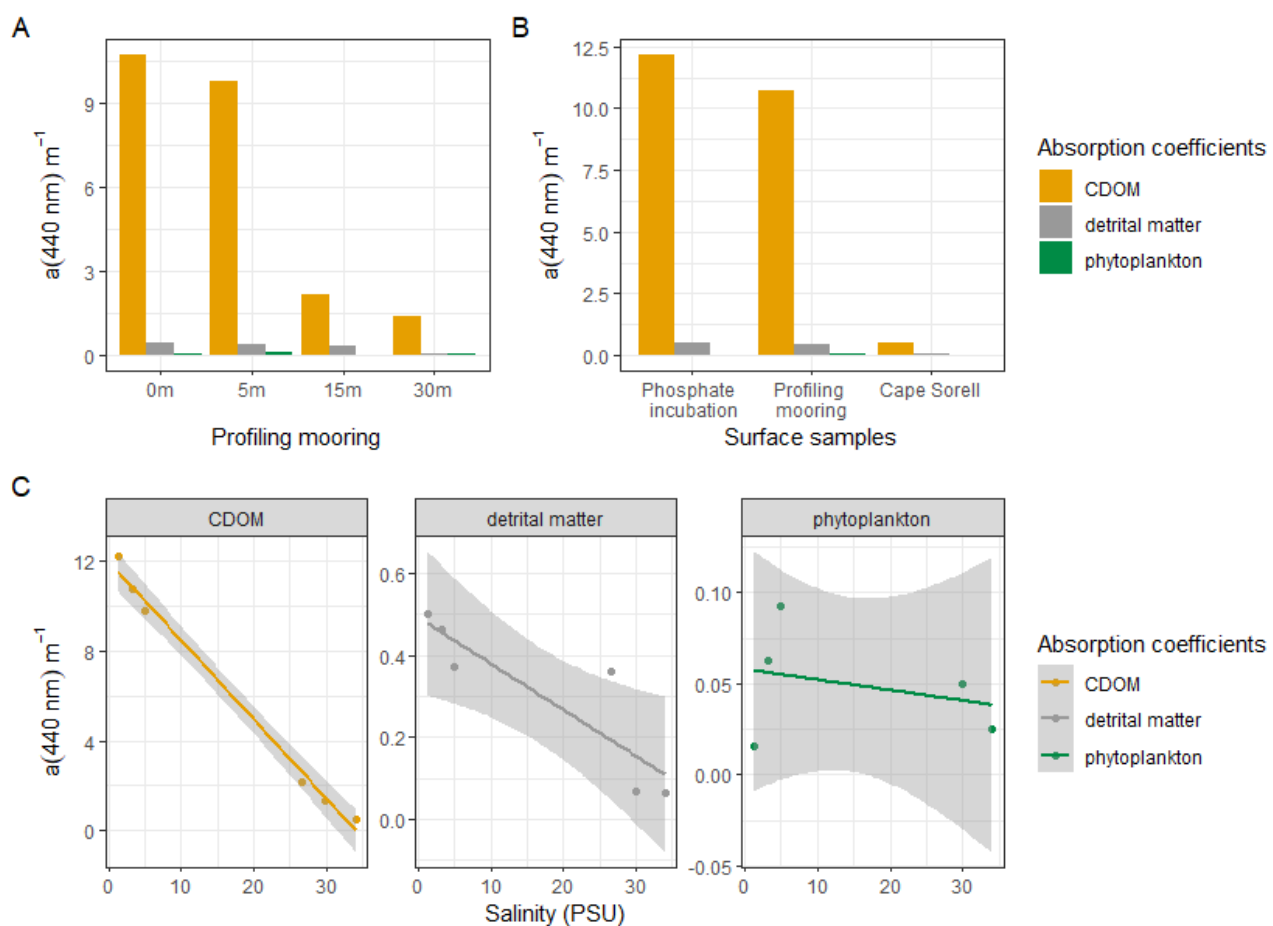


Figure 5.1 Absorption coefficient for chromophoric dissolved organic matter (CDOM), detrital or non-algal matter, and phytoplankton at 440 nm, for A) samples collected from the profiling mooring B) surface samples from within (incubation site and profiling mooring) and outside (Cape Sorell) of the harbour and C) the relationship between  $a(440nm) m^{-1}$  and salinity for all samples.

At the profiling mooring,  $a_{CDOM}(440 nm)$  dominates the absorption properties at all depths (Figure 5.1), with levels highest in the surface sample ( $10.75 m^{-1}$ ), and decreasing slightly at 5 m ( $9.78 m^{-1}$ ), and then greatly reduced in the more saline waters at depth ( $2.16$  and  $1.37 m^{-1}$  respectively). High values in surface

waters and lower values in more saline waters are similar to data reported for detailed surveys of the Huon Estuary (range 12.78 to 0.58 m<sup>-1</sup>, Clementson et al 2004) and other tannin affected freshwater bodies in Tasmania. Both CDOM and detrital matter contribute significantly greater to the total absorption than phytoplankton. The absorption spectra over the whole range of wavelengths scanned (350 – 800 nm) for all surface samples (**Error! Not a valid bookmark self-reference.**, and the 4 depths sampled at the profiling mooring samples (Figure ) show that high salinity waters outside the harbour, or at depth have similar properties with low contributions of CDOM, detrital or phytoplankton compared to DOC rich surface waters.

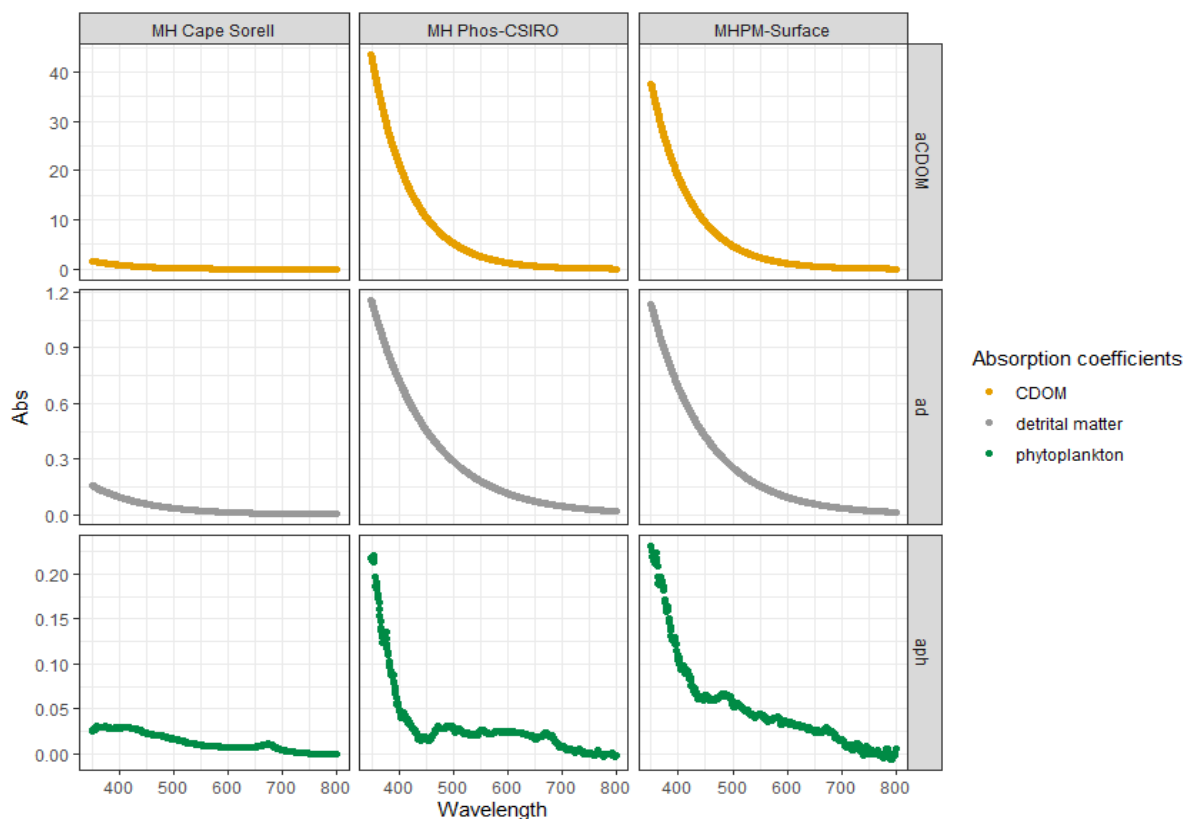


Figure 5.2 Absorption spectra for surface samples collected outside (Cape Sorell) and inside (Phosphate incubation site, Profiling mooring site) the harbour in December 2019.

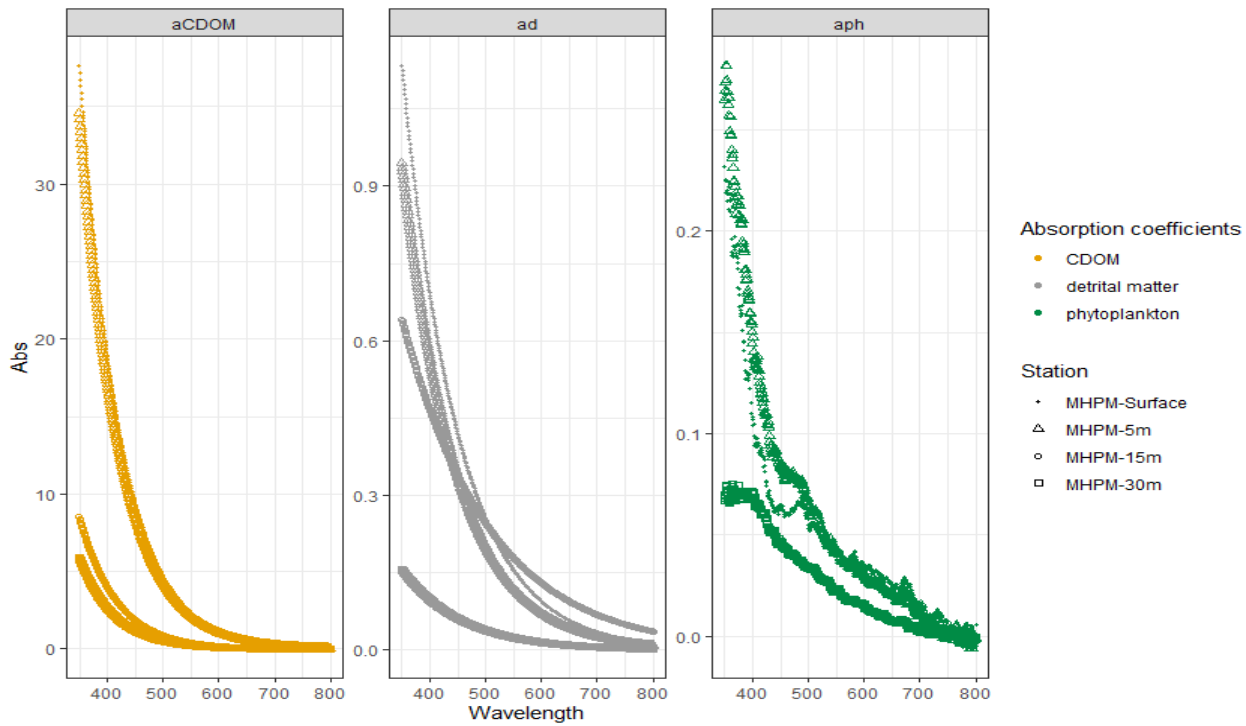


Figure 5.3 Absorption spectra for samples collected from 4 depths at the profiling mooring location, December 2019.

Using other measures of surface water clarity, Total Suspended Sediment (TSS) concentrations at the surface were relatively low at all sites, varying between 1.64 and 2.04 g m<sup>-3</sup>, with organic fraction > inorganic fraction inside the harbour, and the opposite in marine waters outside (Figure 5.4).

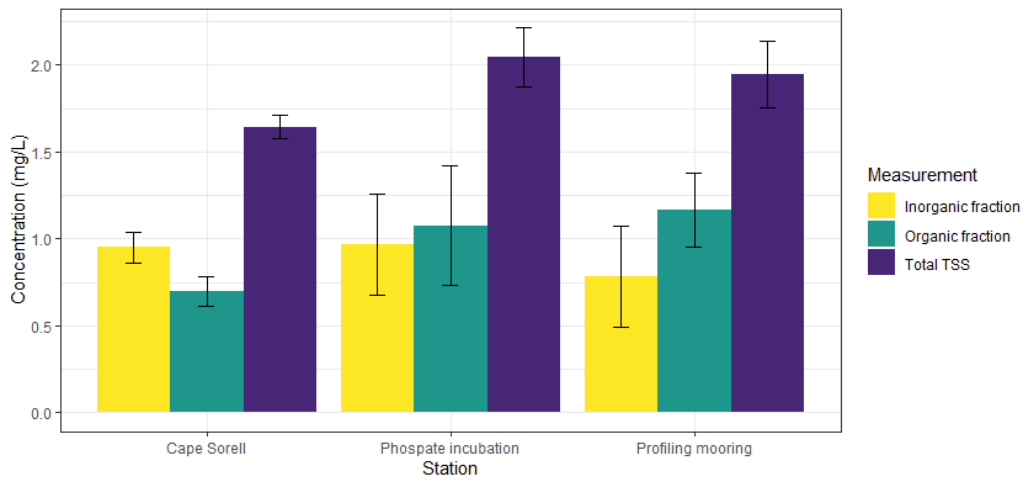


Figure 5.4 Inorganic, organic and Total Suspended Solids (TSS) concentrations in surface samples during the December 2019 survey.

## 5.2 Water column profiles

As part of the December 2019 survey work, water column profiles at several sites were measured with multiple sensor packages. The primary data source was a Xylem EXO2 unit on the CSIRO2 profiling mooring, equipped with sensors for temperature, salinity, dissolved, oxygen, chlorophyll a fluorescence, phycoerythrin fluorescence, DOM fluorescence, and pH. The profiling mooring collects data on the downcast every 2 hours, at 1 m intervals. A hand-held Xylem EXO2 unit which replicated the profiling

mooring sensor package was also deployed, as was a Seabird CTD with temperature, salinity, oxygen, chlorophyll *a* fluorescence and PAR sensors.

Data from all three packages deployed at the profiling mooring during the December calibration exercise are shown in Figure . The three sensor packages show good agreement with salinity and oxygen samples analysed from 4 discrete depths by the CSIRO Hydrochemistry Laboratory. There is some variation between profiles recorded on two separate days with the hand-held EXO2 unit. The Seabird PAR sensor shows light penetration is limited to the first 1-2 meters before becoming negligible below ~4m, attributed to the high concentrations of CDOM observed in surface waters (Figures 5.2-5.4).

Whilst the agreement between all sensor packages is reasonably consistent for chlorophyll *a* (i.e. all sensors show the same broad trend of higher concentrations in the surface waters and lower and invariant concentrations below 10m), the offset between the discrete bottle samples collected at 4 depths and analysed by HPLC is significant. For phycoerythrin (PE, indicative of red algae and cryptophytes) a significant offset was observed between the two EXO2 packages, and interestingly the hand-deployed unit which had been factory calibrated prior to the December survey reported consistently higher concentrations, but the same trends. An expanded view of the PE data only (Figure 5.6) shows that PE values, analysed by spectrofluorometry, are very low, and at maximum concentration at 5m depth. As with the chlorophyll *a* data, the PE data shows that the fluorescence measured by the EXO2 sensors overestimate the pigment concentrations. The most striking problem is that both sensors record high concentrations at depth, i.e.  $> 1 \text{ mg m}^{-3}$  of chlorophyll *a* at depths where the concentrations should be close to 0 (Figure 5.7). This may be caused by the incorrect calibration of the sensor (both in terms of dark count and gain) and/or interference of other optically active constituents present in the water and fluorescing at 685 nm. The comparison between the HPLC and the profiler data indicated an offset of about  $0.56 \text{ mg m}^{-3}$  and the slope of the fit close to 0.5 (Figure 5.8).

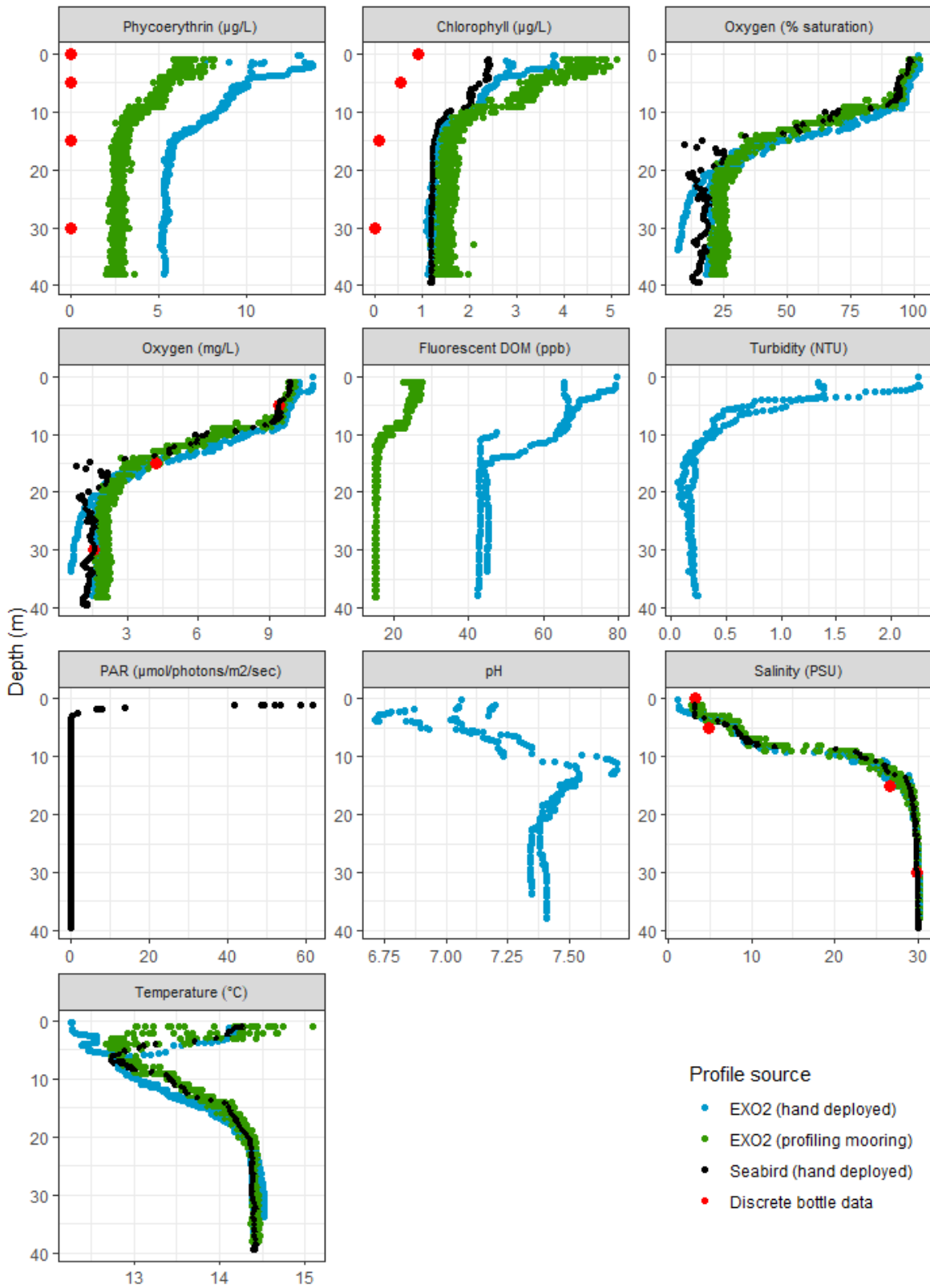


Figure 5.5 Sensor data from 3 profiling instruments December 10 -11 2019. Note that all 2 hourly profiles collected by the profiling mooring over this time period are shown in the plots. Calibration samples for salinity, oxygen and chlorophyll a (by HPLC) are shown as red dots.

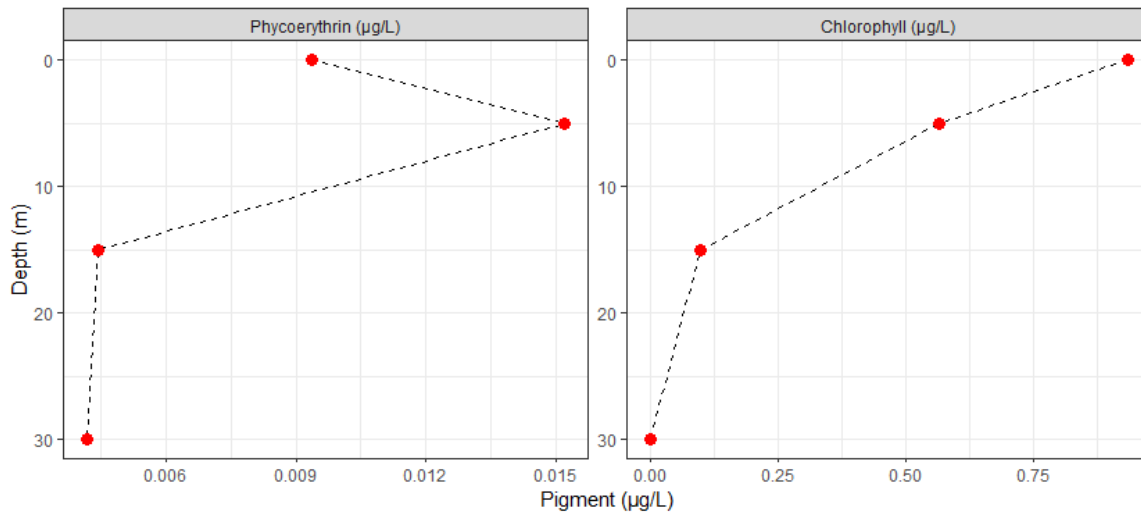


Figure 5.6 Phycoerythrin and MV chlorophyll *a* concentration measured by HPLC sampled from 4 discrete depths at the Macquarie Harbour profiling mooring, December 2019. Pigment concentration axes are expanded compared to Figure 5.5.

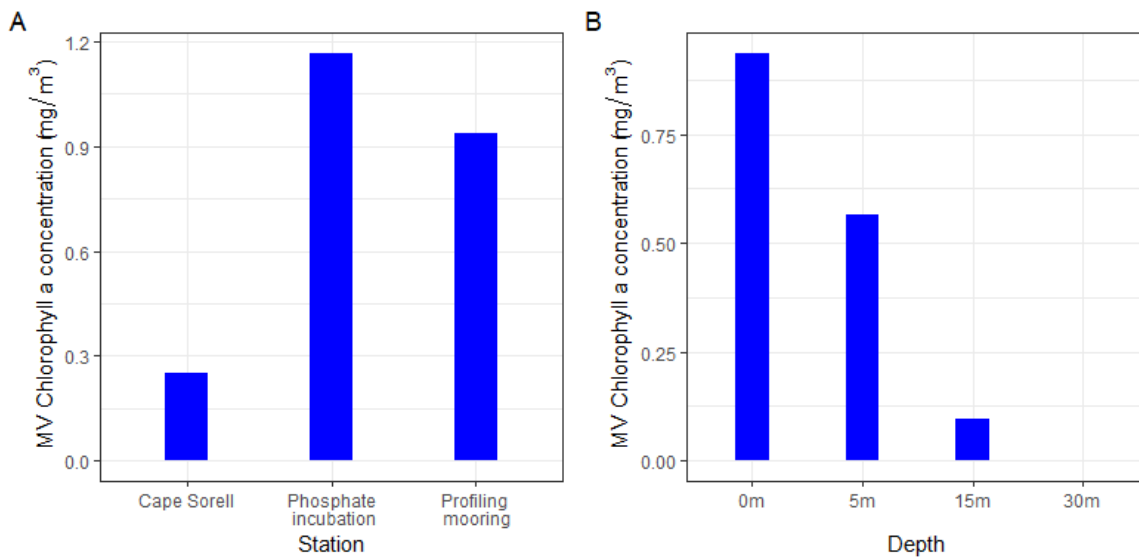


Figure 5.7 Chlorophyll *a* concentration in A) surface samples and B) discrete depths at the profiling mooring locations.

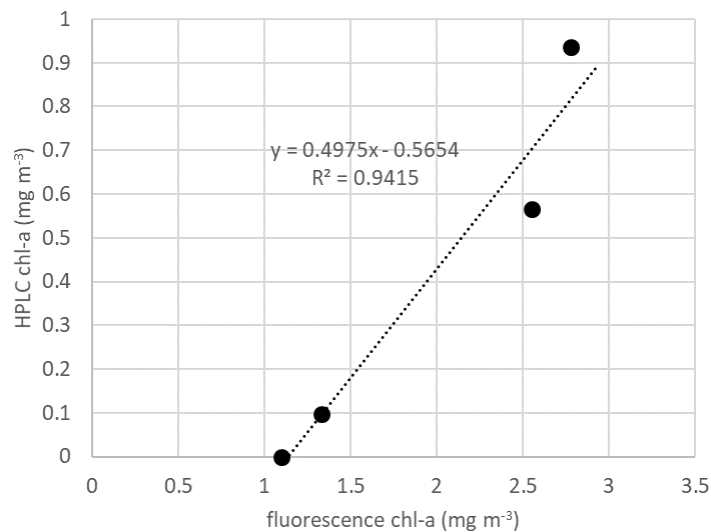


Figure 5.8 Comparison between fluorescence and HPLC-derived chlorophyll *a* concentration.

Nutrient samples (unfiltered) collected as part of the profiling mooring calibration exercise and the broader survey (Figure 5.9) showed that nitrate + nitrite and phosphate were low in surface waters, relative to deeper more saline waters, while ammonium and silicate were higher in surface waters. Note that no samples were collected from Cape Sorell.

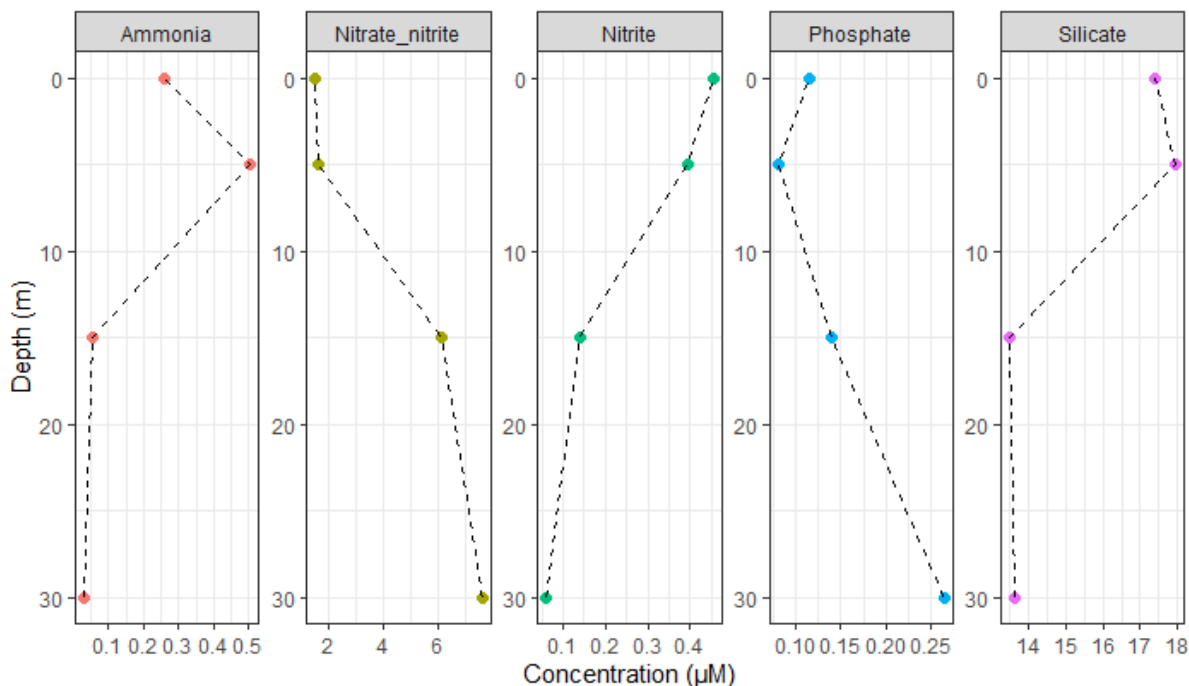


Figure 5.9 Nutrient concentrations (unfiltered) at the Profiling Mooring during the December 2019 field survey.

## 5.3 Phytoplankton composition

### 5.3.1 Marker Pigments

Certain pigments are unique to particular groups of phytoplankton and thus “marker” pigments can help resolve the phytoplankton community composition by normalising their concentrations against MV chlorophyll *a*. Marker pigments provide insights into many groups that cannot be resolved or suitably preserved for analysis by light microscopy. Plots of the marker pigments (normalised to MV Chlorophyll *a* concentration) for the December 2019 survey are shown in Figure 5.10.

The presence of alloxanthin indicates cryptophytes were present in all samples except the deepest profiling mooring sample. Alloxanthin concentrations in surface waters were higher inside the harbour than outside. Crocoxanthin is also indicative of cryptophytes but was only observed at the phosphate incubation site further south in the harbour. The diatom marker pigments, fucoxanthin, along with associated diadinoxanthin were observed in the surface samples from all sites but were not detected at depth at the profiling mooring. At Cape Sorell, haptophytes (Hex-fuco) and prasinophytes (prasincoxanthin, chl-b) were also present. The surface waters of the profiling mooring also contained dinoflagellates (indicated by peridinin). This data is broadly consistent with the microscopy analyses (see later discussion). The phycoerythrin data from the same samples are shown in Figure 5.11. Concentrations of this accessory pigment were highest inside the harbour, with maximum concentrations observed in the 5m sample. Cryptophytes have flexible nutrition strategies and are low light adapted, and the data suggests there is an

optimal niche in the upper layers of the harbour that provides an advantage to cryptophytes over other autotrophic taxa.

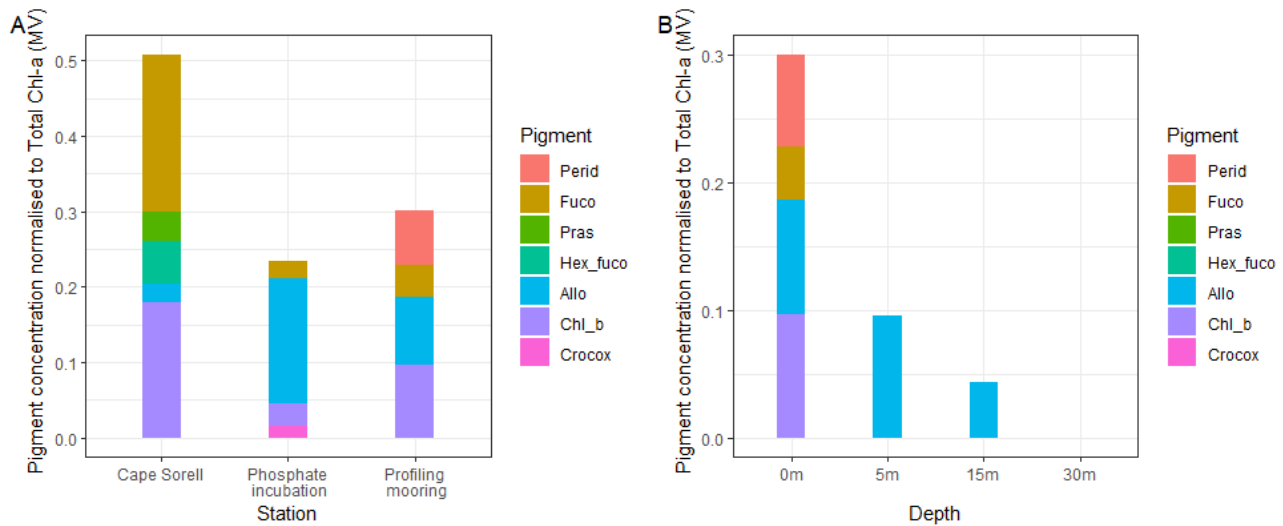


Figure 5.10 Pigment concentration normalised to chlorophyll a concentration from HPLC analysis for A) surface samples and B) at four depths from the profiling mooring, in December 2019.

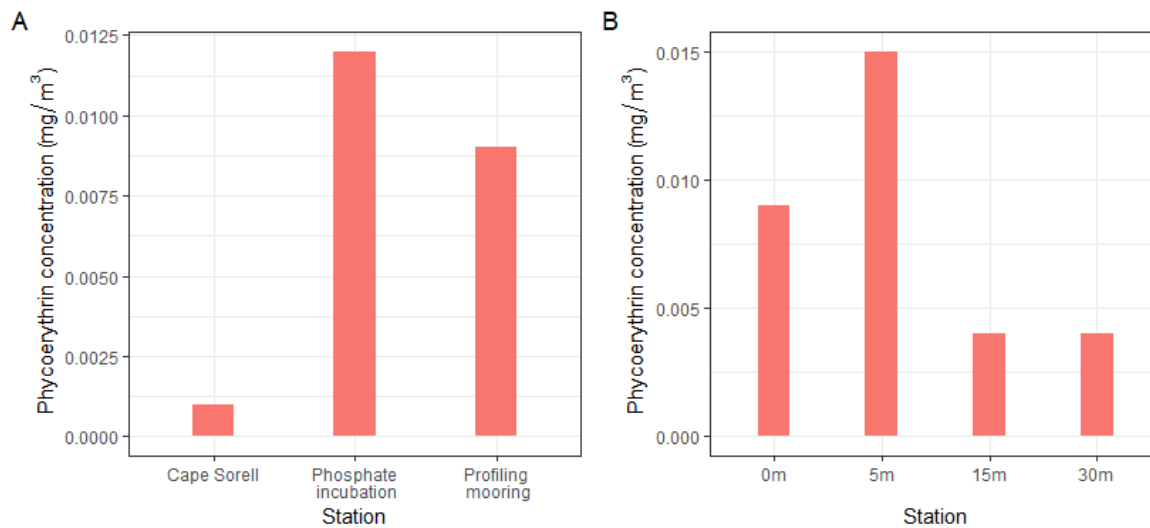


Figure 5.11 Concentrations of the accessory pigment phycoerythrin measured at A) surface samples from Cape Sorell, the phosphate incubation site and the profiling mooring and B) at four depths from the profiling mooring, in December 2019.

### 5.3.2 Picoplankton communities

As part of the investigations into phytoplankton communities and the calibration of the profiling mooring, samples for picocyanobacteria (*Prochlorococcus* and *Synechococcus*) were collected from the same sites and depths as the absorption and pigment data. No previous data exists for picocyanobacteria composition in the harbour, and because of their very small size (< 2 µm), they are not routinely discriminated in phytoplankton samples analysed by light microscopy.

Surface samples from Cape Sorell had the highest concentration of *Synechococcus*, but no *Prochlorococcus* were detected at the marine site. This sample was dominated by eukaryotes < 5 µm, and lesser amounts of eukaryotes > 5 µm. The southern harbour site (where surface water was collected from for the phosphate

incubation; -42.32701°S, 145.40901°E) had similar proportions of eukaryotes, but no *Synechococcus* or *Prochlorococcus*. Surface waters from the profiling mooring had traces of *Synechococcus*, most likely due to its closer proximity to the mouth of the harbour and the influence of more saline waters (Figure ).

At the profiling mooring site (Figure ), samples from the surface and 5 m depths showed similar composition, with the exception of trace amounts of *Synechococcus* present only in the surface waters. Abundances were significantly reduced in deeper samples from 15 and 30 m, and *Prochlorococcus* was absent from all samples. *Prochlorococcus* and *Synechococcus* both can produce phycoerythrin (PE) under certain light conditions (Kim et al., 2011; Steglich et al., 2005), but it can be inferred from these data that they are not contributing to the fluorescence response observed in Figure 5.5. The observations from the microbial community analysis confirmed that picocyanobacterial were only present in low concentrations in the surface sample from the profiling mooring site.

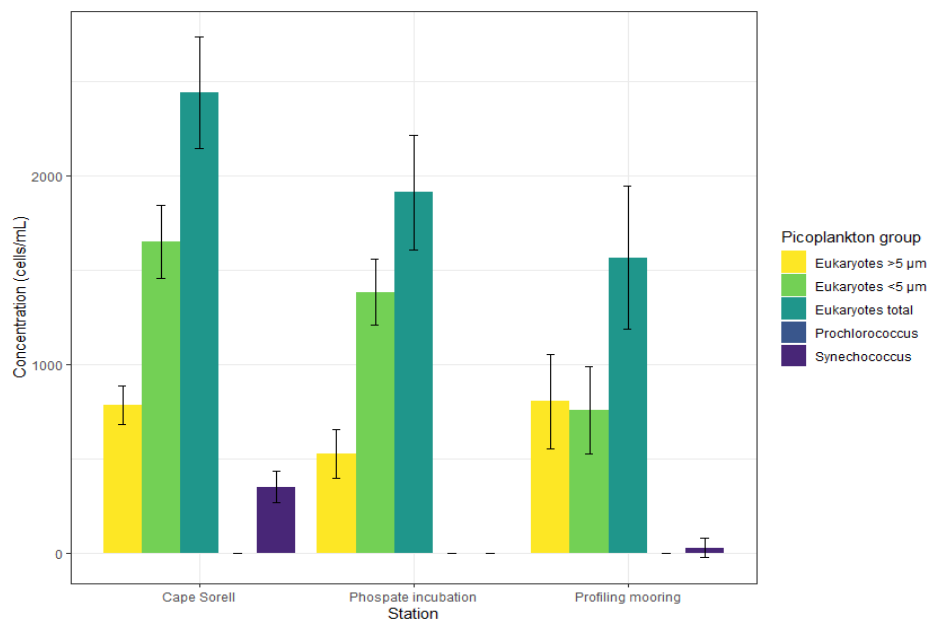


Figure 5.12 Abundance of picoplankton community in surface samples collected outside (Cape Sorell) and inside (Phosphate incubation site, Profiling mooring) Macquarie Harbour during the December field campaign.

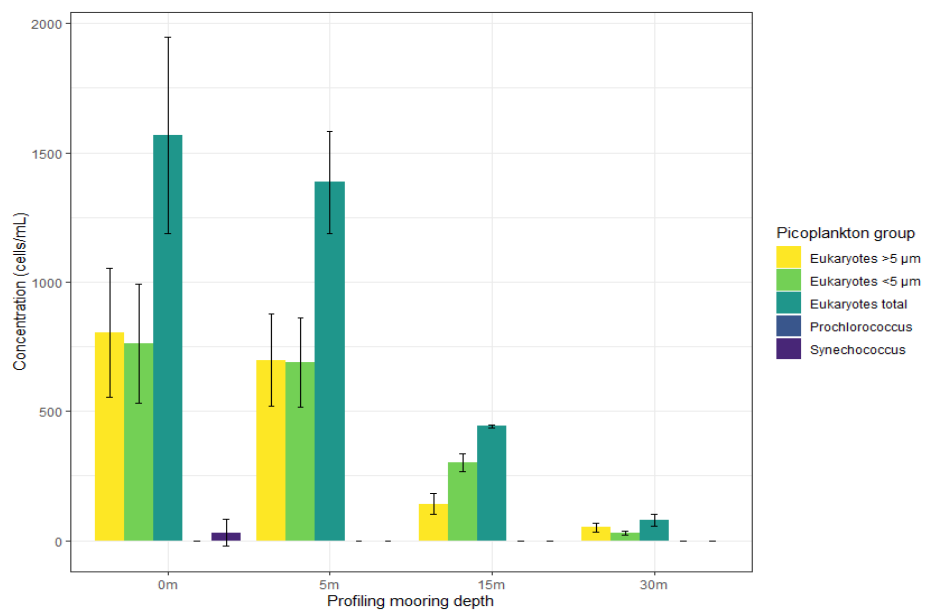
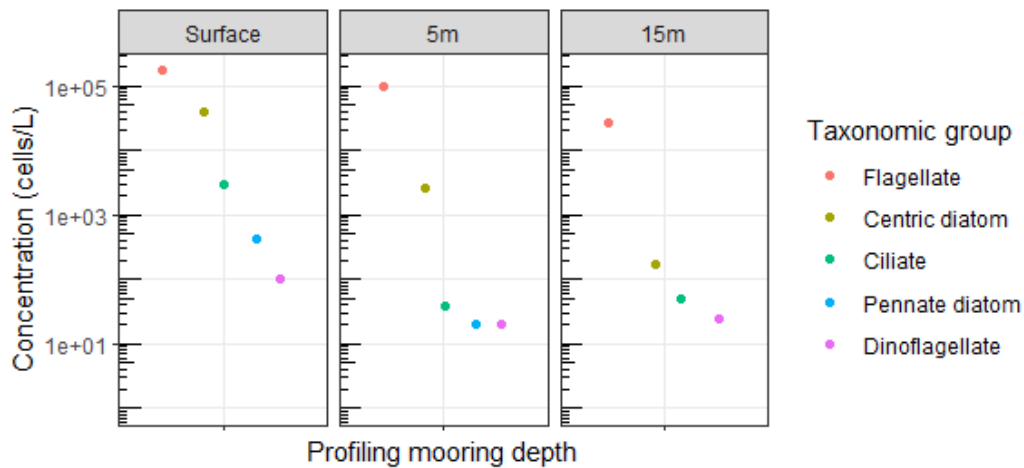


Figure 5.13 Picoplankton abundances for samples collected from 4 depths at the profiling mooring location, December 2019.

### 5.3.3 Light microscopy

A



B

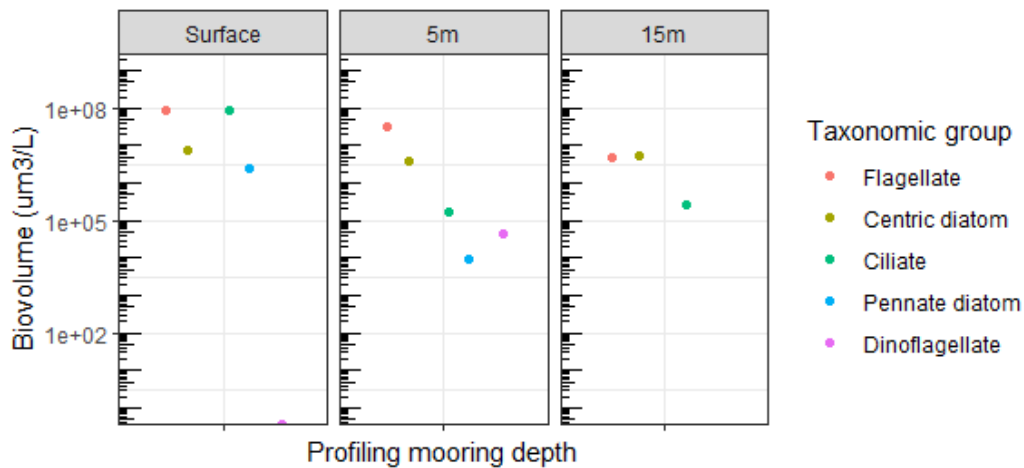


Figure 5.14 Major taxonomic groups present in the profiling mooring samples during the December 2019 field survey. No data for 30 m sample. Note log scale for A) abundance as cells/L and B) biovolume as  $\mu\text{m}^3/\text{L}$ .

Light microscopy on the profiling mooring samples was consistent with the community composition determined by HPLC. The most abundant group were the flagellates (Figure 5.14), which were dominated by cryptophytes in all samples. Small ( $< 10 \mu\text{m}$ ) chain forming centric diatoms were the next most abundant, followed by small numbers of naked ciliates around  $50 \mu\text{m}$  diameter. Pennate diatoms and dinoflagellates were present in all samples, but rare as were prasinophytes and filamentous cyanobacteria. Overall concentrations decreased with depth, consistent with the chlorophyll *a* (Figure 5.7), and picoplankton abundances (Figure 5.13). Surface samples had higher biovolumes than deeper samples for all taxonomic groups.

## 5.4 Phosphate addition process study

Results of the spatial nutrient survey in 2018 suggested that the waters of the harbour are phosphorous limited. To test the short time-scale effects of phosphorous addition on the bacterial and eukaryote community, we ran a pilot trial growth assay with surface waters collected in bulk in the December 2019 survey (collection site -42.32701°S, 145.40901°E). The surface water properties at the collection site were similar to those observed at the CSIRO profiling mooring site (see section 5.2).

Surface water was pre-filtered through 200 µm mesh to remove grazers and transferred into 2L clear polycarbonate bottles for a 48-hour incubation. A control (no phosphate addition), and two treatments (+0.5 µM phosphate and +2 µM phosphate) were run, in both natural light and complete dark conditions. Individual bottles were placed in 6 large tanks connected in series on the Strahan wharf to give natural light conditions. Surface water was pumped through the experimental tanks to maintain a realistic temperature regime. Samples were collected at the commencement (T0), after 24 hours (T1) and 48 hours (T2) to monitor biological response to the phosphate addition (Table 5.1).

Due to the large volume of water required for some of the analyses (pigment analyses, phycoerythrin, microbial community composition, microscopy), individual replicates (n=3) for each treatment (control, +0.5 µM phosphate added, + 2 µM phosphate added) were subsampled and pooled at each time point to provide sufficient water for those analyses. Nutrient samples (phosphate, ammonium, nitrate + nitrite, silicate) were collected from each replicate (with the average and SD presented in figures) and from the pooled sample to monitor how representative the pooled samples are of the conditions. Nutrients were monitored over the course of the experiment, and both filtered and unfiltered samples were collected from the pooled sample.

Table 5.1: Phosphate addition experiment sampling protocol. Parameters marked with \* indicate triplicate samples were pooled to provide enough volume for analysis.

	Treatment	Picocyanobacteria and total bacteria count	Nutrients	Microbial community composition (*pooled sample)	Pigments (*pooled sample)	Phycoerythrin (*pooled sample)	Phytoplankton community (*microscopy pooled sample)
LIGHT	Control	x	x	x	x	x	x
	+0.5 µM	x	x	x	x	x	x
	+2 µM	x	x	x	x	x	x
DARK	Control	x	x	x			
	+0.5 µM	x	x	x			
	+2 µM	x	x	x			

Samples for microbial community analysis from the pooled water samples were filtered onto 0.2 µm Sterivex filters, snap frozen in liquid nitrogen to stabilize the community found at the end of the

experimental incubation, and transferred to a -80°C freezer upon arrival to the CSIRO lab. DNA was extracted using the Qiagen PowerWater Sterivex Extraction kit following the manufacturer’s instructions. The DNA was used as template for tag sequencing of archaeal 16S rRNA, bacterial 16S rRNA and eukaryote 18S rRNA, respectively. Sequencing was done at the Ramaciotti Sequencing Centre (UNSW, Sydney, Australia) following the standard protocols for the Australian Microbiome initiative (Brown et al., 2018). Sequences were analysed following the standard informatics pipeline of the Australian Microbiome initiative (<https://www.australianmicrobiome.com/protocols/>). Statistical analysis of the results was carried out using the Primer statistical package and Microsoft Excel. The results will indicate which bacterial, archaeal and phytoplankton groups reacted to the addition of phosphate under light and dark conditions, providing an insight into the effect of phosphate limitation on the phytoplankton community of Macquarie Harbour. Only samples from light conditions are presented here.

### 5.4.1 Start conditions

To assess any potential change in the biological communities present in bulk water used for the incubation, samples collected as part of the field survey were compared to the start (T0) samples from the incubation. Pigment profiles were very similar with all pigments detected present in both samples (Figure 5.15). There was an increase in the picoplankton concentrations detected at the start of the incubation although small analysis volumes may contribute to increased uncertainty (Figure 5.16). No *Synechococcus* or *Prochlorococcus* were observed either via pigment or genomics analyses.

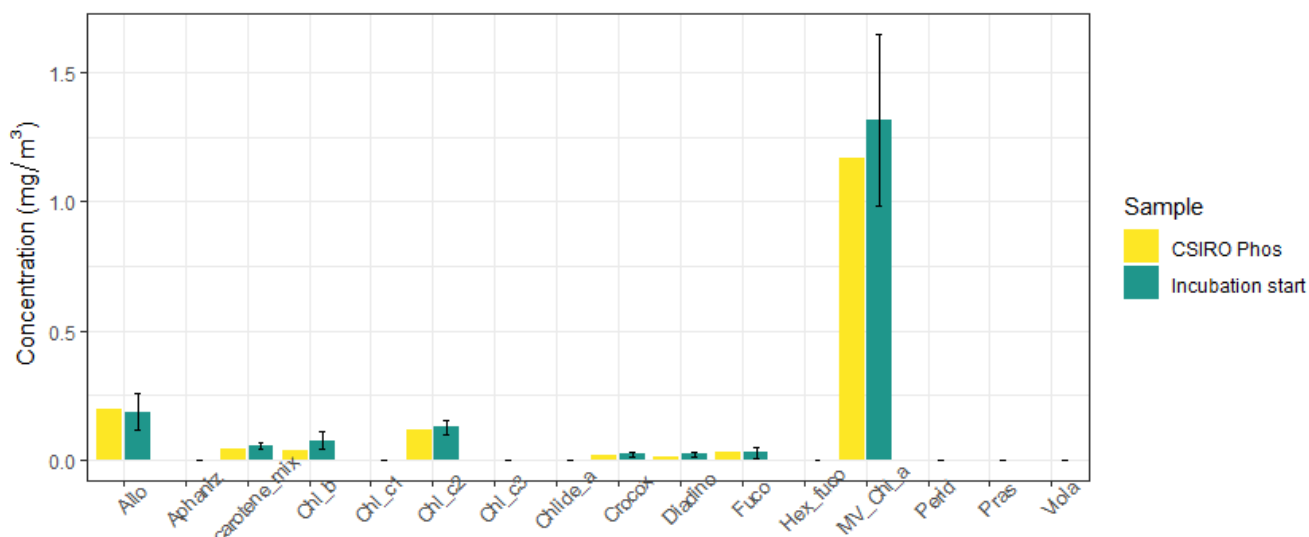


Figure 5.15 Comparison of pigments collected from the site survey and at the start of the incubation (T0).

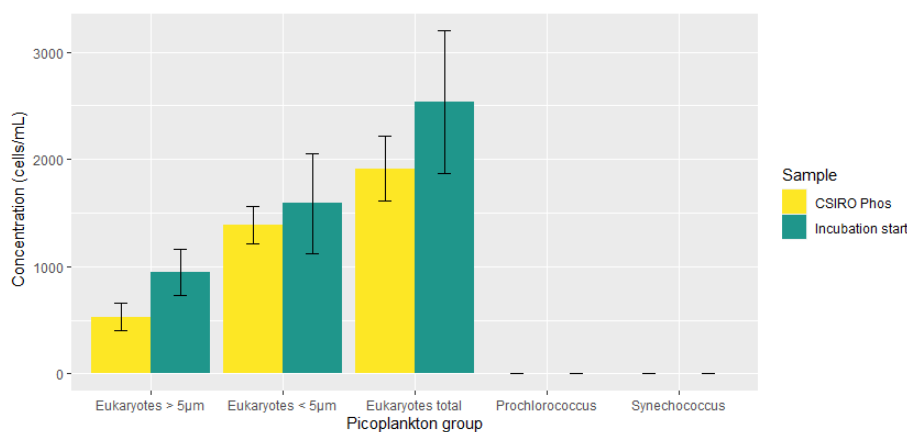


Figure 5.16 Comparison of picoplankton communities collected from the site survey and at the start of the incubation (T0).

Nutrient samples at the start of the incubation showed dissolved phosphate was significantly lower than total phosphate, while concentrations of nitrate + nitrite and silicate were similar in filtered and unfiltered samples. Ammonium samples suggest some contamination of the filtered sample with filtered > unfiltered but the concentration of unfiltered ammonium is consistent with surface data from the harbour recorded during previous spatial surveys.

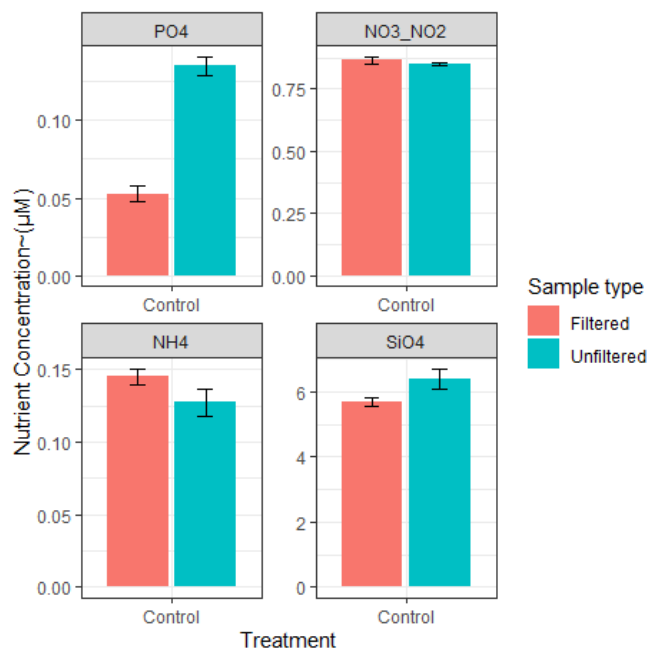


Figure 5.17 Comparison of nutrients (total and dissolved) at the start of the incubation (T0).

### 5.4.2 Incubation results

Nutrients results (Figure 5.17) show that the targeted range of phosphate spikes were achieved, with good agreement between the average of replicates from each treatment (n=3) and the corresponding pooled samples. Phosphate concentrations decreased from initial (T0) conditions at both T1 and T2 in the spiked samples, with a reduction of ~ 0.17 µM PO<sub>4</sub>/day in the light incubation. Phosphate loss or draw-down was similar for the first 24 hours in the dark incubation with negligible loss (~0.03 µM PO<sub>4</sub>) in the following 24 hours. Silicate, an essential nutrient for diatoms and other silicifying plankton, remained relatively stable over the course of the experiment, as did ammonium although some potential contamination of samples at T2 in the dark incubation is evident.

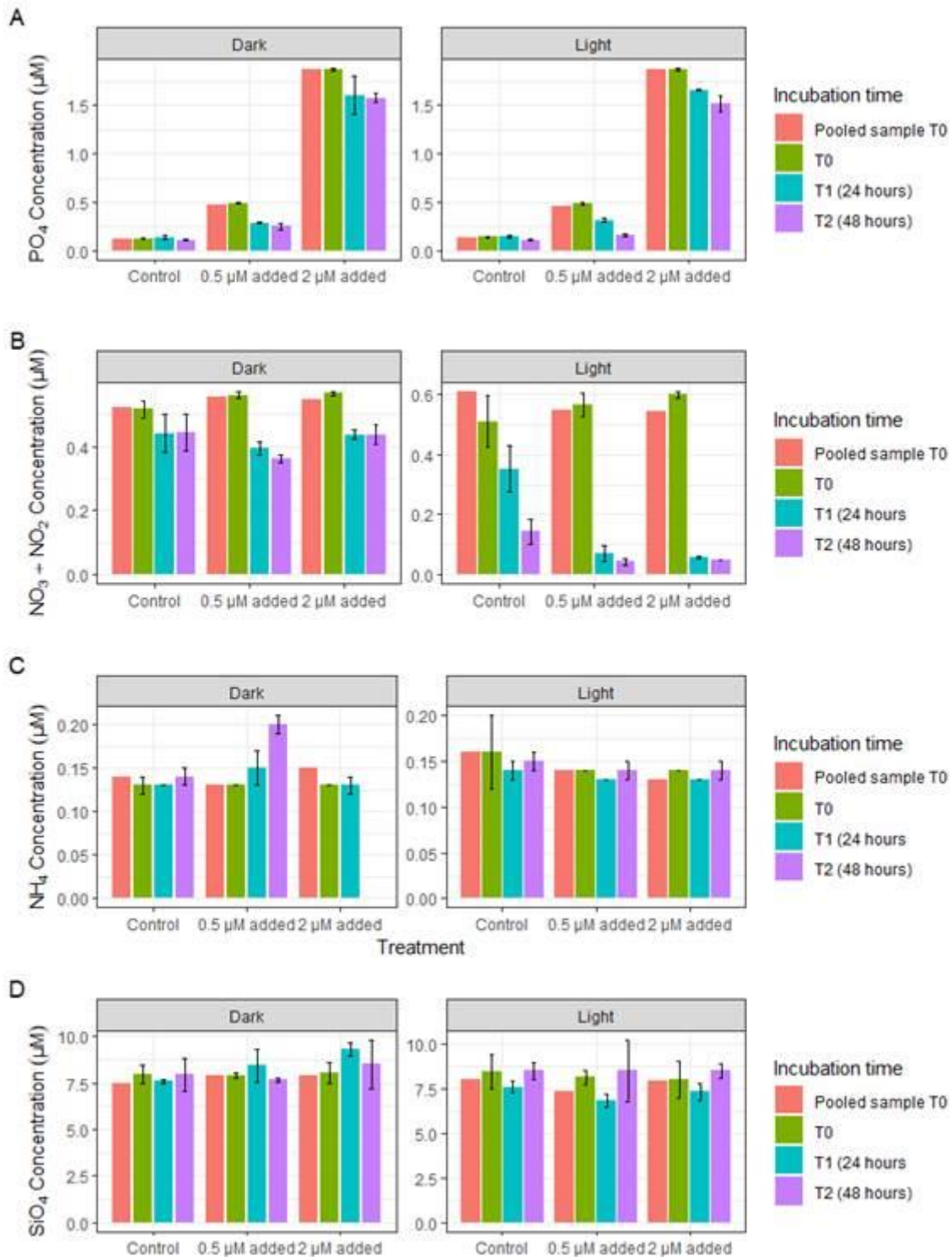


Figure 5.18: Nutrient concentrations throughout the 48-hour nutrient incubation where T0 = incubation start, T1 = 24 hours and T2 = 48 hours. P= pooled sample at T0, shown for comparison to replicates.

Pigment data from the Light incubation (Figure 5.19) shows that chlorophyll *a* decreased over the incubation period in the controls, with no consistent trend in the phosphate addition treatments. The pigment composition (normalised to MV Chl *a*) indicated that cryptophytes (alloxanthin) were abundant in all samples (Figure 5.20). Crocoxanthin, also indicative of cryptophytes, was present in all T0 samples and the Control T1 sample but was not detected in the phosphate addition treatments after T0. This could be due to a smaller volume of sample being collected for T1 and T2 samples; that is the crocoxanthin is

present but below detection level. Diatoms were also present in all samples, as indicated by the presence of fucoxanthin. The relative proportion of the diatoms appears to be more stable through time in the Controls, increasing over time with the higher phosphate addition (+2  $\mu\text{M}$ ). It is interesting to note that Chl-b, indicative of the presence of green algae, is present in the T0 samples, but not in any other of the time series samples, but again this may be due to the volume filtered.

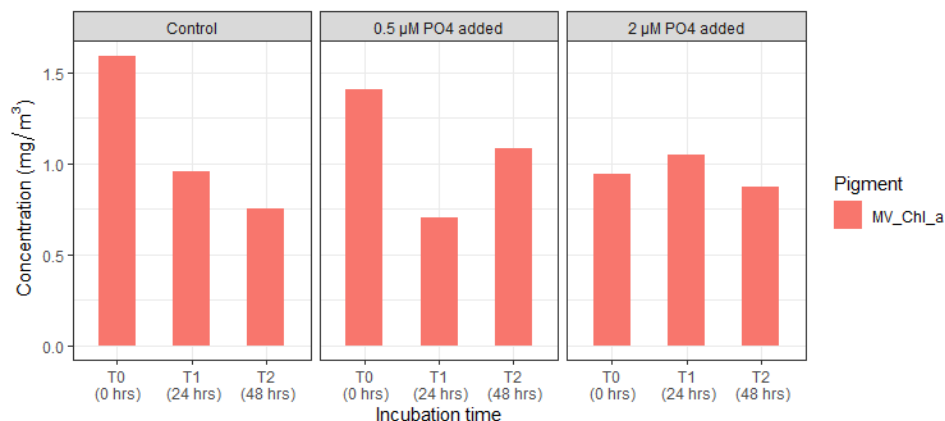


Figure 5.19 Concentration of MV chlorophyll *a* for each incubation sampling point during the incubation.

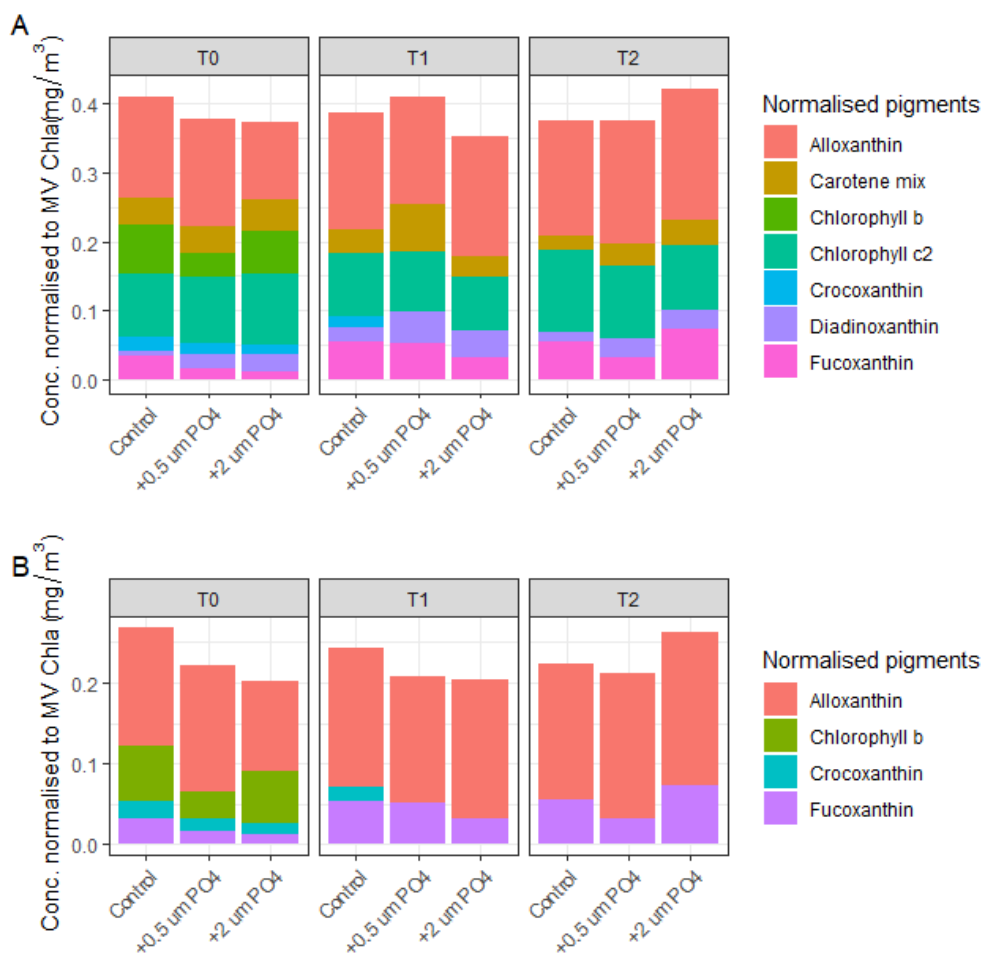


Figure 5.20 Concentration of marker pigments (normalised to MV chlorophyll *a*) for A) each incubation sampling point and B) a subset of the main marker pigments of interest.

Phycoerythrin concentrations (Figure 5.21) increased over the course of the Light incubation in both the Control and the +2  $\mu\text{M}$  PO<sub>4</sub> treatment, showing the opposite trend to the MV Chl *a* data in each treatment. The picoplankton analyses showed an increase in total eukaryotes over time in each treatment. The

relative proportions of eukaryotes determined by flow cytometry was unchanged for the control and +2  $\mu\text{M}$   $\text{PO}_4$  treatments, with a gradual increase in the larger size class in the +0.5  $\mu\text{M}$   $\text{PO}_4$  treatment.

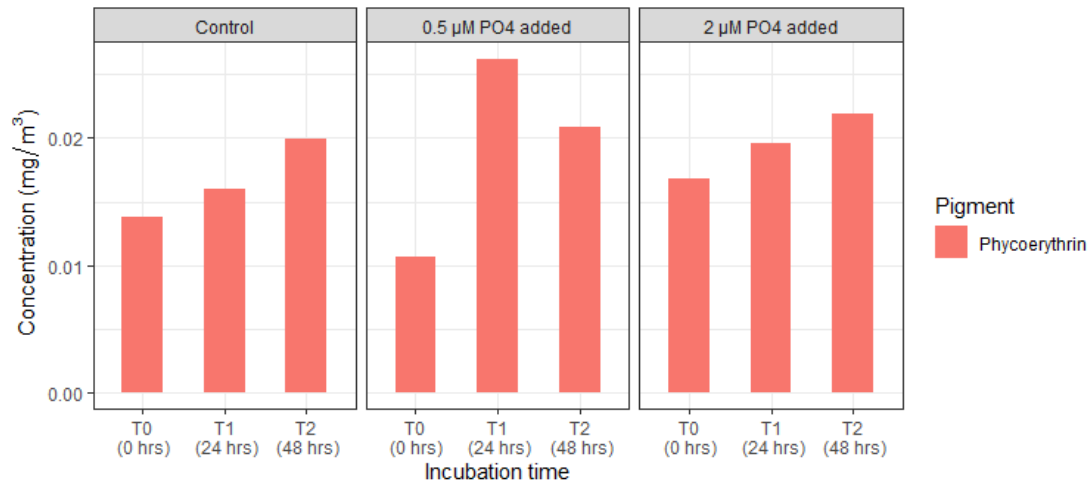


Figure 5.21 Concentration of phycoerythrin throughout the phosphate incubation.

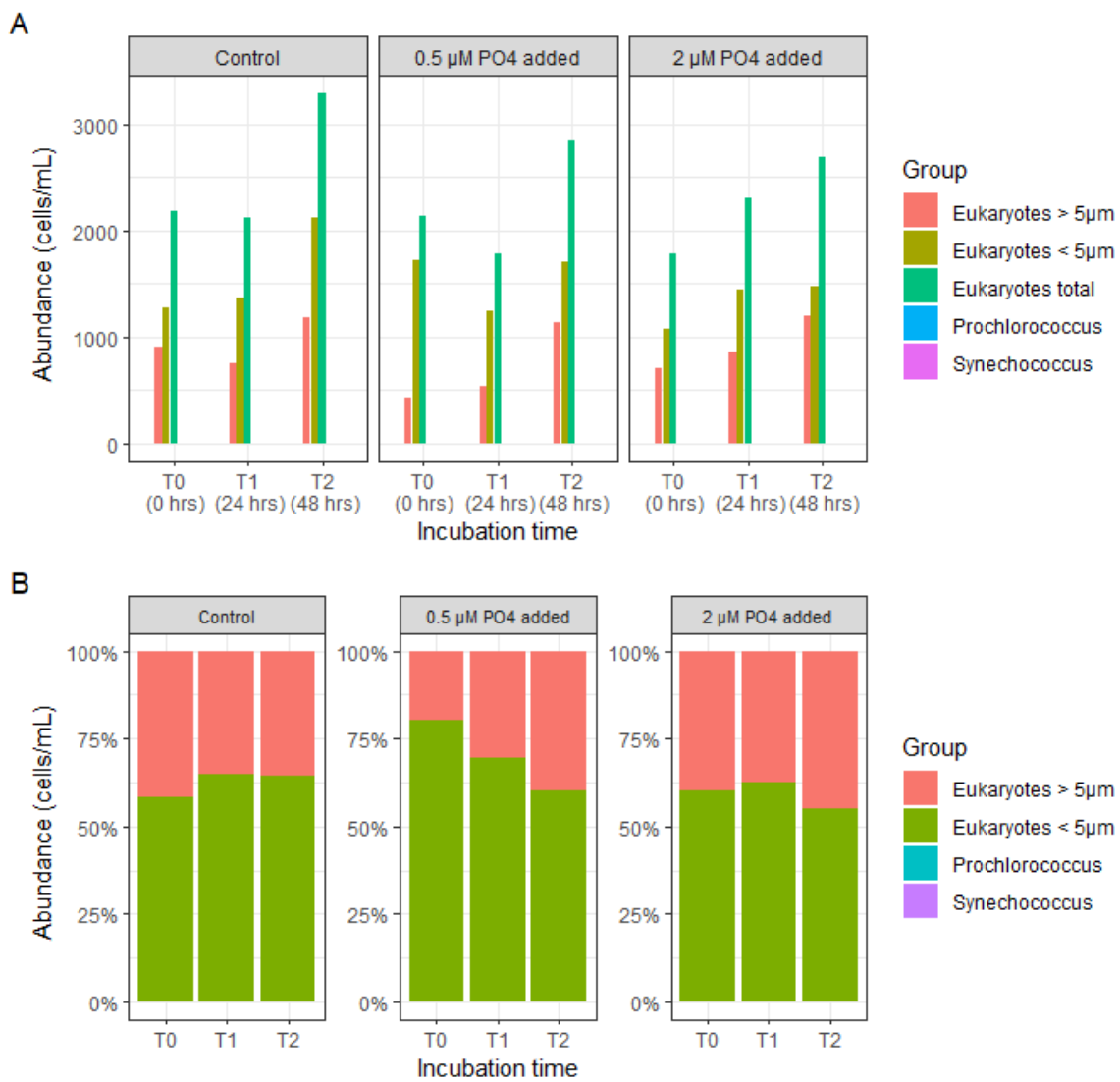


Figure 5.22 Picoplankton abundances throughout the 48-hour nutrient incubation where T0 = incubation start, T1 = 24 hours and T2 = 48 hours.

Microscopy data from the incubation shows some variability in the phytoplankton composition in the controls over the 48 hours, (Figure 5.22), with little change in the overall structure in the phosphate addition treatments.

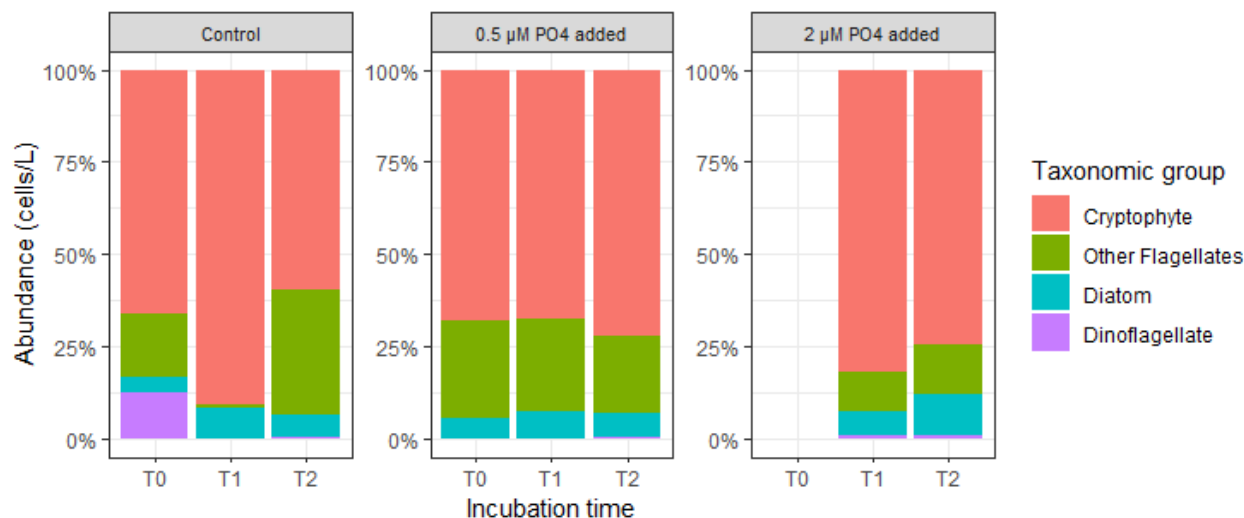


Figure 5.23 Microplankton abundances (proportion contribution to total) throughout the 48-hour nutrient incubation where T0 = incubation start, T1 = 24 hours and T2 = 48 hours.

### 5.4.3 Molecular analyses

The 16S and 18S ribosomal DNA analyses from the Light incubation showed no significant reaction to the addition of phosphate in the abundance of eukaryotes (phytoplankton) (Table 5.2). Similarly, there was no significant change detected in the relative abundance of the archaeal or bacterial taxa due to phosphate addition during the course of the experiment (data not shown). This and the other lines of evidence examined here (pigments and light microscopy) suggest that phosphate limitation may not be a major factor shaping Macquarie Harbour communities and that other factors such as light limitation due to high levels of DOC in the surface waters may have a greater influence. Alternatively, it is also possible that the experimental timeframe wasn't long enough for a change in the communities to occur in the form of population growth. The genomics analysis applied here detects cell division, but not an initial increase in activity (prior to cell division).

Table 5.2 Microbial community abundances throughout the 48-hour nutrient incubation where T0 = incubation start, T1 = 24 hours and T2 = 48 hours. Numbers indicate the relative abundance of the phytoplankton groups in percentage of the total eukaryote community, as reflected by their 18S rDNA copy numbers.

Group	In situ	PO <sub>4</sub> addition: T0			PO <sub>4</sub> addition: T1.			PO <sub>4</sub> add <sup>n</sup> : T2	
		0	0.5uM	2uM	0	0.5uM	2uM	0	0.5uM
	In situ	P-LC-T0	P-L0.5-T0	P-L2-T0	P-LC-T1	P-L0.5-T1	P-L2-T1	P-LC-T2	P-L0.5-T2
Cryptophytes	8.05	25.43	5.77	16.68	36.87	22.77	14.76	25.24	34.35
Dinophytes	19.06	15.77	15.08	13.16	17.76	10.40	10.31	8.14	10.45
Chrysophyceae	2.01	7.25	2.29	3.27	7.59	12.34	3.24	11.91	13.52
Dictyochophyceae	0.02	0.59	0.32	0.21	0.82	0.47	0.36	1.43	2.22
Chlorophyceae	0.42	0.41	0.26	0.30	0.33	0.52	0.07	0.70	2.31
Diatoms	1.40	0.38	0.39	0.12	0.24	0.44	1.00	0.32	0.44

## 5.5 Dissolved oxygen drawdown process study

The mechanisms of dissolved oxygen drawdown within the harbour are still not well understood. As part of trying to further understand the possible processes involved, we undertook a series of incubation experiments with water collected from depths of 10 m and 20 m adjacent to and ~100m from a cage. Unfortunately, a third more distant sample intended as a control couldn't be sampled due to poor weather.

Half the water collected from each depth was aerated to raise its DO as far as possible, while the rest was kept at ambient concentrations. Aerated and non-aerated water from each depth were each decanted into nine 1L Nalgene bottles which were placed in ambient water baths covered with tarpaulin. All incubations were undertaken in triplicate under dark conditions. Incubations ran over approximately 16 h with time points collected at 0, 8 and 16 h. DO was measured on the initial water collected from the two depths, again following aeration to assess the magnitude of the aeration processes and at the time of harvesting. DO was also measured continuously within one aerated incubation bottle from each depth throughout the incubation period to facilitate a real time assessment of how the incubations were progressing. Prior to the final 16 h harvest, DO was measured in the control incubations. At each time point, samples were collected for nutrient analyses and filtered for transcriptomics as follows:

Individual samples were collected from each of the three bottles at each time step on 0.2 mm Sterivex filters and snap frozen in liquid nitrogen, then transferred to -80°C and stored there until RNA was extracted. RNA was extracted using the Qiagen PowerWater Sterivex Extraction kit following the manufacturer's recommended protocol for RNA extraction (<https://dx.doi.org/10.17504/protocols.io.gmkbu4w>). The resulting RNA was in vitro transcribed into cDNA using the Superscript IV kit (Thermo Fisher) and random hexamers, following the manufacturer's recommendation. The cDNA was used as template for tag sequencing of archaeal 16S rRNA, bacterial 16S rRNA and eukaryote 18S rRNA, respectively. Sequencing was done at the Ramaciotti Sequencing Centre (UNSW, Sydney, Australia) following the standard protocols for the Australian Microbiome initiative (Brown et al., 2018). Sequences were analysed following the standard informatics pipeline of the Australian Microbiome initiative (<https://www.australianmicrobiome.com/protocols/>). Statistical analysis of the results was carried out using the Primer statistical package and Microsoft Excel.

### 5.5.1 Results

Vertical profiles of dissolved oxygen at the two sites were very similar at the time of sampling (Figure 5.24). There was little impact on ambient dissolved oxygen levels during transport to the laboratory, but once there, 30 minutes of aeration successfully elevated DO to 100% (Table 5.3; Figure 5.25).

Non-aerated samples from 10 m deep showed a slight decrease in DO over the time of the incubations while similar samples from 20 m showed little change and possibly a slight increase (Table 5.3; Figure 5.25). This apparent increase during incubation of samples with a very low initial DO concentration has been observed in previous experiments in Macquarie Harbour (Revill et al., 2016) and probably represents oxygen being desorbed from the container. Aerated water typically exhibited a decrease in DO concentration during incubation of 10-12 % (ca. 1 mg/L) over the course of the incubations (Table 5.3; Figure 5.25). It is worth noting that during the incubation period there was a slight increase in the temperature of the water bath (ca. 2°C) but this is compensated for in the oxygen concentration calculation.

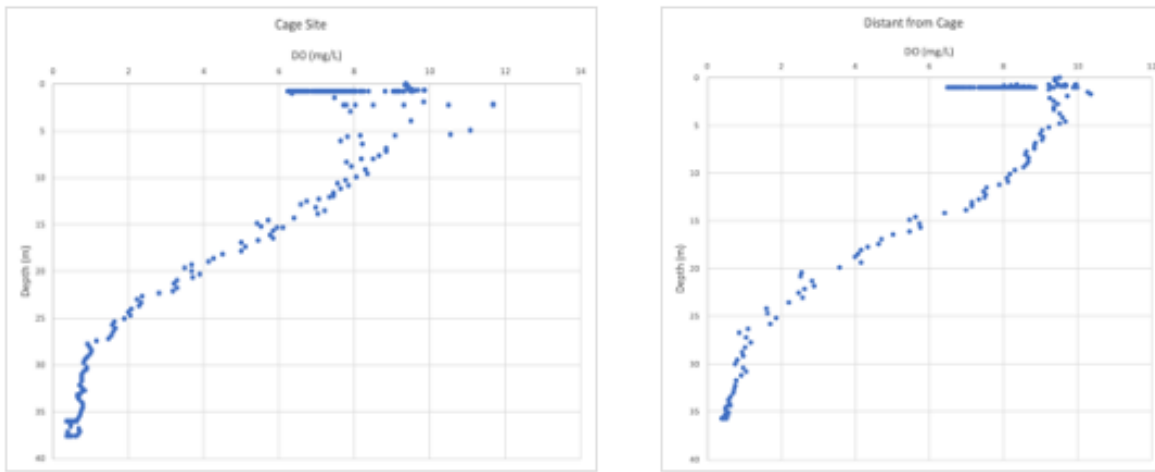


Figure 5.24 CTD casts showing dissolved oxygen profiles with depth at the cage site (L) and distant from cage site (R).

All the aerated water incubations exhibited an initial increase in ammonium concentration compared to their non-aerated counterparts, suggesting an increase in ammonification in these samples associated with the increase in oxygen. This increased concentration then slowly decreased over the incubation period. However, there was no apparent concurrent increase in nitrate or nitrite (Table 5.3; Figure 5.25) which suggests that either:

- There was no associated stimulation of nitrification and the liberated ammonium was being taken up directly (possibly by bacteria), or
- There was stimulation of nitrification, but denitrification was also occurring at a similar rate resulting in no net nitrate production

Results from the transcriptomics showed a 25x surge in copiotroph activity at T1 (approximately 8 hours after oxygenation) and a 100x surge at T2 (approximately 16 to 18 hours after oxygenation), due to aeration (Table 5.4). A more detailed view is shown in Figure 5.26, where the individual levels of each of the four genera in each sample is shown. The 20 m samples at the fish farm location had comparatively lower levels of copiotrophs in both oxygenated and control experiments but a similar increase in magnitude occurred as noted for the other site/depth combinations. Interestingly, the *Vibrio* genus only showed an increase in the 10m samples, but not in the 20m samples. The other 3 copiotroph genera showed the same strong increase in activity in samples from both depths.

These four genera, *Alteromonas*, *Pseudoalteromonas*, *Vibrio* and *Marinobacter* are well documented marine copiotrophs (Lopez-Perez et al., 2012; Tout et al., 2014; Simonato et al., 2010; Mounier et al., 2014). Copiotrophs live on complex organic compounds and thrive when they are available in copious amounts. The same analysis did not show any noticeable increase in other bacterial groups. In particular, we did not identify any increase in nitrifier or in methanotroph (methane oxidising) activities due to oxygenation. Similarly, no noticeable increase was shown in the activities of any of the eukaryotic microbes or any of the archaea.

Finally, the same analysis did not indicate any dramatic drop in the activity of any of the abundant microbial groups (bacterial, archaeal or eukaryote) due to oxygenation. This indicates that aeration did not cause a significant die-off event in the microbial community. A significant die-off would have resulted in the release of organic compounds, which could be an alternative explanation for the increased copiotroph activity detected. Based on these results we were able to exclude this alternative explanation.

Table 5.3 Dissolved oxygen and nutrient data for the incubation experiments. Shaded data are from non-aerated water, non-shaded are from water aerated for 30 min prior to commencing the experiment. Samples were collected prior to aeration (T0), immediately following aeration (T01), 8 hours post aeration (T1), and 16 hours post aeration (T2).

		Depth	Treatment	Oxygen (%)	Ammonium ( $\mu\text{M}$ )	NOx ( $\mu\text{M}$ )	Nitrite ( $\mu\text{M}$ )	Phosphate ( $\mu\text{M}$ )	Silicate ( $\mu\text{M}$ )
Cage Site	10 metres	T0	78.7	0.23	5.18	0.11	0.07	14.20	
		T01_C	81.2	0.25	5.07	0.12	0.08	14.00	
		T1_C		0.25	4.87	0.11	0.07	13.37	
		T2_C	71.9	0.19	5.09	0.12	0.07	14.03	
		T01_A	102.0	0.42	5.23	0.12	0.09	14.20	
		T1_A	101.4	0.36	5.12	0.12	0.07	14.17	
		T2_A	87.7	0.32	5.11	0.12	0.08	14.13	
	20 metres	T0	26.1	0.12	7.53	0.05	0.20	15.40	
		T01_C	33.0	0.14	7.52	0.05	0.22	15.43	
		T1_C		0.07	7.49	0.06	0.19	15.37	
		T2_C	31.8	0.05	7.50	0.06	0.18	15.40	
		T01_A	103.0	0.21	7.54	0.05	0.21	15.35	
		T1_A	99.0	0.28	7.61	0.05	0.21	15.37	
		T2_A	88.0	0.28	7.60	0.05	0.20	15.33	

Distant from Cage	10 metres	T0	84.5	0.08	5.74	0.08	0.08	13.50
		T01_C	74.9	0.15	6.53	0.04	0.19	13.20
		T1_C		0.07	5.68	0.08	0.07	13.37
		T2_C	65.8	0.05	5.72	0.09	0.07	13.40
		T01_A	100.2	0.18	5.74	0.09	0.09	13.50
		T1_A	96.9	0.18	5.45	0.09	0.07	12.87
		T2_A	89.0	0.11	5.72	0.09	0.06	13.47
	20 metres	T0	39.4	0.12	7.53	0.06	0.19	15.40
		T01_C	44.0	0.21	7.52	0.07	0.22	15.40
		T1_C		0.08	7.21	0.05	0.18	14.80
		T2_C	45.5	0.04	7.47	0.06	0.18	15.30
		T01_A	100.5	0.06	5.73	0.09	0.08	13.40
		T1_A	95.9	0.17	7.51	0.07	0.20	15.37
		T2_A	88.7	0.11	7.50	0.07	0.20	15.37

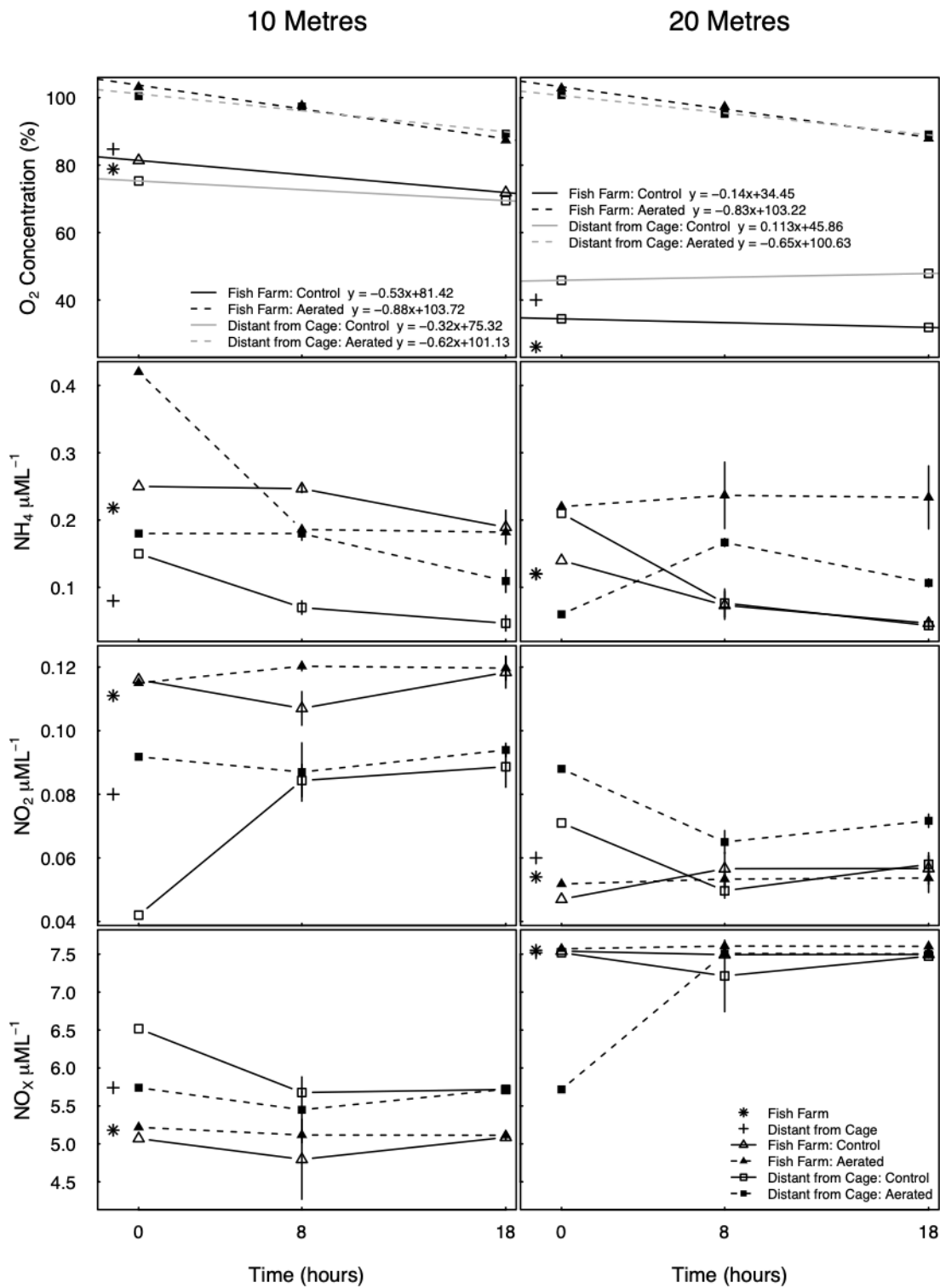


Figure 5.25 Dissolved oxygen and nutrient data from the dissolved oxygen drawdown incubation experiments.

Table 5.4 Very high oxygen enrichment indices for four copiotroph genera at T1 (8 hours post aeration), and T2 (18 hours post aeration). Oxygen enrichment indices were calculated as the ratios between the average 16S rRNA relative abundances for the oxygenated vs. the control (non-oxygenated) samples.

Genus	O <sub>2</sub> enrichment index T1	O <sub>2</sub> enrichment index T2
<i>Alteromonas</i>	7.8	40.8
<i>Marinobacter</i>	23.9	52.2
<i>Pseudoalteromonas</i>	9.2	101.1
<i>Vibrio</i>	31.3	120.6
4 copiotroph genera together	24.4	106.8

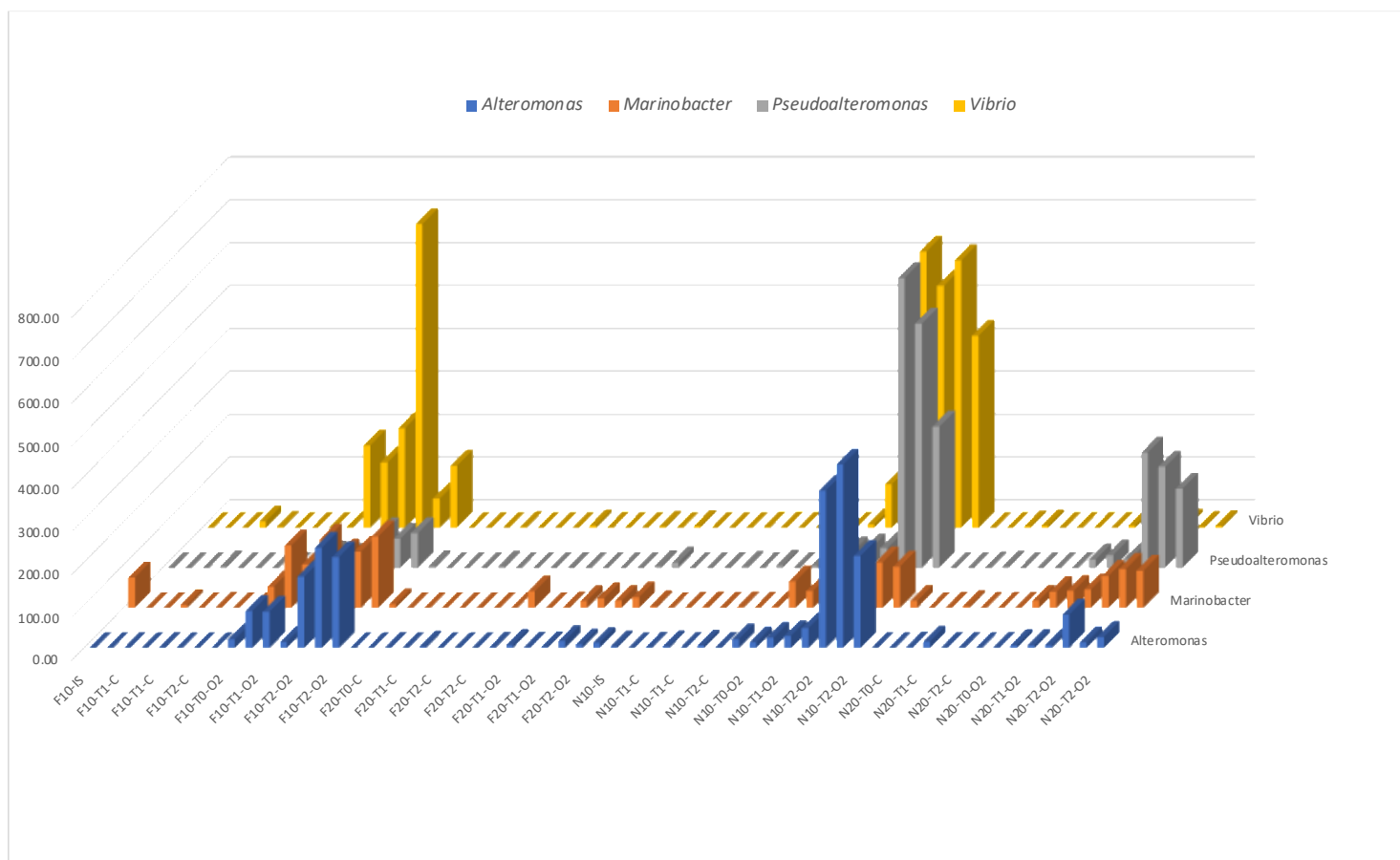


Figure 5.26 Individual levels of 16S rRNA (relative abundance values) for the four copiotroph genera in each sample. F=at Fish farm. N=Near fish farm. IS = in situ samples. C = Control samples. O<sub>2</sub> = oxygenated samples.

### 5.5.2 Discussion

Long term net pelagic dissolved oxygen drawdown has previously been estimated to be approximately 0.03 mg/L/day and 0.01 mg/L/day at 10 and 20 m respectively (Revill et al, 2016). Attempts to measure actual drawdown have previously proved to be difficult, with some incubations resulting in an increase in the measured DO (Revill et al 2016). In this series of incubations, background DO consumption was measured to be of the order of 0.02 mg/L/h (0.48 mg/L/day) at 10 m, which is significantly greater than the previous gross net estimate. At 20 m there was no measured background DO consumption. As previously described,

aeration caused an increase in measured DO consumption, with all samples recording 0.04 mg/L/h (0.96 mg/L/day) and this is attributed to the increase in copiotroph activity.

Spietz et al. (2015) reported that DO concentrations between 5.17 and 7.12 mg/L were associated with a marked change in estuarine microbial community composition and activity. This is significantly above the threshold for hypoxic conditions ( $\sim 2$  mg/L), traditionally considered to be the point at which impacts would occur. In-situ CTD data from the sampling sites show that DO concentrations at the time of sampling were approximately 7.5 mg/L and 3.7 mg/L at 10 m and 20 m respectively, putting them close to or within the range of concentrations potentially inducing a change in activity as identified by Spietz et al (2015). Thus, while copiotrophs were detected in the non-aerated samples from these depths, their measured low activity likely reflects the prevailing DO conditions. Organisms at 10 m were experiencing conditions that allowed them to function but at significantly reduced rate, while organisms at 20 m were at DO concentrations which fully inhibited their ability to function. Aeration elevated the DO concentrations in all the samples, removing any limitation to copiotroph activity and thus the measured DO consumption was similar across all the samples.

This raises the question as to what was being consumed during this increased activity. Release and subsequent consumption of nitrogen in the form of ammonium was apparent from the measured nutrient concentrations. The up to 100x increase in copiotroph activity strongly suggests organic carbon as the primary source of oxygen drawdown. Unfortunately, for this experiment, the volumes of water being incubated precluded any measurement of organic carbon. However, in previous studies (Revill et al., 2016) it has been shown that there are organic compounds present at depths of 10 m and 20 m and there was an inferred relationship between their concentration and the measured DO consumption, suggesting this is an area requiring more investigation. With a refined experimental set-up, it should be possible to measure DO consumption, microbial activity and organic carbon utilisation from the same incubations, confirming the primary biogeochemical mechanism responsible for oxygen drawdown in Macquarie Harbour.

## 6 Conclusions

This report delivers CSIRO's Final Report for the project: Understanding oxygen dynamics and the importance for benthic recovery in Macquarie Harbour (FRDC 2016-067). Specifically, we have reported on the completion of our four project objectives:

### **1. Maintenance of the CSIRO profiler and ongoing delivery of near real time and short term forecast model results**

The CSIRO profiling mooring continues to operate and has delivered an impressive dataset of hourly profiles of temperature, salinity, dissolved oxygen, chlorophyll, BGA and CDOM fluorescence in near real time since June 2019 with very little down time. These data (together with available IMAS mooring string data and fish farm data) are routinely used to assess the performance of the operational hydrodynamic and oxygen tracer model that runs in near real time with a short-term forecast. Recently the forecast has been extended out to +10 days, using BOM ACCESS-G, although the accuracy of the harbour forecast is limited by the accuracy of the meteorological forecast and estimated river flows, both of which can deteriorate significantly over the extended +10 day forecast period.

### **2. Updated visualisation dashboard**

The visualisation dashboard has been upgraded to deliver a robust and secure platform consistent with latest developments on similar platforms (e.g. the Storm Bay Information System). Output from the mooring and operational model are available on the Macquarie Harbour dashboard at: <https://macqmodelling.csiro.au/> [user login: CSIRO; password: HitchikersGuide], to inform stakeholders of evolving and predicted harbour conditions. A recent example demonstrating stakeholder use of the dashboard occurred in February 2020, when farmers were informed (with 3 days notice) of a predicted intrusion event and risk of reduced near surface dissolved oxygen in areas of the harbour shown on the dashboard.

### **3. Description of the harbour water quality simulated by the biogeochemical model; evaluation of oxygen and nitrogen budgets; scenario results and analysis**

A biogeochemical and optical water quality model has been implemented for Macquarie Harbour and generally reproduces the hydrodynamics, biogeochemical cycling and dissolved oxygen conditions observed in 2017-18 very well. The model performed best in the main harbour basin with slightly poorer skill near the Gordon and King Rivers, due to unconstrained uncertainty in river flows and biogeochemical loads. For simulated properties and scales that were not observed the model provides a hypothesis of system dynamics consistent with the properties that were observed at the sites within the Harbour.

Surface water in the harbour is seasonally warmer in summer and cooler in winter resulting in a persistent temperature inversion in winter and spring, maintained by the strong salinity driven density gradient. Should low river flow occur in winter or spring this could potentially allow overturning of the water column to re-establish a stable thermal structure.

Surface waters have very low phosphorous content with model and observations suggesting a deficit in phosphorous supply for phytoplankton growth (c.f. Redfield 16 mol N : 1 mol P). Simulated nutrient concentrations at depth were generally higher in 2017 and lower in 2018, particularly for nitrogen, due to a corresponding reduction in fish farm nutrient load in 2018. The largest input of nitrogen to the harbour in 2017-18 was from rivers (45%), fish farms and sewerage (25%), and marine intrusions (23%) [note that for the Gordon river only 30% of the nitrogen load was labile (reactive) material c.f. 100% of fish farm and

sewerage treatment plant waste]; nitrogen loss from the harbour was by export to the ocean (80%), and by sediment and water column denitrification (20%). The simulated harbour nitrogen budget shows a small net deficit of -100 tN/y, suggesting that the harbour was not in steady state but was eroding nitrogen to the surrounding environment. Given the relatively large fluxes of nitrogen into and out of the system, and the uncertainty in river nutrient loads, the absolute accuracy of this budget should be treated with caution.

Phytoplankton growth throughout the harbour is limited by light (CDOM and detrital matter dominate total absorption) and low nutrient concentrations in surface waters. Peak concentrations of chlorophyll were simulated at around 15m depth towards the northern end of the harbour which was subject to greater marine phosphorous supply and more transparent water in summer. It should be noted, that phytoplankton increase their pigment concentration under low light conditions and chlorophyll concentration does not directly correspond to phytoplankton biomass.

Dissolved oxygen concentrations in harbour surface waters are generally high, whilst concentrations at depth are depleted, primarily due to stratification and slow flushing of deep water in the harbour. No anoxic (<1% oxygen saturation) water or sediment areas were simulated by the biogeochemical model. Mean conditions simulated in 2017-18 showed that 14% of the whole harbour water volume and 33% of the sediment surface area was hypoxic (1-30% oxygen saturation) with the World Heritage Area (WHA) more impacted than the other basins. Oxygen budget analysis found the largest influx of oxygen to the harbour was from rivers (66%), marine input (10%) and air-sea flux (6%); the greatest loss terms were from export to the ocean (87%), biogeochemical remineralisation processes in the sediment (8%) and estimated farmed fish respiration (3%). Seasonal analysis for 2017-18 showed a net increase in harbour oxygen in winter and less consistently in autumn, and a net loss of oxygen in spring. The simulated harbour oxygen budget is very close to balanced being in deficit by only around -2900 tO/y. Given the large fluxes of oxygen into and out of the harbour, the accuracy of this small net sum should be considered in the context of potential uncertainty in the estimates of river flow and harbour entrance bathymetry.

Scenario simulations were achieved for drier (lower river flow) and wetter (higher river flow) conditions. Under reduced river flow, there was ~20% greater influx of marine water into the deeper parts of the harbour and reduced hypoxia; with increased river flow, marine influx was suppressed (by ~20%), deep water residence time increased and hypoxia increased. These patterns were persistent when scenarios were extended for a further 2 years and strong linear relationships were found between river flow, marine influx of oxygen and hypoxia. Further scenario simulations were achieved to explore reduced anthropogenic load on harbour water quality (by omission of fish farm respiration and nutrient loads). This reduction in anthropogenic load resulted in a 50% reduction in hypoxic water and a 40% reduction in hypoxic sediment compared to the 2017-18 model run and was persistent in the extended model run. The reduced anthropogenic load scenarios showed a larger reduction in hypoxia under comparable ocean oxygen influx c.f. all other scenarios.

#### ***4. Analysis of observational process studies for phosphate addition and oxygen drawdown***

The phosphate addition process study achieved the targeted range of phosphate spikes and demonstrated rapid phosphate draw-down within 24 hours in both dark and light incubations, plus ongoing utilisation of phosphate over 48 hours in the light incubation. Picoplankton analyses showed an increase in total eukaryotes over time and pigment data indicated the presence of cryptophytes and diatoms. Molecular analysis of 16S and 18S ribosomal DNA samples were however inconclusive and no significant reactions to the addition of phosphate were detected [although the experimental timeframe may not have been long enough to observe significant cell division]. On balance, this experiment suggests that phosphate

limitation may not be a major factor shaping the Macquarie Harbour microbial community and that light limitation due to high levels of CDOM in surface waters may have a greater influence.

The oxygen drawdown process study found that, following aeration of Macquarie harbour water collected from 10 m and 20 m, there was a substantial increase in the activity of specialised bacteria known as copiotrophs; these increased 25x within 8 and 100x within 18 hours. These bacteria are known to utilise labile organic carbon and we also observed a simultaneous uptake of available ammonium. Our results show that, even at 80% dissolved oxygen saturation, the activity of these bacteria would have been suppressed, which indicates that if more dissolved oxygen were to become available at depth, it would likely be rapidly utilised by these bacteria (assuming sufficient availability of labile carbon and nitrogen).

In conclusion this body of work integrates multiple lines of evidence to characterise the water quality and oxygen dynamics of Macquarie Harbour. Through modelling studies we now understand that river flows control the flushing time and influx of marine water and together with anthropogenic load, this ultimately defines the hypoxic condition of the harbour. Our observations confirm the skill of the model and identify the key microbial communities driving the biogeochemical cycling of nutrients, the remineralisation of organic matter and the ecological drawdown of oxygen. The findings documented in this report are available to inform ongoing sustainable management of the harbour to minimise the deleterious impacts of anthropogenic activities on water quality and local environmental values.

## 7 Recommendations

During this study the accuracy of the models was compromised by lack of river flow gauge data for the main rivers entering the Harbour, and interruptions in the tide gauge record due to instrument down time. We recommend installation of river flow gauges on the lower reaches of the Franklin-Gordon and King-Queen River catchments and priority maintenance of the Strahan tide gauge should it fail.

The short term forecasting hydrodynamic and oxygen tracer model has proven useful in alerting industry to potential low oxygen events near farm sites, however the forecast becomes less reliable as it extends forwards in time beyond a few days. We recommend investing in this model to include ensemble model forecasting (using the available range of BoM model forecasts), data assimilation of near real time data sets, a catchment model (including predicted dam releases) and an automated alert system to improve forecast delivery.

Skill assessment of the biogeochemical model against observations benefitted from a large number of observing stations within the harbour and a wide range of parameters, however spatial and temporal sampling was inconsistent and the resolution of some parameters (e.g. chlorophyll, phosphorous) was quite limited. We recommend reviewing the monitoring program to better integrate industry, EPA and research sampling programs and deliver a superior data set.

The modelling scenarios identified the key role of river flow and anthropogenic loads in modulating the oxygen status of Macquarie Harbour. We recommend further scenario simulations to better characterise the impact of contrasting anthropogenic loads. There is also evidence that variation in seasonal hydro dam release can impact flushing and harbour oxygen status and this should be investigated further (especially in the context of changing hydro demand and future investment in a second Basslink energy transmission cable).

Nutrient budget analysis for the harbour suggests that ~60% of fish farm nitrogen is exported to the ocean and this likely enhances local algal blooms (evident in remotely sensed images of Macquarie Harbour plumes). We recommend further characterisation of the west coast shelf (with models and remote sensing) to better understand the fate of anthropogenic loads on this environment and local environmental values.

## 8 References

- Andrewartha, J. & Wild-Allen, K. 2017. Hydrodynamic and Oxygen Tracer Modelling in Macquarie Harbour. Technical report. CSIRO Oceans & Atmosphere, Hobart, Australia.
- Baird, M. E., Ralph, P. J., Rizwi, F., Wild-Allen, K. A., Steven, A. D. L., 2013. A dynamic model of the cellular carbon to chlorophyll ratio applied to a batch culture and a continental shelf ecosystem. *Limnol. Oceanogr.* 58, 1215-1226.
- Baird, M. E., N. Cherukuru, E. Jones, N. Margvelashvili, M. Mongin, K. Oubelkheir, P. J. Ralph, F. Rizwi, B. J. Robson, T. Schroeder, J. Skerratt, A. D. L. Steven and K. A. Wild-Allen 2016. Remote-sensing reflectance and true colour produced by a coupled hydrodynamic, optical, sediment, biogeochemical model of the Great Barrier Reef, Australia: comparison with satellite data. *Env. Model. Software* 78: 79-96
- Bell J., Ross j., Jorge Mardones J., Macleod C. 2018 Assessment of the Macquarie Harbour Broadscale Environmental Monitoring Program. August 2018, IMAS University of Tasmania 129p
- Brown, M.V., van de Kamp, J., Ostrowski, M., Seymour, J.R., Ingleton, T., Messer, L.F., Jeffries, T., Siboni, N., Laverock, B., Bibiloni-Isaksson, J., Nelson, T.M., Coman, F., Davies, C.H., Frampton, D., Rayner, M., Goossen, K., Robert, S., Holmes, B., Abell, G.C.J., Craw, P., Kahlke, T., Sow, S.L.S., McAllister, K., Windsor, J., Skuza, M., Crossing, R., Patten, N., Malthouse, P., van Ruth, P.D., Paulsen, I., Fuhrman, J.A., Richardson, A., Koval, J., Bissett, A., Fitzgerald, A., Moltmann, T., Bodrossy, L., 2018. Systematic, continental scale temporal monitoring of marine pelagic microbiota by the Australian Marine Microbial Biodiversity Initiative. *Scientific Data* 5, 180130.
- Cherukuru, Nagur; Brando, Vittorio; Schroeder, Thomas; Clementson, Lesley; Dekker, Arnold. Influence of river discharge and ocean currents on coastal optical properties. *Continental Shelf Research*. 2014; 84:188–203. <https://doi.org/10.1016/j.csr.2014.04.022>
- Clementson, L.A., Parslow, J.S., Turnbull, A., and Bonham, P.I (2004) Properties of light absorption in a highly coloured estuarine system in south-east Australia which is prone to blooms of the toxic dinoflagellate *Gymnodinium catenatum*. *Estuarine and Coastal Shelf Science*, 60, p 101- 112
- CSIRO Coastal Environmental Modelling Team. 2018. CSIRO Environmental Modelling Suite: Scientific description of the optical, carbon chemistry and biogeochemical models. CSIRO Report, Hobart. [online access at <https://research.csiro.au/cem/software/ems/>].
- Environment Protection Authority (EPA) 2017. Macquarie Harbour 2013-2016 Nutrient Review May 2017, EPA Tasmania. 23p
- Gervais, F (1998) Ecology of cryptophytes coexisting near a freshwater chemocline. *Freshwater Biology* 39, 61-78.
- Herzfeld, M., 2006. An alternative coordinate system for solving finite difference ocean models. *Ocean Modelling*, 14, 174 – 196.
- Herzfeld, M., Andrewartha, J., Baird, M., Brinkman, R., Furnas, M., Gillibrand, P., Hemer, M., Joehnk, K., Jones, E., McKinnon, D., Margvelashvili, N., Mongin, M., Oke, P., Rizwi, F., Robson, B., Seaton, S., Skerratt, J., Tonin, H., Wild-Allen K. 2016. eReefs Marine Modelling: Final Report 497 p. [http://www.marine.csiro.au/cem/gbr4/eReefs\\_Marine\\_Modelling.pdf](http://www.marine.csiro.au/cem/gbr4/eReefs_Marine_Modelling.pdf)
- Johnson, MD, Beaudoin, DJ, Frada, MJ, Brownlee, EF, Stoecker, DK (2018) High Grazing Rates on Cryptophyte Algae in Chesapeake Bay. *Frontiers in Marine Science* 5, 241.

- Knight B, Forrest B, Johnston C 2015. Macquarie Harbour Environmental and Fish Health Monitoring Review. Prepared for Department of Primary Industries, Parks, Water and Environment Tasmania. Cawthron Report No.2729. 93 p. plus appendices.
- López-Pérez, M., Gonzaga, A., Martin-Cuadrado, A.-B., Onyshchenko, O., Ghavidel, A., Ghai, R., Rodriguez-Valera, F., 2012. Genomes of surface isolates of *Alteromonas macleodii*: the life of a widespread marine opportunistic copiotroph. *Scientific Reports* 2, 696.
- Margvelashvili, N., Saint-Cast, F., Condie, S., 2008. Numerical modelling of the suspended sediment transport in Torres Strait. *Continental Shelf Research*, 28, 2241-2256.
- Mounier, J., Camus, A., Mitteau, I., Vaysse, P.-J., Goulas, P., Grimaud, R., Sivadon, P., 2014. The marine bacterium *Marinobacter hydrocarbonoclasticus* SP17 degrades a wide range of lipids and hydrocarbons through the formation of oleolytic biofilms with distinct gene expression profiles. *FEMS Microbiology Ecology* 90, 816–831.
- Nechad, B; Ruddick, Kevin; Schroeder, Thomas; Oubelkheir, Kadija; Blondeau-Patissier, David; Cherukuru, Nagur; et al. CoastColour Round Robin datasets: a database to evaluate the performance of algorithms for the retrieval of water quality parameters in coastal waters. *Earth Systems Science Data*. 2015; 8:173–258. <https://doi.org/10.5194/essdd-8-173-2015>
- O'Connor, NA, Cannon, F, Zampatti, B, Cottingham, P, Reid, M (1996) A pilot biological survey of Macquarie Harbour, western Tasmania. Supervising Scientist.
- Revill, A.T., Ross, J. and Thompson, P.A. (2016) Investigating Dissolved Oxygen Drawdown in Macquarie Harbour. CSIRO, Australia.
- Robson, B.J., Arhonditsis, G.B., Baird, M.E., Brebion, J., Edwards, K.F., Geoffroy, L., Hébert, M-P, van Dongen-Vogels, V., Jones, E.M., Kruk, C., Mongin, M., Shimoda, Y., Skerrat, J.H., Trevathan-Tackett, S., Wild-Allen, K., Kong, X., Steven, A. 2018. Towards evidence-based parameter priors for aquatic ecosystem modelling. *Environmental Modelling & Software* 100: 74-81
- Simonato, F., Gómez-Pereira, P.R., Fuchs, B.M., Amann, R., 2010. Bacterioplankton diversity and community composition in the Southern Lagoon of Venice. *Systematic and Applied Microbiology* 33, 128–138.
- Spietz, R.L., Williams, C.M., Rocap, G., Horner-Devine, M.C., 2015. A Dissolved Oxygen Threshold for Shifts in Bacterial Community Structure in a Seasonally Hypoxic Estuary. *PLOS ONE* 10, e0135731.
- Stramski, D., M. Babin, S. B. Wozniak (2007) Variations in the optical properties of terrigenous mineral-rich particulate matter suspended in seawater. 52, 2418-2433.
- Tout, J., Jeffries, T.C., Webster, N.S., Stocker, R., Ralph, P.J., Seymour, J.R., 2014. Variability in Microbial Community Composition and Function Between Different Niches Within a Coral Reef. *Microbial Ecology* 67, 540–552.
- Wild-Allen, K. & Andrewartha, J. 2016. Connectivity between estuaries influences nutrient transport, cycling and water quality. *Marine Chemistry* 185:12-26. doi:10.1016/j.marchem.2016.05.011
- Wild-Allen, K., Skerratt, J., Whitehead, J., Rizwi, F. and Parslow, J. 2013. Mechanisms driving estuarine water quality: a 3D biogeochemical model for informed management. *Estuarine, Coastal & Shelf Science* 135:33-45.

Wild-Allen, K., Andrewartha, J., Skerratt, J., Eriksen, R., Revill, A., Schwanger, C., Sherrin, K. and Wild, D. (2019) Understanding oxygen dynamics and the importance for benthic recovery in Macquarie Harbour (FRDC 2016-067): CSIRO Milestone 3 Report. CSIRO, Australia.

Wild-Allen, K., Andrewartha, J., Baird, M., Bodrossy, L., Brewer, E., Eriksen, R., Skerratt, J., Revill, A., Sherrin, K., Wild, D. (2020) Macquarie Harbour Oxygen Process model (FRDC 2016-067): CSIRO Milestone 4 Report. CSIRO, Australia

## **9 Appendix: Summary figures of model comparison with observations**

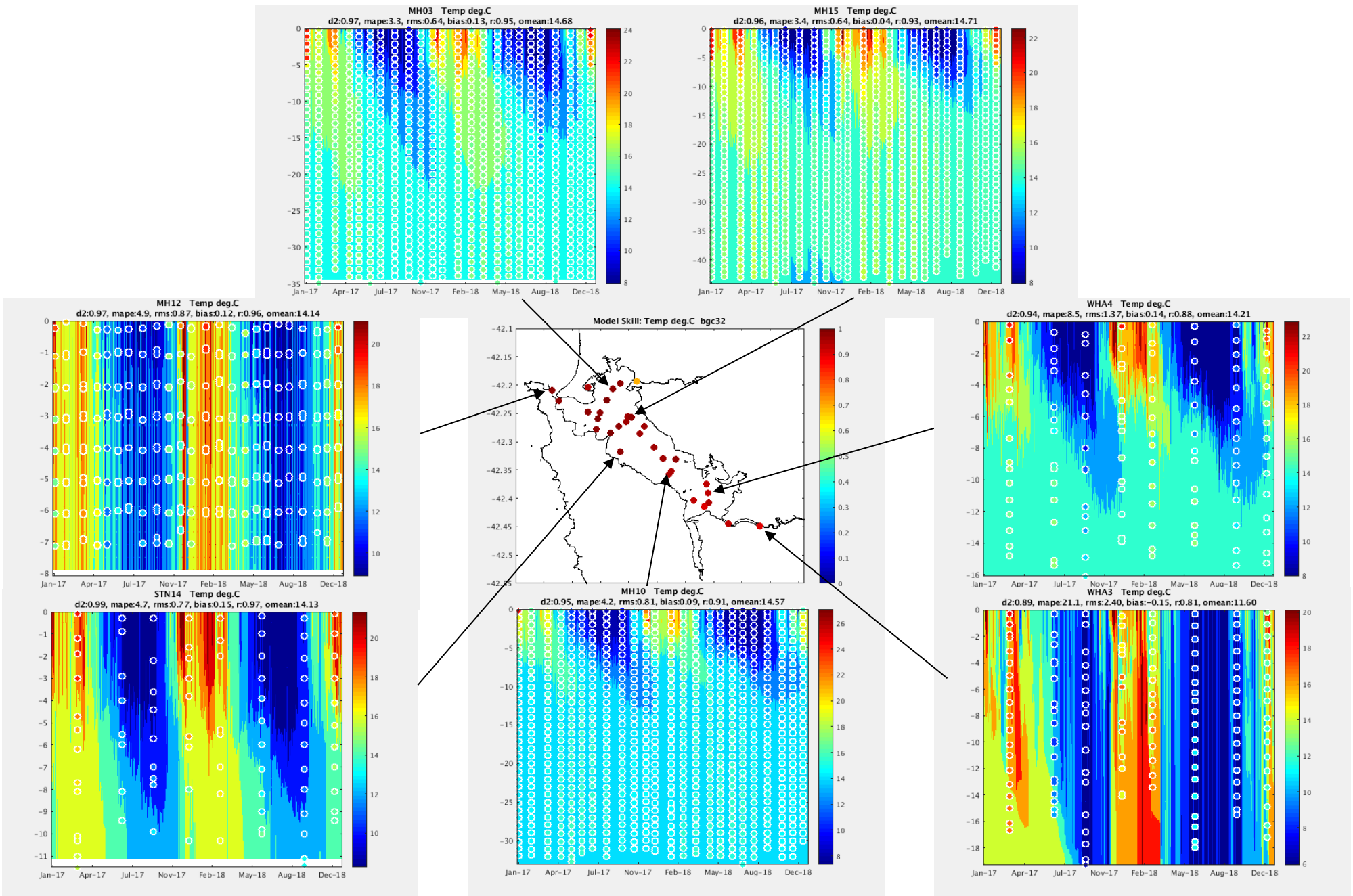


Figure 7.1 Simulated (background) and observed (circles) vertical evolution of temperature during 2017-2018 at sites throughout Macquarie Harbour. Skill metrics summarised in subplot titles; Willmott score shown in centre image (1 = best, 0 = poor fit).

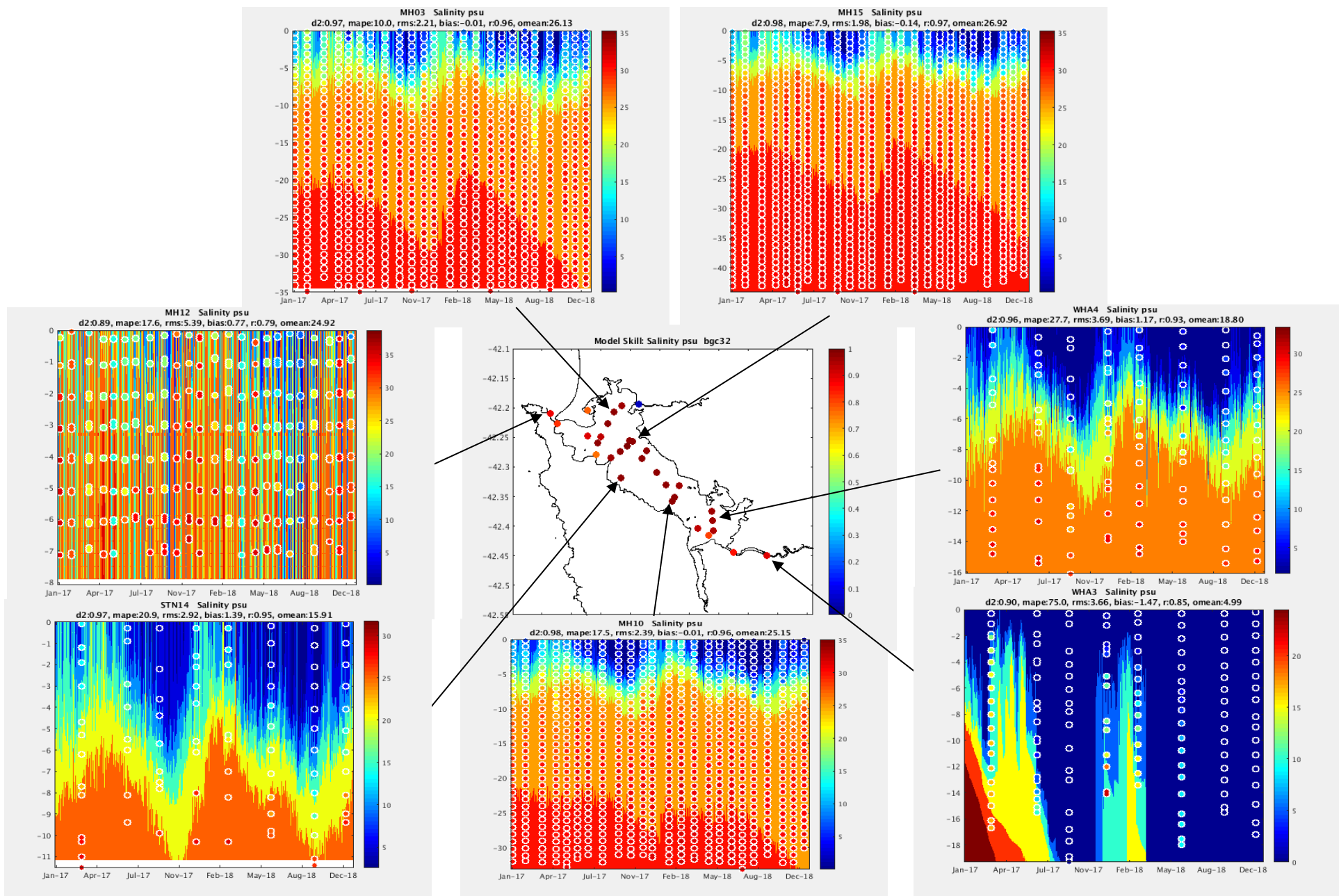


Figure 7.2 Simulated (background) and observed (circles) vertical evolution of salinity during 2017-2018 at sites throughout Macquarie Harbour. Skill metrics summarised in subplot titles; Willmott score shown in centre image (1 = best, 0 = poor fit).

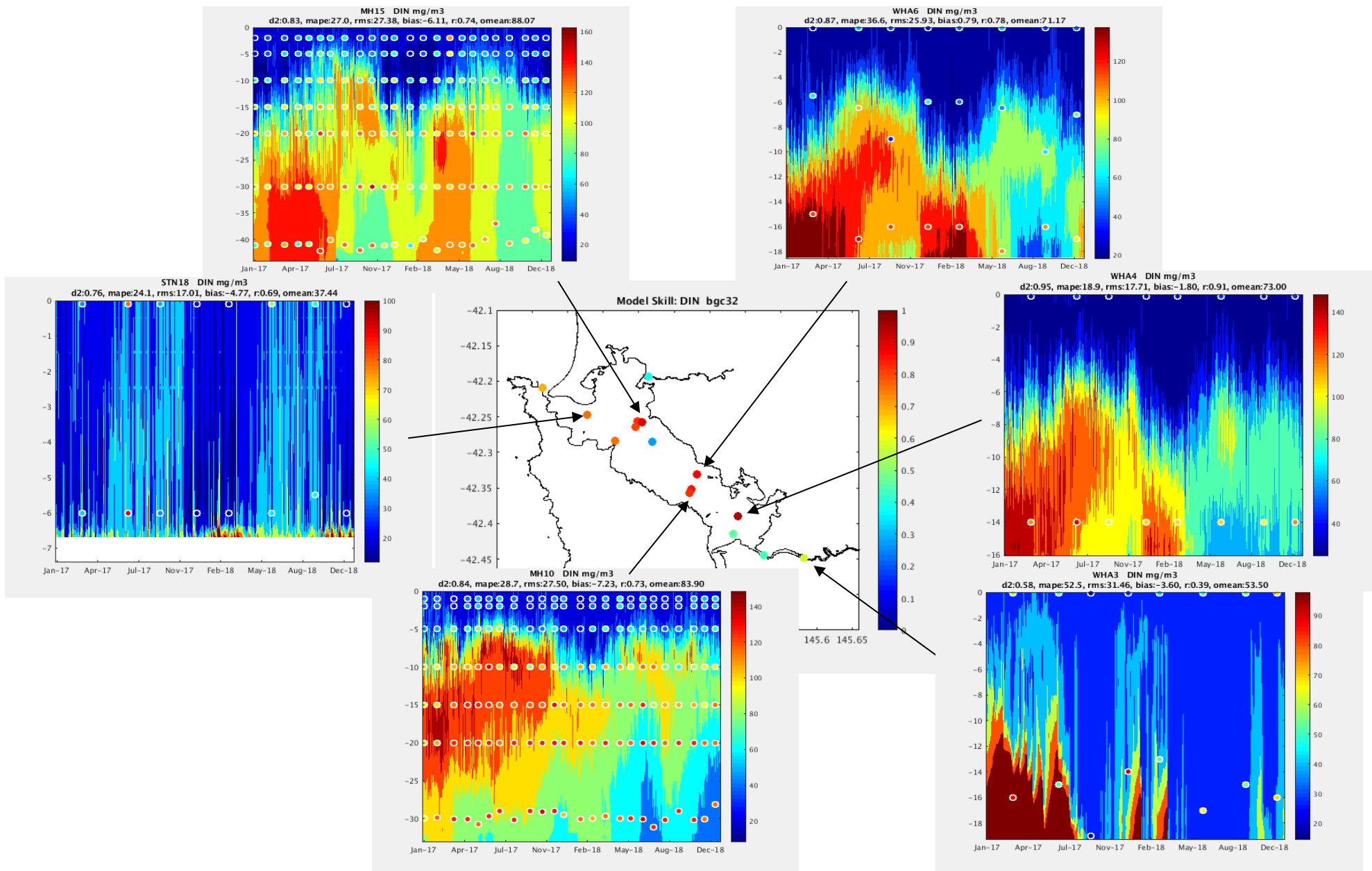


Figure 7.3 Simulated (background) and observed (circles) vertical evolution of dissolved inorganic nitrogen during 2017-2018 at sites throughout Macquarie Harbour. Skill metrics summarised in subplot titles; Willmott score shown in centre image (1 = best, 0 = poor fit).

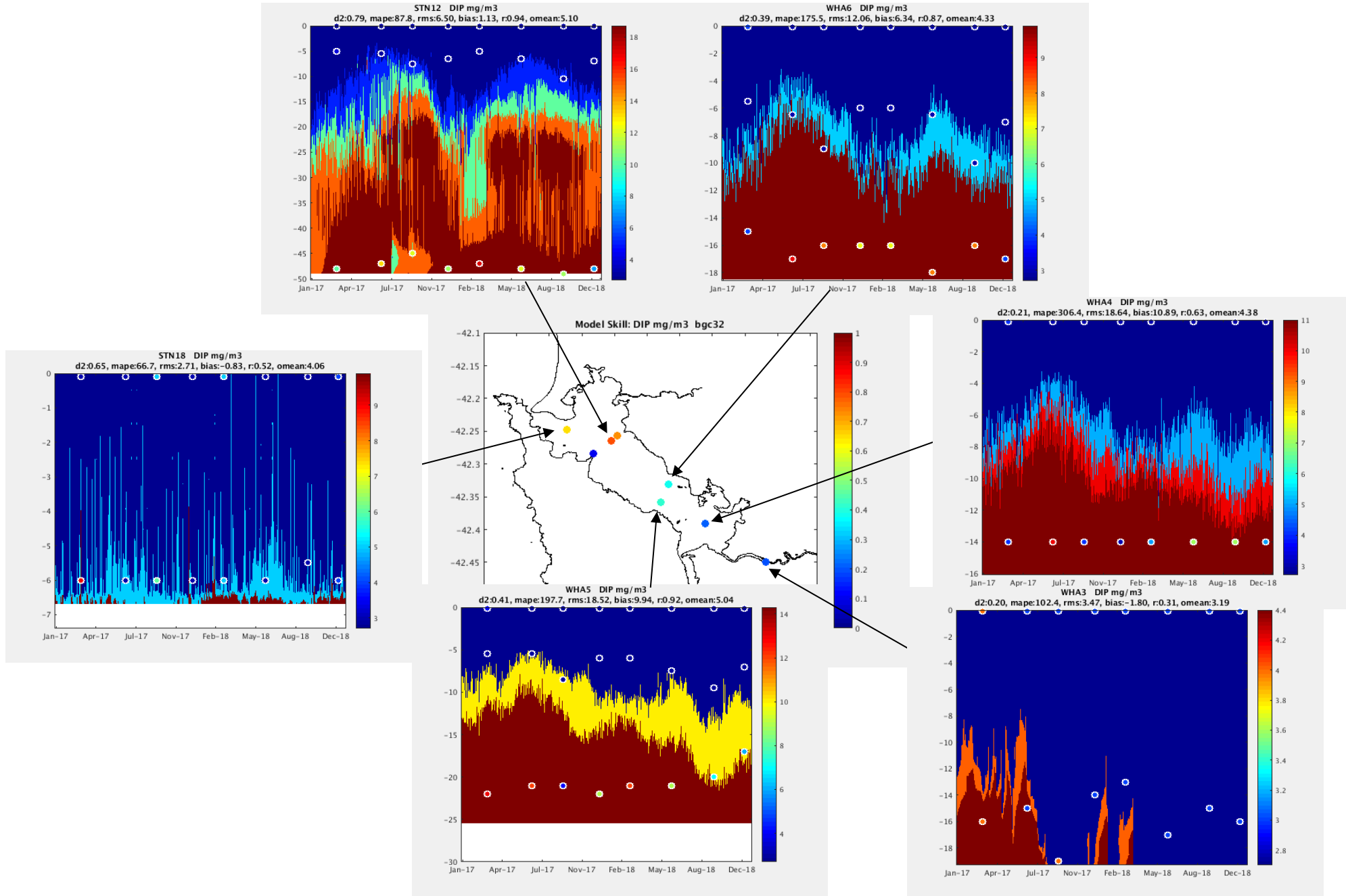


Figure 7.4 Simulated (background) and observed (circles) vertical evolution of dissolved inorganic phosphate during 2017-2018 at sites throughout Macquarie Harbour. Skill metrics summarised in subplot titles; Willmott score shown in centre image (1 = best, 0 = poor fit).

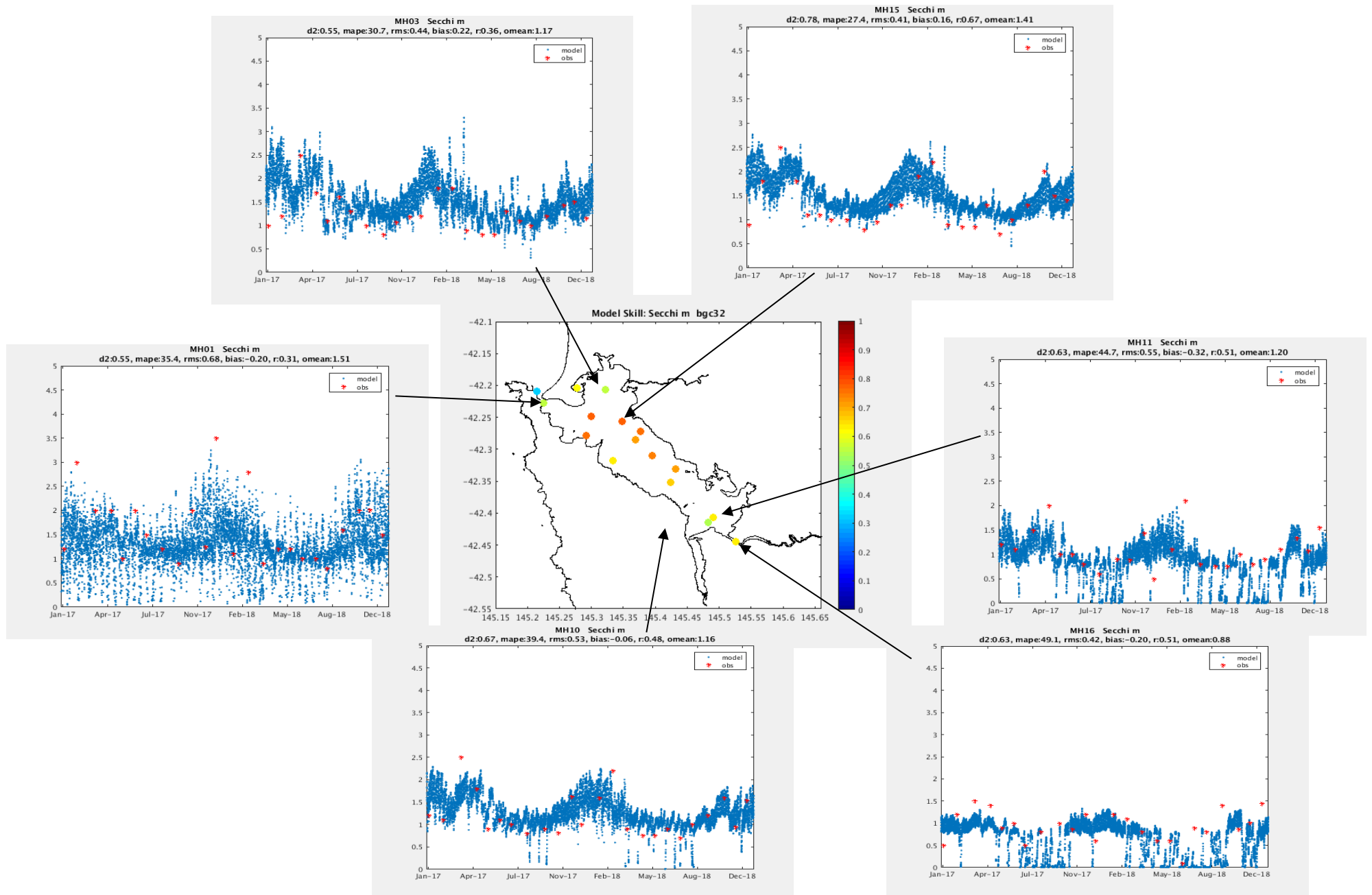


Figure 7.5 Simulated (blue) and observed (red) temporal evolution of secchi depth during 2017-2018 at sites throughout Macquarie Harbour. Skill metrics summarised in subplot titles; Willmott score shown in centre image (1 = best, 0 = poor fit).

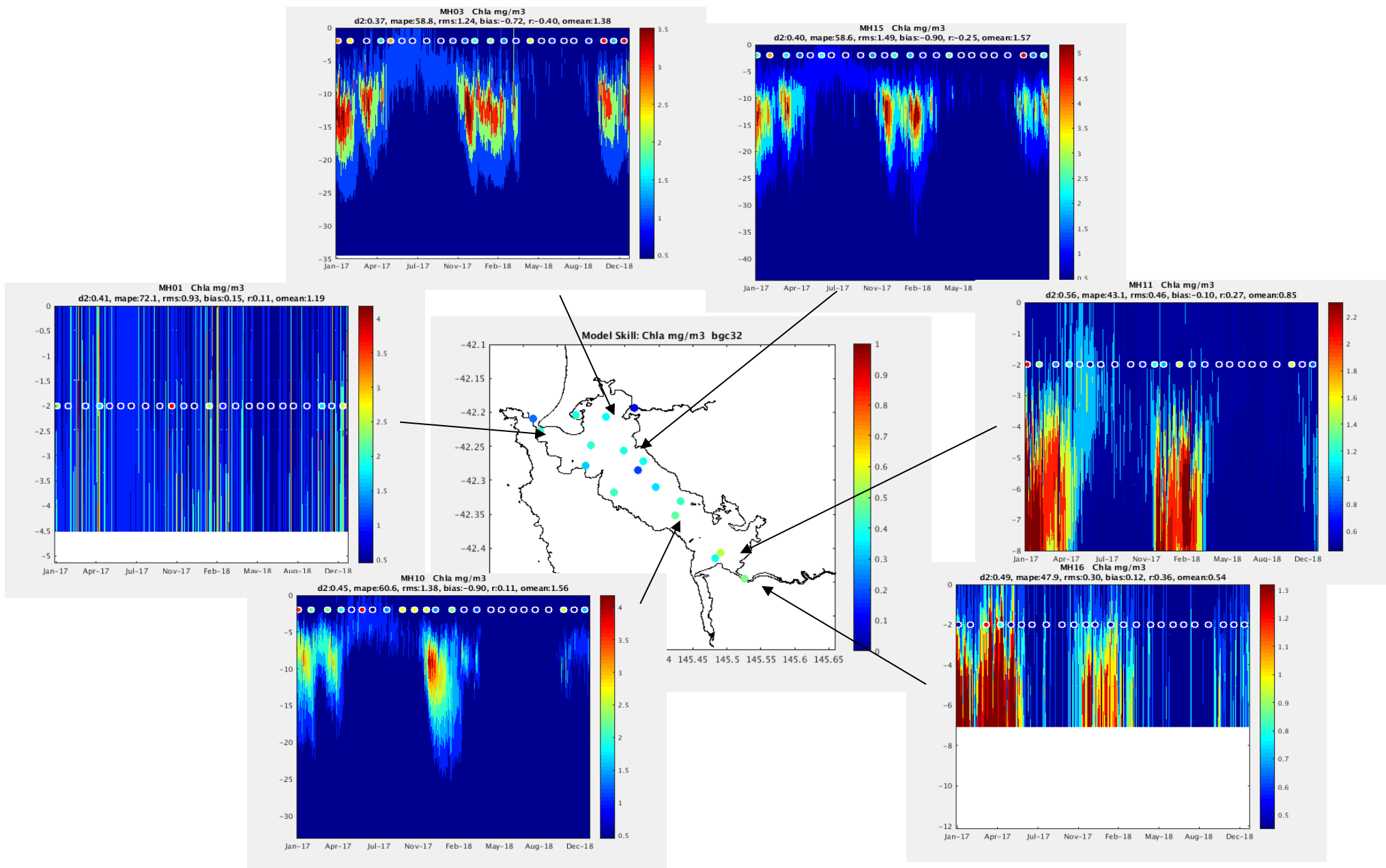


Figure 7.6 Simulated (background) and observed (circles) vertical evolution of chlorophyll during 2017-2018 at sites throughout Macquarie Harbour. Skill metrics summarised in subplot titles; Willmott score shown in centre image (1 = best, 0 = poor fit).

CONTACT US

**t** 1300 363 400  
+61 3 9545 2176  
**e** [csiroenquiries@csiro.au](mailto:csiroenquiries@csiro.au)  
**w** [www.csiro.au](http://www.csiro.au)

AT CSIRO, WE DO THE  
EXTRAORDINARY EVERY DAY

We innovate for tomorrow and help improve today – for our customers, all Australians and the world.

Our innovations contribute billions of dollars to the Australian economy every year. As the largest patent holder in the nation, our vast wealth of intellectual property has led to more than 150 spin-off companies.

With more than 5,000 experts and a burning desire to get things done, we are Australia's catalyst for innovation.

CSIRO. WE IMAGINE. WE COLLABORATE.  
WE INNOVATE.

FOR FURTHER INFORMATION

**OCEANS & ATMOSPHERE**

Karen Wild-Allen  
**t** +61 3 6232 5010  
**e** [Karen.wild-allen@csiro.au](mailto:Karen.wild-allen@csiro.au)  
**w** [www.csiro.au/Oanda](http://www.csiro.au/Oanda)